

An Advanced Assessment of Ski Bindings

A Major Qualifying Project Report

submitted to the Faculty

of the

WORCESTER POLYTECHNIC INSTITUTE

in partial fulfillment of the requirements for the

Degree of Bachelor of Science

by

Kelsey Wall

Brendan Walsh

Date:

Approved:

Professor Christopher Brown, Major Advisor

Abstract:

The leading causes of death among skiers are uncontrollable falls and collisions, which are often caused by a phenomenon called inadvertent release. Using Nam Suh's Axiomatic Design method, this project focused on developing a torque-displacement system, which could determine the work required to release a ski boot from its binding. Measuring work-to-release identifies bindings' susceptibility to inadvertent release through assessing its shock absorptive capabilities. However, due to the tested displacement sensors having an unacceptably high uncertainty, $\pm 0.68\text{mm}$ or greater, a work-to-release device was not created. However, an electronic torque to release dynamometer that could be integrated with several identified displacement methods, was designed, manufactured, and tested. The device measured values within $\pm 3.2\text{ Nm}$ of clockwise applied moments, within $\pm 3.06\text{ Nm}$ of counterclockwise applied moments, and within $\pm 52.2\text{ Nm}$ of moments applied in forward lean. This system could be improved through better definition of the calibration curves used to generate torque values.

Authorship:

All design and testing was an equal collaboration between the group members, while editing was performed by Kelsey Wall. Primary authorship of each chapter of the report is as follows:

Brendan Walsh: Ch. 4 Tolerancing, Ch. 5 Prototype Construction, Ch.7 Design Iteration

Kelsey Wall: Ch.1 Introduction, Ch. 2 Design Process, Ch.3 Physical Integration, Ch.6 Testing of the Design, Ch.9 Conclusion

The Abstract and Ch.8 Discussion sections of the report were created through equal collaboration of the group members.

Acknowledgements:

The team would like to acknowledge

Professor Christopher Brown, for his dedicated advising

Jeffrey Elloian, for his help in configuring and troubleshooting our circuitry

Connor Morette, for instructing us on how to machine

Niravkumar Patel, for his assistance with the NDI Polaris

Richard Howell, for his guidance and input on ski binding testing

Richard Kirby, for providing information on optical mouse use for displacement measurements

Contents

An Advanced Assessment of Ski Bindings.....	i
Abstract:.....	i
Authorship:	i
Acknowledgements:.....	i
Table of Figures.....	v
Table of Tables	vii
1. Introduction	1
1.1 Objective	1
1.2 Rationale	1
1.3 State of the Art.....	3
1.4 Approach.....	7
2. Design Process	9
2.1 Design Constraints	10
2.2 Design Decomposition	11
2.2.1 Zero Level Decomposition	12
2.2.2 Functional Requirement 1	13
2.2.3 Functional Requirement 2	21
3. Physical Integration.....	27
3.1 Design Matrix.....	27
4. Tolerancing.....	28
5. Prototype Construction.....	29
6. Testing of the Final Design and Results	31
6.1 Calibration Testing for Clockwise Twist Release Testing	35
6.1.1 Test setup and methods for clockwise twist release testing.....	35
6.1.2 Calibration curve, results, and analysis for clockwise twist release testing.....	37
6.2 Calibration Testing for Counterclockwise Twist Release Testing.....	41
6.2.1 Test setup and methods for counterclockwise twist release testing	41
6.2.2 Calibration curve, results, and analysis for counterclockwise twist release testing	41
6.3 Calibration Testing for Forward Bending Release Testing.....	45
6.3.1 Test setup and methods for forward bending release testing	46

6.3.2 Calibration curve, results, and analysis for forward bending release testing.....	48
6.4 SBB System Testing for Clockwise and Counterclockwise Release Testing	51
6.4.1 Clockwise testing results and analysis	52
6.4.2 Counter clockwise testing results and analysis.....	55
6.5 Additional Calibration Curve Validation Testing for Forward Bending Testing	58
6.5.1 Testing results and analysis.....	58
7. Design Iteration.....	59
7.1 Optical Mouse	61
7.1.1 Design Decomposition	61
7.1.2 Shortcomings of Optical Mouse.....	62
7.2 NDI Polaris.....	63
2.2.1 Design Decomposition	64
7.2.2 Shortcomings of NDI Polaris	65
7.3 Additional Displacement Sensors	65
7.3.1 Rotary and String Potentiometers	65
7.3.2 Rotary Encoders	66
7.3.3 Leap Motion	67
8. Discussion.....	68
8.1 Satisfaction of the Objective.....	68
8.1 Results and Satisfaction of Constraints.....	68
8.3 Impact of Solution.....	70
8.4 Future Recommendations	71
9. Conclusions	71
Appendix B: Axiomatic Design Concepts	76
Appendix C: Supplements to Our Approach	78
Appendix D: CAD Drawings of System	80
Appendix E: SignalExpress Instructions (NI, 2010).....	86
Appendix F: Clockwise SBB System Torque vs. Time Graph	88
Appendix G: Counter Clockwise SBB System Torque vs. Time Graph.....	89
Appendix H: Optical Mouse Data Analysis.....	90
H.1 Testing Setup and Procedure	91
H.1.1 Labview Program for Tracking Mouse Position.....	91

H.1.2 Physical Testing Setup	92
H.1.3 Data and Analysis	93
H.1.4 Findings.....	96
Appendix I: Polaris Measurement Analysis.....	98
I.1 Test Setup	98
I.2 Data and Analysis	99
Appendix J: Prototype and Consumer Costs.....	101
References	102

Table of Figures

Figure 1: Idealized Torque Displacement Curve for a Binding ($W = Td\theta$) (Brown, 2006).....	2
Figure 2: Testing Axes (ASTM, 2005)	2
Figure 3: General Static Release Moment Tester Configuration (ASTM, 2005)	3
Figure 4: Lipe Check Tester (Lipe et al., 1966)	4
Figure 5: Single Handle Torque Wrench (Vermont Ski, 2010)	5
Figure 6: Double Sided Handle (Epitoux, 1989)	5
Figure 7: Heel Release Caused by Vertical Force at the Heel (Ski Gear, 2012).....	6
Figure 8: Tester Prototype (Merrill, 2013)	6
Figure 9: Torque tester in Bending Configuration (Left) and in Twist Configuration (Right).....	13
Figure 10: DPs for Functional Requirement 1.1.1 and its Constituents (Full system far left, Exploded view middle, Bottom piece second from right, Top Piece far right)	15
Figure 11: DP 1.1.1.2 Cylindrical Torque Applicator	16
Figure 12: DP 1.1.1.3.2 Prosthetic foot interface	17
Figure 13: Complete circuit diagram including DPs 1.1.2.1 to 1.1.2.4.....	18
Figure 14: Full Wheatstone bridge configuration DP 1.1.2.2 (Hoffman, 1986)	18
Figure 15: Proper setup of the dual polarity power supply, DP 1.1.2.1	19
Figure 16: SignalExpress window for tester.....	20
Figure 17: DPs for functional requirement 2.1.1 and its constituents (full system, right; exploded view, left).....	23
Figure 18: DP 2.1.1.2 Cylindrical torque applicator	24
Figure 19: DP 2.1.2.2 full wheatstone bridge configuration (Hoffman, 1986)	26
Figure 20: Complete circuit diagram including DPs 2.1.2.1 to 2.1.2.4.....	26
Figure 21: Design Matrix	27
Figure 22: Completed device components	30
Figure 23: Completed part assembly	30
Figure 24: Running and Recording Testing Information	33
Figure 25: Clockwise calibration pulley applicator system	36
Figure 26: Mean Outputs and Standard Deviations at Specified Torque Values.....	38
Figure 27: Calibration Curve for Torque Applied in the Clockwise Direction	39
Figure 28: Correlation between Applied Torque and Strain.....	40
Figure 29: Counterclockwise torque applicator pulley system.....	41
Figure 30: Mean outputs and standard deviations at specified torque values applied in the counterclockwise direction.....	43
Figure 31: Calibration Curve for Torque Applied in the Counter Clockwise Direction	43
Figure 32: Correlation between strain and torque applied in the counterclockwise direction	45
Figure 33: Forward bending torque applicator pulley system.....	47
Figure 34: Mean outputs and standard deviations at specified forward bending torque values	49
Figure 35: Calibration curve for torque applied in the forward bending direction	49
Figure 36: Correlation between strain and torque applied in forward bending	51

Figure 37: Ski Boot Binding Testing Setup for the Vermont Release Calibrator (left) and the designed device (right)	52
Figure 38: Torque to release over time for clockwise run 1 with our device	53
Figure 39: Torque to release over time for counterclockwise run 1 with our device	56
Figure 40: Volume of Polaris measurement range (NDI, 2014)	64
Figure 41: Displacement measurement with string potentiometers	66
Figure 42: Working range of a LeapMotion (LeapMotion, 2014)	67
Figure 43: "Bow Effect" Inadvertent Release (Brown and Ettlinger, 1985)	74
Figure 44: Failure of Ski to Release	75
Figure 45: Bending Moment Sensed by the Binding vs. the Tibia (Brown and Ettlinger, 1985).....	75
Figure 46: Relationship Between FRs and DPs (Suh, 1990)	76
Figure 47: Failure of Independence Axiom	76
Figure 48: Information Axiom Satisfied by Altering k	77
Figure 49: Objectives Tree Representation of Objectives and Sub-Objectives	78
Figure 50: MAX Configuration.....	86
Figure 51: A compilation of all torque vs time graphs generated during clockwise SBB system testing ...	88
Figure 52: A compilation of all torque vs time graphs produced during counterclockwise SBB system testing	89
Figure 53: Labview program for documenting mouse position.....	92
Figure 54: Physical test setup for mouse position data acquisition	92
Figure 55: Changing the pointer speed, or sensitivity, of an optical mouse	93
Figure 56: Mean and standard deviation of mouse displacement measurements from a 2000 DPI mouse at pointer speed 7.....	96
Figure 57: Ski boot with attached passive marker and passive marker reference marker on testing bench	98

Table of Tables

Table 1: Paired Functional Requirements and Design Parameters	12
Table 2: FR1 Determine Binding Response to tibial axis torsion	13
Table 3: FR 1.1 Measure torsion about z-axis accurately in time	14
Table 4: FR 1.1.1 Transmit torque through system for measurement	14
Table 5: FR 1.1.2 Acquire Strain Measurements.....	18
Table 6: Selection of a resistor value for a specified gain (Texas Instruments, 2005).....	20
Table 7: FR 2 Determine binding response to forward bending loads	21
Table 8: FR 2.1 Measure torque applied about the positive y-axis in time	22
Table 9: Transmit torque through system for measurement	22
Table 10: FR 2.1.2 Acquire strain measurements	25
Table 11: Machining error analysis.....	31
Table 12: FR 1.1.3 Create a strain to torque calibration curve for twist release.....	32
Table 13: FR 2.1.3 Create a strain to torque calibration curve for forward bending release.....	32
Table 14: FR 1.2 and 2.2 Validate torque measurements.....	32
Table 15: FR 1.1.3.1 Create strain to torque calibration curves in clockwise release	36
Table 16: The relationship between the mass applied to each side of the pulley system and the applied torque	37
Table 17: Relative Rang of Output Values from Clockwise Testing	38
Table 18: Percent Difference and Relative Rang of Torque Testing in the Clockwise Direction	39
Table 19: Relative range of output values from counterclockwise testing	42
Table 20: Percent Difference and Relative Rang of Torque Measurements in the Counter Clockwise Direction.....	44
Table 21: Create strain to torque calibration curve in forward bending release	46
Table 22: The relationship between the applied mass and the applied torque.....	47
Table 23: Relative range of output values from forward bending testing	48
Table 24: Percent Difference and Relative Range of Torque in the Forward Bending Direction	50
Table 25: Characterization of torque to release measurements from a Vermont Release Calibrator and the designed device	53
Table 26: Percent difference and relative range of the Vermont Release Calibrator and the designed device.....	54
Table 27: Characterization of torque to release measurements from a Vermont Release Calibrator and the designed device	56
Table 28: Percent difference and relative range of the Vermont Release Calibrator and the designed device.....	57
Table 29: Percent difference and relative range of the forward bending calibration curve at 148.6 Nm of applied torque.....	59
Table 30: Displacement sensor comparison	60
Table 31: Initial decomposition for torque-displacement binding tester.....	61
Table 32: Decomposition for a displacement measurement system utilizing an optical mouse	62

Table 33: Decomposition for a displacement measuring system utilizing the NDI Polaris	64
Table 34: Satisfaction of project constraints	68
Table 35: Pairwise Comparison Chart of Objectives	79
Table 36: Terminal/pin locations	87
Table 37: Location for software tutorials.....	87
Table 38: Mouse position and linear displacement calculations.....	94
Table 39: Displacement measurements obtained by a standard mouse at pointer speed 1	94
Table 40: Displacement measurements obtained by a standard mouse at pointer speed 5.....	95
Table 41: Displacement measurements obtained by a standard mouse at pointer speed 10.....	95
Table 42: Displacement measurement from a 2000 DPI mouse at pointer speed 7.....	96
Table 43: Polaris position tracking of a ski boot	99
Table 44: Average Polaris Error (cm)	100

1. Introduction

1.1 Objective

The objective of this Major Qualifying Project is to design an alpine ski binding testing device that measures the torque, displacement, and work to release ski boots from bindings in response to multiple quasi-static loading configurations in the y and z axis. The test device would be able to identify ski binding devices' susceptibility for inadvertent release [Appendix A].

1.2 Rationale

On average forty-one people die per year in skiing accidents, while another forty-four sustain serious injuries such as paralysis or head trauma (Hawks, 2012). However, in 2012 there was a 32% increase in fatalities and a 17% percent increase in severe injuries. The leading causes of death among skiers are uncontrollable falls and collisions (Lagran, 2012), which are often caused by a phenomenon called inadvertent release (Ettlenger et al., 2005). Inadvertent release is one of the two modes of failure for the ski-binding-boot system (SBB) (Shealy et al., 1999). In this type of failure the binding releases the boot from the ski at an unnecessary or inappropriate time, when the load is not large enough to cause injury (Ettlenger et al., 2005). The other mode of failure deemed a "miss", is when the binding fails to release under an injurious load, often resulting in tibial fractures and other lower leg injuries (Shealy et al., 1999). A thirty year study found that the rates of both inadvertent releases and "misses" have increased in the last 15 years (Ettlenger et al., 2005). However, the rate of inadvertent releases was found to be 2.3 times higher than "misses" in the 17-49 age group, which composes 76.3% of the skiing population. Creating a binding testing device that could measure work to release is important because it could help identify if bindings are prone to inadvertent release.

Inadvertent release can be caused by retention problems, inherent flaws in the heel piece design, skier error, as well as issues with release torque [Appendix A] (Ettlenger et al., 2009). The unavailability of binding testers that can identify issues with more than just the release torque leads to under evaluated bindings going on the slopes and resulting in injuries. Some skiers' ignorance to the mechanisms of inadvertent release also leads them to needlessly elevate their release torques to dangerously high levels (Ettlenger, 2010). They do this to prevent inadvertent release when in fact they only put themselves at risk for severe lower leg injuries. Developing a binding tester that could determine the work to release would allow for ski-binding retention capabilities to be analyzed in a new way. Work to

release indicates a way to measure the anti-shock capabilities of SBB systems because it is a measure of the work a binding can absorb from its environment before release [Figure 1] (Brown, 2006). Work to release is defined as the integral of torque in terms of displacement, or simply the area under the torque displacement curve. The work to release can be increased by increasing the displacement up to the release point. In this manner the binding could prevent inadvertent releases caused by instantaneous large torques.

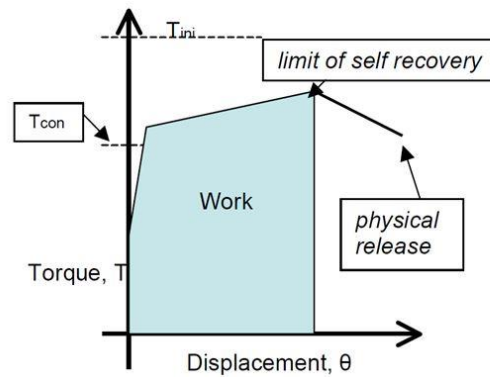


Figure 1: Idealized Torque Displacement Curve for a Binding ($W = \int T d\theta$) (Brown, 2006)

This would be especially beneficial in the case of the bow effect (Brown and Ettlinger, 1985; Young, 1989) where the heel piece senses a higher moment than the tibia due to an instantaneous force experienced by the shovel of the ski couple with forward lean of the skier. In an ideal situation displacement would occur above the torque limit necessary for control (T_{con}), so that steering forces applied by the skier's legs under normal conditions would not be dampened, but below the injury threshold (T_{inj}). By creating a device that measures work to release the ski boot binding system could be analyzed in a way that would identify issues with retention as well as release. This could lead to improvements in binding designs that would mitigate the danger of inadvertent releases. Currently, there are limited means to test for work to release; testing options are available, but they are prohibitively expensive and used to test bindings before they are put onto the market (ISO, 2009). There are currently no testing devices available for ski shop or average consumer usage. The objective of this project is to

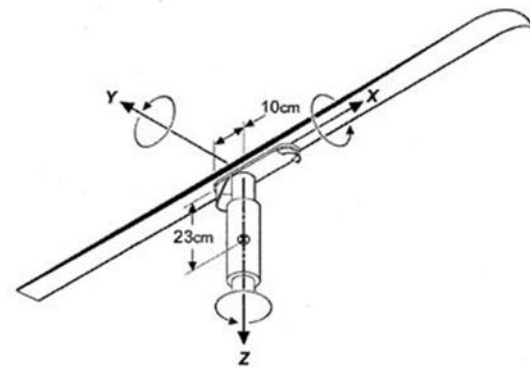


Figure 2: Testing Axes (ASTM, 2005)

address this gap in technology by designing a binding test device that finds torque to release as well as release displacement. We will find torque to release in the y and z axes [Figure 2]. The torques experienced around the y axis correspond to forward and backward lean of the skier and are the mechanism for vertical boot release at the heel. The torques experienced around the z axis correspond to tibia torsion and are responsible for the clockwise and counterclockwise release of the boot at the toe. We will also be taking angular displacement measurements in the xy and xz planes. Angular displacement in the xy plane corresponds to the displacement of the boot in the binding during applied

twist torques. The angular displacement of the boot in the xz plane corresponds to the displacement of the boot in the binding during forward or backward lean and subsequent heel release. Valgus torques along the x axis, commonly attributed to knee injuries (Dodge et al, 2010), are rarely addressed in SBB systems and are not addressed in current commercial binding testers. Due to this we will not be measuring torque to release, displacement, or work to release in regards to the x axis.

1.3 State of the Art

Alpine skiing is an extremely popular sport, with over 8 million participants in the United States alone in the year 2013 (SIA, 2013). However, due to the high velocities experienced, it can be a dangerous activity. Major causes of serious ski injuries are inadvertent release, or pre-release, of the boot from the binding, as well as failure of the binding to release under injurious loads [Appendix A]. These forms of ski boot binding (SBB) failure can be contributed to problems with either the release or retention characteristics of a binding (Shealy et al., 1999). Release is defined as a SBB's ability to release the boot from the binding at a pre-set release torque, while retention is the ability of the binding to maintain the boot in the binding under non-injurious loading situations. There can be an appropriate release response combined with an inappropriate retention response when a binding releases under a large instantaneous load that would not have resulted in a lower leg injury. However, most of the binding testers available to consumers and ski shops only have the ability to measure release, or a binding's ability to release at a desired pre-set torque threshold, not retention. A work to release binding tester would be able to measure the shock absorptive capabilities of a binding, and thus its retention capabilities, but these tests are unavailable to the general public and are only used to initially verify a binding. Our proposed design would make it easier to identify the retention capabilities of individual bindings and provide a new metric for safety in ski bindings that could lead to newer, safer, and more marketable ski binding designs.

There are many different types of test mechanisms used to test ski binding release. ASTM F504-05 outlines the general method of testing static release moments [Figure 3], which is what is tested with modern ski binding testers found in ski shops (ASTM, 2005). The basic test for static release is to apply forces to a system adapted to fit into a ski boot firmly attached to a ski in order to apply torsional and bending moments on the ski until it releases;

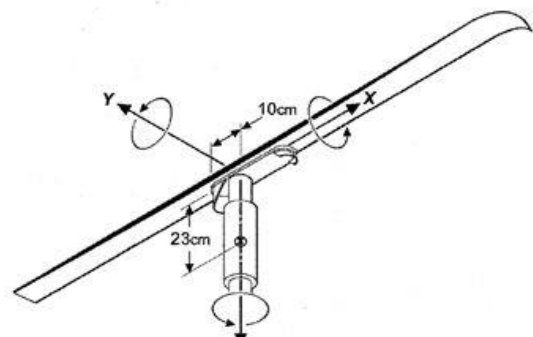


Figure 3: General Static Release Moment Tester Configuration (ASTM, 2005)

documenting the torques required for release. However, the standards also detail how to test for quasi-static release moments, which more accurately identify retention. The quasi-static tests detail using a cable and pulley system to apply pre-loads on different standardized locations on the ski. When the preload is used it will produce a release moment that is a certain percentage of the moment in test 2.1, which is used as a base. This serves as an indicator as to how release torques will vary based on different loading conditions, such as forward or backward lean in a skier. Previously mentioned tests 2.3 and 2.5 are both examples of quasi-static testing in ASTM F504. Though these tests can be reliable in predicting many different loading situations they are limited in the fact that they are only applied in specific regions and are not subjected to dynamic testing conditions. This means that they are unable to identify some of the possible mechanisms of release such as inadvertent release. The quasi-static tests are more comprehensive but are not performed in ski test shops, as they are difficult to set up, require multiple configurations for different tests, and are time intensive.

An early method of ski binding tester that pre-dated the F504 standards, and standardized release settings, was the Lipe Check tester [Figure 4]. The Lipe Check was invented in 1966 and pre-dates the releasable heel mechanism in ski bindings (Lipe et al., 1966). As such the tester purely measured toe piece release. It did this in a unique way, by measuring the force to release the boot from the binding. When the lever arm actuator is pulled forward, springs push a plunger against the side of the boot. The plunger pushes against the side of the boot until the boot releases, whereupon the force is measured through an “O” ring’s resultant position on one of the graduation

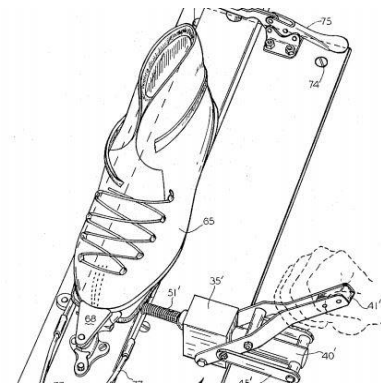


Figure 4: Lipe Check Tester (Lipe et al., 1966)

marks that lie on the reduced diameter portion of the plunger. The number of the graduation mark that the “O” ring lies upon on the bindings release is then compared with the preferred number given by the designer based on weight and skier ability. This method introduced the idea of binding release testing, but could only measure force applied. Release torque could be calculated using force times displacement but were less accurate.

The Vermont Release Calibrator, originally invented in 1974, is an early torque to release measuring device still commonly used in the United States (Ettliger, 1974). The Vermont Calibrator is a simple torque wrench adapted to measure both twist release at the toe piece and bending release at the heel piece and is currently sold at \$3,975 to \$4,975 (Vermont Ski, 2010). There are three different parts to the device, a foot, a leg, and an arm. The foot is inserted into the boot, the leg is attached to the foot for forward/backward bending tests, and the arm is a torque wrench that is attached to the foot for twist tests and the leg for bending tests. To perform a twist release the foot is put in the boot and attached to the arm, the arm is held with a hand on each end and rotated clockwise or counter clockwise until release. However, true couples are desired in twist release tests, which is impossible when the lever arm only has one handle [Figure 5]. The idea is to get rotation without translation, which would be better accomplished with two equally sized handles. To perform a bending test the foot is inserted into the boot, under which a strap is placed, then the leg is attached to the foot and the arm attached to the leg. The arm is then grabbed and pulled either forward until release. All measurements from this device are given in Nm and can be used directly with ASTM F 939-05a standards.



Figure 5: Single Handle Torque Wrench (Vermont Ski, 2010)

A similar device to the Vermont Release Calibrator was the Epitoux binding tester, which employed a similar lever mechanism (Epitoux, 1989). Though the Epitoux is no longer in use it had several design improvements over the Vermont tester. The foot mechanism that slid into the boot was equipped with wheels that allowed for easier placement within the boot and the handle used for the twist test used a large two-sided handle to ensure a true couple during testing [Figure 6]. This device also included some electrical

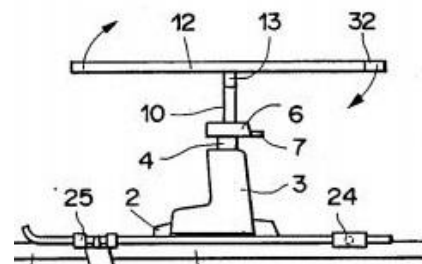


Figure 6: Double Sided Handle (Epitoux, 1989)

components that would be useful for a work displacement tester. Instead of utilizing a torque wrench the Epitoux uses two strain gauges to gain the release torque in both the twist and bending tests. When measuring the work to release torque to release and displacement have to be simultaneously measured to perform a proper integration meaning that the data needs to be gained electronically so that it can be input into a computer. The way the strain gauge works is that when torque, or rather the turning force, is applied to the system, stress is experienced by the metal bar labeled “10” in Figure 5, this stress

causes a deformation, or strain, to the bar that is read by the gauge. The torque can be measured as it is proportional to the strain experienced by the system.

The Speedtronic Pro tester is one of the modern binding testers produced by Wintersteiger, that incorporates a user friendly and predominantly hands free design (Wintersteiger, 2011). Though these machines are uncommon in the United States they are popular in countries such as Austria and Switzerland (Ski Gear, 2012). The testing system is completely electronic once the ski, with the attached boot, is correctly loaded onto the instrument, which eliminates most user error. The tester



Figure 7: Heel Release Caused by Vertical Force at the Heel (Ski Gear, 2012)

simply enters the user weight, height, age, and skier type as well as boot sole length and binding type, and then the machine produces the correct release settings based on the standards. The machine then tests the binding by directly applying forces to either side of the front of the boot in the twist test, and directly under the heel of the boot [Figure 7] in the case of the bending test. The problem with this testing is that applying a force directly under the heel does not accurately reproduce the bending moments generated by skier lean. This makes the heel release tests much less reliable. Another problem with this testing device is that it is prohibitively large and expensive for most ski shops.

Despite the amount of ski binding testers and tests that have been created and are available on the market today, none measure work to release. Recent work at Worcester Polytechnic Institute was done on a torque-displacement binding tester (Merrill, 2013). The tester utilized a strain gauge, fitted to a Vermont Release Calibrator, and computer mice to input data into a Labview program that would simultaneously measure release torque and displacement [Figure 8]. In this project Bradley Merrill was able to prove that computer mice have the required accuracy to measure ski-boot displacement, and was able to identify Labview as a program that could process torque and displacement data. Unfortunately, there was difficulty in indexing the mouse



Figure 8: Tester Prototype (Merrill, 2013)

displacement data in the software; so while data from the mouse was able to be read, it could not be simultaneously processed with data from a strain gauge. There was also no presented data on torque to release for the binding, though a Labview model was developed. Though there is no completed model of

a work to release binding tester, Merrill's work identified key requirements and possible solutions for a successful design.

Current binding testers and standards are focused on the torque necessary for lateral toe release and vertical release at the heel (ASTM, 2005; Vermont Ski, 2010; Wintersteiger, 2011). However, there are retention issues, key elements in inadvertent releases, which have failed to be addressed in modern ski binding testing technology. These issues could be addressed by a tester that not only looks at release torques, but at the work it takes for bindings to release. If work to release could be identified, then binding safety could be measured in a more comprehensive manner and new and more robust binding systems could be produced. This is because an increase in work to release would mean an increase in the amount of energy bindings could absorb before release (Brown, 2006). This would decrease or eliminate the risk of pre-release through large instantaneous torques, such as those seen in the bow effect (Brown and Ettlinger, 1985; Young, 1989).

1.4 Approach

Client Statement and Objectives:

Our initial client statement, Appendix C, was first refined to concentrate the focus of the project, the final client statement is as follows.

To design an inexpensive torque and work to release binding tester that would be able to demonstrate response to multiple quasi-static loading conditions, whose design could be downloadable off the web and be safely usable by ski shops and ski teams.

Objectives for our project based on our client statement and ASTM and ISO standards can be viewed in Appendix C.

Strategy:

The following strategy was used to develop our project. Using Suh's Axiomatic design method [Appendix B] and Acclaro software a design for a work to release binding tester that met our functional requirements was created. Through using readily available resources and inexpensive components, or components which have inexpensive counter-parts, we were able to create an inexpensive torque tester that has the capability of outputting continuous torque data to a computerized system. If a further method of measuring displacement was developed, that could be integrated into this system, the work to release could be obtained by integrating the area under the torque/displacement curve. To the end of displacement measurements, we have explored and described several alternatives, the Polaris Optical

Tracker, rotary encoders and string potentiometers, and Leap Motion optical controller. Additionally, we created an iteration of our design that included a wireless optical mouse for displacement measurements; however we found this design to be ineffectual for our purposes, and disproved the optical mouse as a means of measuring displacement to release in ski-bindings.

This device was designed to interact with the prosthetic foot component of the Vermont Release Calibrator, but have independent components that measure torque to release in twist and forward bending. The device was also designed to be useable with any type of boot or ski type available on the market. The torque tester for twist release was designed to withstand loads of up to 462 Nm, safety factor of 3, and the torque tester for forward lean release was designed to withstand loads of up to 1200Nm, safety factor of 1.75. However, the methods of displacement measurement that we explored in-depth, the optical mouse and Polaris Tracker, were not capable of measuring within 0.2 mm as per the ISO standards for alpine ski bindings test methods (ISO, 2009). Our design prototype was inexpensive, due to the availability of resources at Worcester Polytechnic Institute (WPI); however the cost for customer production would be slightly higher due to outside machining costs and the need to purchase a DAQ and Signal Express Software.

Each component of the torque tester design was modeled in SolidWorks. Manual calculations and finite element analysis, using ANSYS Workbench, was performed to verify that the parts would not permanently deform under the required loads, but provide enough plastic deformation for strain gauge readings. After the torque tester parts were modeled, tool paths for the manufacturing process were generated in Esprit. The components were machined using the HAAS CNC machine center in the Washburn Shops at WPI. The raw data obtained through our torque testing instrument was collected by a National Instruments (NI) DAQ and was synthesized and exported to Excel using NI Labview SignalExpress Software. Wireless optical gaming mice were tested via Labview to determine if they were accurate enough for displacement measurements, the feasibility of their implementation into our design was also discussed as an option for ski boot displacement with Mr. Richard Kirby, an expert in displacement measurements. Upon disproving the optical mice, a Polaris Tracker system was also tested and found to be lacking in the required precision.

Specifically for torque measurements, a full Wheatstone bridge, of different configurations, was used on both the twist and bending release testing components, and an operational amplifier was used to enhance the differential voltage for use with our DAQ model. The amplified electrical analogue strain signals, which were calibrated to known torque levels, were acquired through the use of a National

Instruments DAQ and NI Measurement and Automation Software in combination with Labview SignalExpress software. The completed torque testers measured voltage change under an applied load and strain. To calibrate these measurements the strain output of the testers at five known applied torques in twist, four in bending, and at zero loading. The correct torque values were determined through comparing anthropometric data with the ASTM standards for the selection of release torque values (ASTM, 2005). The determined torques were applied via pulley systems designed to apply the correct amount of torque in clockwise and counterclockwise twist release and forward lean release. The results of this testing were plotted in Excel and a calibration curve was produced. The tester was then used to release a ski boot from the SBB system in twist. The amount of torque needed to release the ski from the binding was first determined through using the Vermont Release Calibrator. Then our tester was used and output values were produced, which were analyzed with our calibration curve to predict the applied torque. The variance between the torque to release documented by our tester compared to the Vermont Release Calibrator was then documented and compared.

Our displacement measurements were made by applying removable fiducials, also known as passive markers, onto the tested ski boot in order for the Polaris Spectra to optically track the three-dimensional motion of the boot, while other passive markers were used to provide a reference frame for the displacement. The position of the boot in relation to the reference marker was determined by the Polaris' optical measurement system and Application Program Interface (API), which allowed for tracking of specific passive markers and output data to Excel. During Polaris testing, the position of the tracking markers was measured and recorded via calipers, and then compared to the positions documented by the Polaris to validate the precision of the measurements. The Polaris measurements were not precise enough to be viable for displacement measurements in our system, and also did not provide a time parameter, which would make it difficult to interface with our torque measurements.

2. Design Process

In this project we utilized Nam Suh's axiomatic design theory [Appendix B], using Acclaro software for our decompositions and matrix production. The functional requirements and their corresponding design parameters were developed in a hierarchical fashion beginning with the main objective as Functional Requirement 0, which acts as a parent to the subsequent requirements also known as children. This process organizes and reduces the number of functional requirements of the system such that any set of "children" are mutually exclusive from one another and collectively exhaustive with respects to their

corresponding “parent”. This creates a more robust design by helping the designer eliminate redundancies, coupling, and complexity from within a design (Suh, 1990). Conversely, the iterative algorithmic approach requires time consuming trial and error and relies on experience, as opposed to rules and axioms, for evaluation.

2.1 Design Constraints

Constraints:

The constraints of our project were based on industry standards for binding testers, WPI budget restrictions, and consideration of our target audiences’ maximum budget, and were considered before the design process was begun to ensure success in satisfying the objectives. Elements of the ASTM F1061 performance requirements for ski binding test devices, section 6, were considered in creating the constraints for our project and those we sought to follow are listed below (ASTM, 2008). The referenced equations are discussed in detail in the testing section and are found in section 9 of ASTM F1062 (ASTM, 2013).

ASTM Requirements:

- Torque testing must be no greater than $\pm 5\%$ of the release torque determined through testing with the standard apparatus of ASTM F504, using the equation from ASTM F1062, in the Z-axis.
- Torque testing must be no greater than $\pm 5\%$ of the release torque determined through testing with the standard apparatus of ASTM F504, using the equation from ASTM F1062, in the Y-axis.

However, as we were unable to test with an ASTM F504 standard testing apparatus, detailed in the state of the art section, we were unable to measure for these values. We instead used the provided equations and constraints to develop the constraints for our testing device.

Constraints for Calibration Testing Based on ASTM Standards:

- Torque testing must be no greater than $\pm 5\%$ of the known applied torque during calibration testing, using the equation from ASTM F1062, in the Z-axis.
- Torque testing must be no greater than $\pm 5\%$ of the known applied torque during calibration testing, using the equation from ASTM F1062, in the Y-axis.

Constraints for Testing with a Ski Boot Binding System Based on ASTM Standards:

- Torque testing must be no greater than $\pm 5\%$ of the release torque determined through testing with a Vermont Release Calibrator, using the equation from ASTM F1062, in the Z-axis.
- Torque testing must be no greater than $\pm 5\%$ of the release torque determined through testing with a Vermont Release Calibrator, using the equation from ASTM F1062, in the Y-axis.

We also assessed the relative range of values produced by the tester, in both calibration and SBB system testing for all testing configurations, using a slight alteration to the equation used to calculate the

difference between results produced by a tester to the expected results from a calibration curve. However, these results served as a basic assessment and have no associated constraints.

Additional Constraints:

The additional constraints of our project were based on industry standard for ski boot release, WPI budget restrictions, and consideration of our target audiences' maximum budget and are as follows:

- The device must be compatible with existing ski boot binding setups
- Displacement testing uncertainty must be within 0.2 mm (ASTM, 2009; ISO, 2009; ASTM E2655, 2008)
- Customer cost must be under \$350
- Design prototype must be under \$500

2.2 Design Decomposition

The design decomposition highlights each functional requirement developed in the design process and explains the reasoning behind the selection of a design parameter to satisfy it. Detailed drawings of every torque tester component can be seen in Appendix D. As a note, while most of the dimensions in the following summary of the designed components are described in English units as well as the drawings of the parts, as the CAM software at WPI uses the English system, the parts that interface with the Vermont Release Calibrator prosthetic foot and the lever arm modeled after the Epitoux tester are referred to in metric units. Information on the Vermont Release Calibrator and Epitoux tester can be viewed in the State of the Art section. Table 1 shows the first three levels of the functional requirements and their corresponding design parameters. Some of the FRs in our first three levels of decomposition involved the calibration and testing of our device. These will be discussed in greater detail in Ch.6, Testing of the Design. As the displacement measurement techniques we investigated were not suitable they are not addressed in our final design decomposition, but decompositions of the different displacement techniques can be found in Chapter 7, Iterations. As our tested methods for displacement measurement did not have the required accuracy, we were unable to create a work to release tester. Our decomposition and devise are for an inexpensive torque tester that has the capability of outputting continuous torque data to a computerized system, which could be integrated with a future displacement measuring device for work to release. The various testing axes referenced in the decomposition can be seen in figure 3.

To satisfy the first axiom of axiomatic design, independence, each level of the design was collectively exhaustive and mutually exclusive. At level one of the design we divided our design into two separate components, the first evaluated the response of the binding in twist release, the second evaluated the

binding in forward bending release. This is collectively exhaustive as it evaluates both standard methods for binding release and mutually exclusive because it evaluates two different loading configurations. The second level of the design serves as a mean for measuring applied torque and validating these measurements. This is collectively exhaustive as encompasses both the process of obtaining measurement values and verifying their fulfilment of the constraints. The second level is mutually exclusive because measuring the torque values requires a dynamometer system, while validating these measurements requires pre-existing measurement devices and processing through Excel functions. The third level of the design encompasses the requirements for the dynamometer and validation testing system. All aspects of this level will be defined in detail in the following sections, but are mutually exclusive as they are used to define separate specific requirements of the measurement or validation process. The sum of the third level of the design fully defines the second level of the design, indicating that the third level is collectively exhaustive.

Table 1: Paired Functional Requirements and Design Parameters

0	FR	Determine torque to release in multiple axes over time allowing for displacement	DP	Electronic torque tester
1	FR	Determine binding response to tibial axis torsion	DP	Twist release tester
1.1	FR	Measure torsion about z-axis accurately in time	DP	Twist Dynamometer System
1.2	FR	Validate torque measurements	DP	Vermont Release Calibrator and Excel testing system
2	FR	Determine binding response to forward bending loads	DP	Forward bending release tester
2.1	FR	Measure torque applied about the positive y-axis accurately in time	DP	Bending Dynamometer System
2.2	FR	Validate torque measurements	DP	Known bending torque pulley system and Excel

2.2.1 Zero Level Decomposition

The fundamental requirement of this design is that it should evaluate a binding’s safety by determining if it responds appropriately to different loading situations (Shealy et al, 1999). In order to do this the tester must identify if the binding is releasing at the desired torque value to which the binding is set, by accurately identifying the amount of torque applied to the SBB system in twist and forward lean release. However, torque to release alone may be insufficient to identify injurious situations from non-injurious situations, as is the case in the “bow effect” [Appendix A] (Brown and Ettlinger, 1985; Young, 1989). This is why the zero level DP is an electronic torque tester that would allow for continuous torque measurements over time and later integration with a displacement tester, so that a work to release profile could be created. A distant view of the final design in the twist configuration undergoing calibration testing, as well as a close up view of the device in the bending configuration can be seen in Figure 9.



Figure 9: Torque tester in Bending Configuration (Left) and in Twist Configuration (Right)

2.2.2 Functional Requirement 1

The first level of decomposition [Table 2] separates the different mechanisms of binding release; satisfying the independence axiom (Suh, 1990). Bindings are subjected to torques along different axes, which have different limits before causing injury. FR 1 is to determine the response to tibial axis torsion applied around the z-axis (Figure 10), this functional requirement was satisfied by our twist release tester. Functional requirement 1 was broken into two sub-FRs. The first, FR 1.1, was to measure torsion about the z-axis accurately in time. This FR was satisfied by DP 1.1, a dynamometer system. The second sub-FR, FR 1.2, was to validate the torque measurements, which was accomplished through DP 1.2, a testing system that involves comparing generated torque values for our tester with those produced via a Vermont Release Calibrator in Excel.

Testing was included in multiple levels of our design of the device. This was because testing was necessary to establish the relationship between our collected data and known torques to be able to determine applied torques in a SBB system and because initial validation of the system was required to demonstrate the devices' efficacy. In this section only FR 1.1 will be explored, as FR 1.2, validate torque measurements, will be explained in Chapter 6, testing of the final design.

Table 2: FR1 Determine Binding Response to tibial axis torsion

1	FR	Determine binding response to tibial axis torsion	DP	Twist release tester	
+	1.1	FR	Measure torsion about z-axis accurately in time	DP	Twist Dynamometer System
+	1.2	FR	Validate torque measurements	DP	Vermont Release Calibrator and Excel testing system

FR 1.1

Functional requirement 1.1 [Table 3] was broken into four lower level functional requirements. The first was to create a physical device that could transmit an applied load through the tester to the SBB system,

with a portion of this device being able to elastically deform to allow for strain gauge readings. The second was to create a system which could collect strain information based on the elastic deformation of the body of the tester. The third was to create a system to calibrate strain to torsion by creating a calibration curve in both the clockwise and counterclockwise directions, which would be accomplished through the design of a pulley system for torques applied in the clockwise and counterclockwise directions. The fourth was to measure torque to release in the SBB system using the created calibration curve in Excel. The third and fourth sub-functions are described in chapter 6, Testing.

Table 3: FR 1.1 Measure torsion about z-axis accurately in time

1.1	FR	Measure torsion about z-axis accurately in time	DP	Twist Dynamometer System
1.1.1	FR	Transmit Torque through system for measurement	DP	Lever arm and interfacing twist tube applicator
1.1.2	FR	Acquire strain measurements	DP	Twist Full Wheatstone Bridge Configuration Strain Gauges and NI MAX Software and Labview Signal Express
1.1.3	FR	Create strain to torque calibration curves in clockwise and counterclockwise release	DP	Known twist torque pulley systems and Excel Software
1.1.4	FR	Measure torque to release in SBB system	DP	Excel functions

Functional Requirement 1.1.1

The decomposition of functional requirement 1.1.1 [Table 4] shows the development of the physical components of our torque tester. The functional requirements of the physical tester were broken down into three lower level requirements. The first, FR 1.1.1.1, describes how the tester must include a means to apply torque to the testing applicator from which the measurements will be taken. The second, FR 1.1.1.2, indicates a need for a surface from which to measure the applied torque. This surface would have to elastically deform in the range of applied loads to allow for torsion measurements to be obtained, but should not plastically deform. The third, FR 1.1.1.3, describes how the tester would need to interface with the SBB.

Table 4: FR 1.1.1 Transmit torque through system for measurement

1.1.1	FR	Transmit Torque through system for measurement	DP	Lever arm and interfacing twist tube applicator
1.1.1.1	FR	Apply torque to applicator	DP	Lever arm and interfacing top piece system
1.1.1.1.1	FR	Transmit load to applicator system	DP	1 Meter lever arm
1.1.1.1.2	FR	Interface applicator and lever arm	DP	Top piece releasable pin system
1.1.1.2	FR	Provide surface for applied torque measurement	DP	Cylindrical twist torque applicator
1.1.1.3	FR	Transmit applied load to ski boot	DP	Prosthetic foot interface
1.1.1.3.1	FR	Interface applicator and prosthetic foot	DP	Bottom piece releaseable pin system
1.1.1.3.2	FR	Transmit load to ski boot	DP	Prosthetic foot

In order to apply a load to the applicator we used DP 1.1.1.1.1, a $\frac{1}{2}$ meter tall lever arm with a 1 meter long handle (Figure 10). The lever arm was modeled after the Epitax handle, which we used for testing. This design was used because the dual handles allow for a pure couple while testing on the SBB, and the

1 meter length allows for mechanical advantage while applying a load to the system, facilitating testing. The testing lever is made of two hollow stainless steel bars, each with a thickness of 2.5mm to make it resistant to deformation, but light. The hollow cores of the bars are 15mmx25mm, which allows for the lever arm to interface with the other components. The two bars are welded together to complete the handle.

To interface the lever with the cylindrical torque applicator, we designed a top piece system with a releasable pin DP 1.1.1.1.2 (Figure 10). The top piece was machined out of 2" diameter 6061 Aluminum stock, which is a low cost alternative. The top piece included a 50mm extruded feature that was 14.97x24.97mm to form an RC1, close sliding, fit with the application lever. The cylindrical portion of the top piece was 2" in diameter and 1" long, with a $\frac{3}{4}$ " deep and 1.52" diameter hole that allows for an RC1 fit with the cylindrical torque applicator. The top piece is attached to the torque applicator by a pin that was purchased at McMaster Carr. The pin was 0.25" in diameter and had a 2" working length, length between the depressible ball stopper and the chain attachment. To allow for a pin of this diameter 0.257" holes were drilled into the side of the top piece and the torque applicator 0.387" from their respective edges.

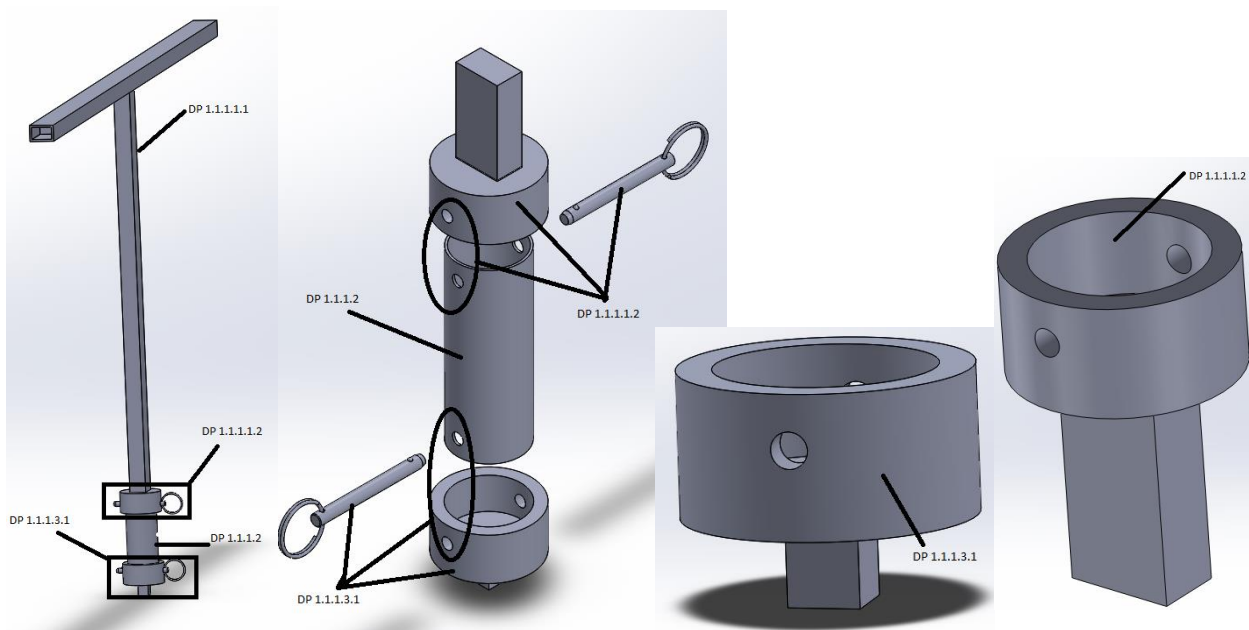


Figure 10: DPs for Functional Requirement 1.1.1 and its Constituents (Full system far left, Exploded view middle, Bottom piece second from right, Top Piece far right)

A cylindrical torque applicator DP 1.1.1.2, is used to satisfy the functional requirement of a part that provides a surface for strain measurements that can be calibrated to determine torque [Figure 11]. The

cylindrical applicator interfaces with the top piece is 4" in length, with 0.257" holes drilled at either end, as already stated, to interface with the top and bottom pieces. The tube has an outer diameter of 1.5" with a thickness of 0.049". The dimensions of the cylindrical applicator were carefully chosen to be able to elastically deform in the expected range of applied torques, while not plastically deforming, with a safety factor of 3. To do this we first found the polar moment of inertia, J , for each possible tube geometry, with r_o and r_i noting the outer and inner radii of the annular tube respectively, using the following equation (Ozkaya et al., 2012).

$$J = \frac{1}{2}\pi(r_o^4 - r_i^4)$$

We then determined the maximum elastic moment, M , each tube could withstand. To do this we first found the shear strength, τ_y , of 6061 Aluminum, 207 MPa (ASM, 2013). We then used the polar moment of inertia, shear strength, and the distance from the neutral axis, the total radius R , to determine the maximum elastic moment (Ozkaya et al., 2012).

$$M = \frac{\tau_y J}{R}$$

The maximum amount of torque needed to release a binding in twist is 142 Nm, as per ASTM F 939-05a standards for the selection of release torque values, so with a safety factor of 3, our tube was to withstand 426 Nm of torque. The tube we selected was calculated to have a maximum elastic moment of 532 Nm.



Figure 11: DP 1.1.1.2 Cylindrical Torque Applicator

In order to satisfy the functional requirement of transmitting the applied torque to the SBB system, a prosthetic foot interface was created, consisting of a bottom piece releasable pin system that attaches

the cylindrical application tube to a prosthetic foot, DP 1.1.1.3.1, and a Vermont Release Calibrator prosthetic foot, DP 1.1.1.3.2, that interfaces the bottom piece with the SBB system.

The bottom piece releasable pin system can be seen in Figure 10. This part has the same dimensions as the top piece releasable pin system, except that its extruded base is 15mm long and 12.649mm x 12.648mm, in order to interface with the Vermont Release Calibrator Prosthetic foot in a close running fit.

The Vermont Release Calibrator prosthetic foot, Figure 12, has a slotted insertion point that is 12.7mm x 12.7mm and 15mm deep, which is designed to interface with the Vermont Release Calibrator bending and twist testers, but also connects to our bottom piece. The body of the tester is able to slip into all adult ski boots and interface with the SBB system.

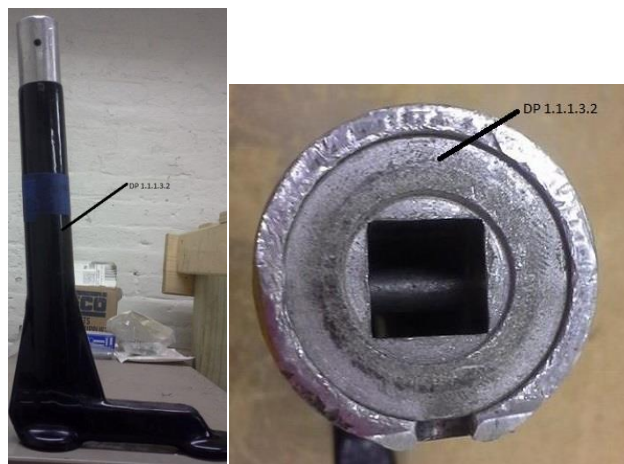


Figure 12: DP 1.1.1.3.2 Prosthetic foot interface

Functional Requirement 1.1.2

The decomposition of functional requirement 1.1 .2, acquire strain measurements, [Table 5] shows the development of the circuit components required for our tester. The functional requirements of the circuit components were broken down into six functional requirements. The first, FR 1.1.2.1, describes the requirement for a power source. The second, FR 1.1.2.2, describes how strain measurements need to be collected from the cylindrical applicator. The third, FR 1.1.2.3, describes how these signals need to be amplified to be read. The fourth, FR 1.1.2.4, describes how the output analogue signals need to be converted to digital signals for processing by the computer. The fifth, FR 1.1.2.5, describes the need to read the initial data and export it to software which can process it further. Finally, the sixth functional

requirement, FR 1.1.2.6, describes the need to synthesize the output data and export it to analysis software, where it can be calibrated.

Table 5: FR 1.1.2 Acquire Strain Measurements

FR	FR Description	DP	DP Description
1.1.2	Acquire strain measurements	DP	Full Wheatstone Bridge Configuration Strain Gauges and NI MAX Software and Labview Signal Express
1.1.2.1	Provide power supply to circuit	DP	Two 9V batteries in a dual polarity power supply configuration
1.1.2.2	Collect strain signals from cylindrical applicator	DP	Four strain gauges in a Full Wheatstone bridge configuration
1.1.2.3	Amplify signals to readable level	DP	Instrumentation Amplifier
1.1.2.4	Convert analogue to digital signals readable by the computer	DP	DAQ module
1.1.2.5	Read and export data signals	DP	NI Measurement and Automation
1.1.2.6	Synthesize data and export to analysis software	DP	Labview Signal Express

To acquire strain measurements we utilized a full Wheatstone bridge configuration, DP 1.1.2.2, to obtain the initial analogue output signals. We connected the strain gauges to the cylindrical torque applicator using the procedure outlined by the Vishay Precision group (Vishay, 2011). We connected the strain gauges onto the applicator at forty-five degree angles, respective of the vertical centerline of the tubes, in the manner shown in Figure 14. The strain gauges we purchased were $120\Omega \pm 5\%$, however, we tested each gauge and only applied those that were within 1% to mitigate bridge imbalance. The strain gauges were then connected into the full Wheatstone bridge configuration in a circuit, the full configuration of which can be seen in Figure 13. Gauge 1 from Figure 14 corresponds to R1 in Figure 13, and the rest of the strain gauges can be corresponded to R2, R3, and R4 in the same manner.

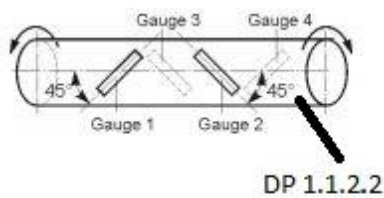


Figure 14: Full Wheatstone bridge configuration DP 1.1.2.2 (Hoffman, 1986)

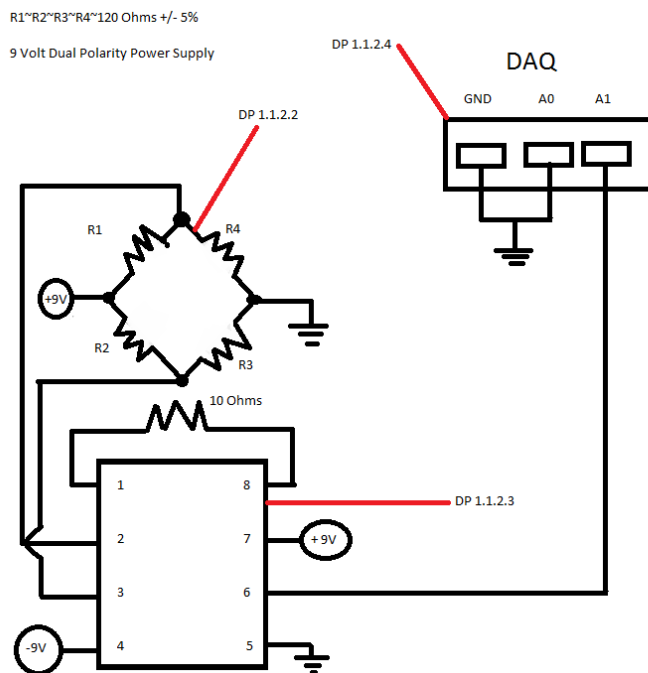


Figure 13: Complete circuit diagram including DPs 1.1.2.1 to 1.1.2.4

As previously stated Figure 13 reflects the circuit diagram for our dynamometer setup. The circuit was powered by a 9V battery dual polarity power supply, DP 1.1.2.1. The proper connection of the power supply to a protoboard/circuit can be seen in Figure 15. This power supply was chosen as our DAQ had an analogue voltage range of $\pm 10V$, as the instrumentation amplifier required a dual polarity power supply, and because it doubles the battery life of the testing circuit when two 9V batteries are used.

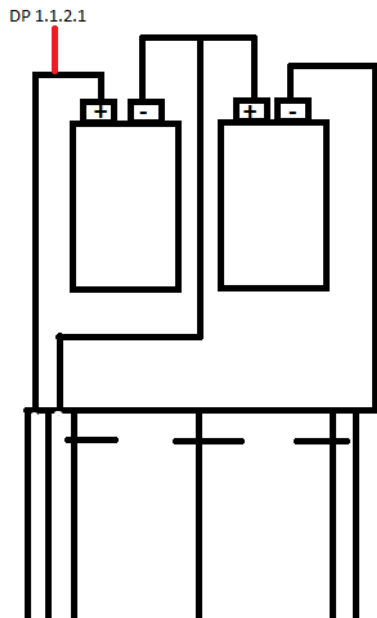


Figure 15: Proper setup of the dual polarity power supply, DP 1.1.2.1

These signals were made readable to the computer through processing, which was accomplished through an NI USB-6008 DAQ, DP 1.1.2.4. However, as these voltage changes were too small to be read by the DAQ, they were first amplified with an INA217AIP instrumentation amplifier, DP 1.1.2.3. In our circuit design we used a 10Ω resistor between pin 1 and 8 of the instrumentation amplifier to produce a gain of 1000, meaning that the voltage changes across the Wheatstone bridge would be multiplied by 1000 before being input to the DAQ. Figure 16 shows the chart through which a resistor value for the desired gain can be determined. On the actual amplifier, pin 1 can be identified by a small circular depression marking the pins location.

Table 6: Selection of a resistor value for a specified gain (Texas Instruments, 2005)

GAIN		R _o (Ω)
(V/V)	(dB)	
1	0	NC ⁽¹⁾
2	6	10000
5	14	2500
10	20	1111
20	26	526
50	34	204
100	40	101
200	46	50
500	54	20
1000	60	10
2000	66	5

After the analogue signal was converted into a digital signal by the DAQ, these readings were read and exported to SignalExpress using NI Measurement and Automation (MAX) software, DP 1.1.2.5. Labview SignalExpress was used to synthesize the data, tracking the input voltage changes over time and converting voltage measurements to strain measurements, and to export this data into Excel where it could be analyzed, DP 1.1.2.6. Instructions on how to configure MAX and SignalExpress and use them for data collection can be seen in Appendix E. In order for SignalExpress to be able to convert voltage measurements to strain measurements several parameters must be filled into the configuration window, as seen in Figure 16. The first parameter is the signal input range, what you expect your strain values to be, however these will automatically update with testing. The gage factor and resistance of your strain gauges must be entered, as well as the measured initial voltage across your Wheatstone bridge. Finally, the excitation voltage of your circuit and the Wheatstone bridge configuration must also be entered. In this window the rate of sampling and the amount of samples can also be determined.

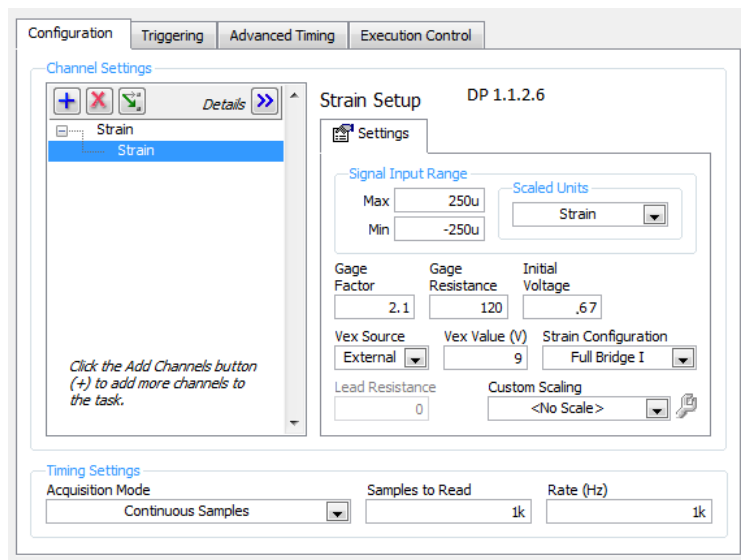


Figure 16: SignalExpress window for tester

2.2.3 Functional Requirement 2

The first level of decomposition [Table 7] separates the different mechanisms of binding release; satisfying the independence axiom (Suh, 1990). Bindings are subjected to torques along different axes, which have different limits before causing injury. FR 2 is to determine the response to forward bending loads (Figure 10), this functional requirement was satisfied by our forward bending tester. Functional requirement 2 was broken into two sub-FRs. The first, FR 2.1, was to measure torque applied about the positive y-axis accurately in time. This FR was satisfied by DP 2.1, a dynamometer system. The second sub-FR, FR 2.2, was to validate the torque measurements, which was accomplished through DP 2.2, a testing system that involves comparing generated torque values for our tester with those produced via a Vermont Release Calibrator in Excel.

In this section only FR 2.1 will be explored, as FR 2.2, validate torque measurements, will be explained in Chapter 6, testing of the final design. Additionally, the forward bending release tester shares or duplicates many of the same elements from the twist release tester. Elements that are shared or duplicated from the twist release tester will be referenced, but not explained in detail in this section.

Table 7: FR 2 Determine binding response to forward bending loads

2	FR	Determine binding response to forward bending loads	DP	Forward bending release tester	
+	2.1	FR	Measure torque applied about the positive y-axis accurately	DP	Bending Dynamometer System
+	2.2	FR	Validate torque measurements	DP	Known bending torque pulley system and Excel

Functional requirement 2.1 [Table 8] was broken into the same four lower level functional requirements as functional requirement 1.1. The first was to create a physical device that could transmit an applied load through the tester to the SBB system, with a portion of this device being able to elastically deform to allow for strain gauge readings. The second was to create a system which could collect strain information based on the elastic deformation of the body of the tester. The third was to create a system to calibrate strain to torsion by creating a calibration curve in both the clockwise and counterclockwise directions, which would be accomplished through the design of a pulley system for torques applied in the clockwise and counterclockwise directions. The fourth was to measure torque to release in the SBB system using the created calibration curve in Excel. The third and fourth sub-functions are described in chapter 6, Testing.

FR 2.1

Table 8: FR 2.1 Measure torque applied about the positive y-axis in time

2.1	FR	Measure torque applied about the positive y-axis accurate	DP	Bending Dynamometer System
2.1.1	FR	Transmit Torque through system for measurement	DP	Lever arm and interfacing bending tube applicator
2.1.2	FR	Aquire strain measurements	DP	Bending Full Wheatstone Bride Configuration Strain Gauges and NI MAX Software and Labview Signal Express
2.1.3	FR	Create strain to torque calibration curve	DP	Known torque bending pulley system applicator for clockwise torsion and Excel Software
2.1.4	FR	Measure torque to release in SBB system	DP	Excel functions

The decomposition of functional requirement 2.1.1 [Table 9] shows the development of the physical components of our torque tester. The functional requirements of the physical tester were broken down into three lower level requirements, which were the same as those seen in the lower levels of FR 1.1.1. The first, FR 2.1.1.1, describes how the tester must include a means to apply torque to the testing applicator from which the measurements will be taken. The second, FR 2.1.1.2, indicates a need for a surface from which to measure the applied torque. This surface would have to elastically deform in the range of applied loads to allow for torsion measurements to be obtained, but should not plastically deform. The third, FR 2.1.1.3, describes how the tester would need to interface with the SBB.

Functional Requirement 2.1.1

Table 9: Transmit torque through system for measurement

2.1.1	FR	Transmit Torque through system for measurement	DP	Lever arm and interfacing bending tube applicator
2.1.1.1	FR	Apply torque to applicator	DP	Lever arm and interfacing top piece system
2.1.1.1.1	FR	Transmit load to applicator system	DP	1 Meter lever arm
2.1.1.1.2	FR	Interface applicator and lever arm	DP	Top piece releasable pin system
2.1.1.2	FR	Provide surface for applied torque measurement	DP	Cyylindrical bending torque applicator
2.1.1.3	FR	Transmit applied load to ski boot	DP	Prosthetic foot interface
2.1.1.3.1	FR	Interface applicator and prosthetic foot	DP	Bottom piece releaseable pin system
2.1.1.3.2	FR	Transmit load to ski boot	DP	Prosthetic foot

In order to apply a load to the applicator we used DP 2.1.1.1.1, a $\frac{1}{2}$ meter tall lever arm with a 1 meter long handle (Figure 18). This was the same handle described and shown in relation to DP 1.1.1.1.1.

To interface the lever with the cylindrical torque applicator, we designed a top piece system with a releasable pin DP 2.1.1.1.2 [Figure 17]. The top piece system was the same series of parts used for DP 1.1.1.1.2.

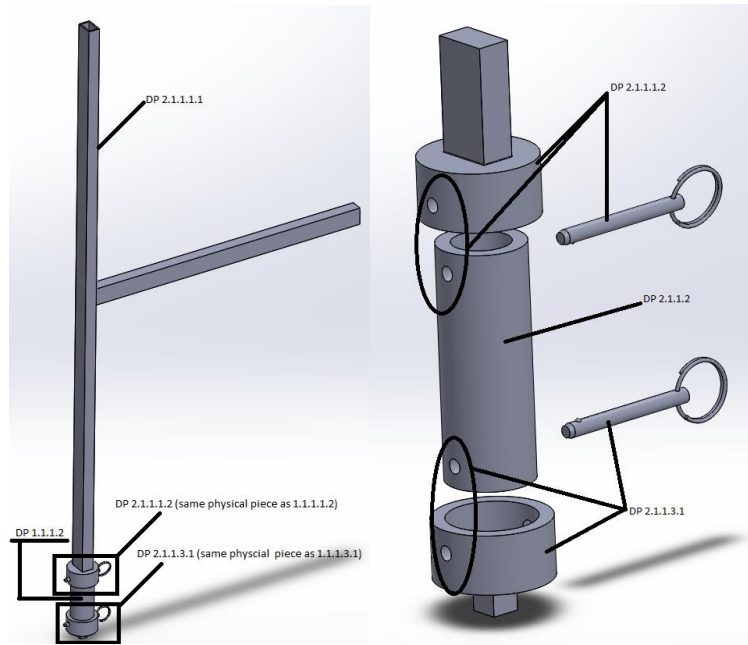


Figure 17: DPs for functional requirement 2.1.1 and its constituents (full system, right; exploded view, left)

A cylindrical torque applicator DP 2.1.1.2, is used to satisfy the functional requirement of a part that provides a surface for strain measurements that can be calibrated to determine torque [Figure 18]. The cylindrical applicator interfaces with the top piece is 4" in length, with 0.257" holes drilled at either end, the same as the cylindrical applicator used for twist testing, to interface with the top and bottom pieces. The tube has an outer diameter of 1.5" with a thickness of 0.25". The dimensions of the cylindrical applicator were carefully chosen to be able to elastically deform in the expected range of applied torques, while not plastically deforming, with a safety factor of 1.75. The safety factor was lowered from three, so that more strain could be observed when testing at lower torque values. To do this we first found the polar moment of inertia, I , for each possible tube geometry, with r_o and r_i noting the outer and inner radii of the annular tube respectively, using the following equation (Ozkaya et al., 2012).

$$I = \frac{1}{4}\pi(r_o^4 - r_i^4)$$

We then determined the maximum elastic moment, M , each tube could withstand. To do this we first found the tensile yield stress, σ_T , of 6061 Aluminum, 276 MPa (ASM, 2013). We then used the polar moment of inertia, tensile yield stress, and the distance from the neutral axis, the total radius y , to determine the maximum elastic moment (Ozkaya et al., 2012).

$$M = \frac{\sigma I}{y}$$

The maximum amount of torque needed to release a binding in bending is 640 Nm, as per ASTM F 939-05a standards for the selection of release torque values, so with a safety factor of 1.75, our tube was to withstand 1120 Nm of torque. The tube we selected was calculated to have a maximum elastic moment of 1201 Nm.



Figure 18: DP 2.1.1.2 Cylindrical torque applicator

In order to satisfy the functional requirement of transmitting the applied torque to the SBB system, a prosthetic foot interface was created, consisting of a bottom piece releasable pin system that attaches the cylindrical application tube to a prosthetic foot, DP 2.1.1.3.1, and a Vermont Release Calibrator prosthetic foot, DP 2.1.1.3.2, that interfaces the bottom piece with the SBB system.

The bottom piece releasable pin system is the same as the one described for DP 1.1.1.3.1 and can be seen in Figure 10.

The Vermont Release Calibrator prosthetic foot, Figure 12, used for our forward bending torque applicator was the same as the one used and mentioned for DP 1.1.1.3.2.

Functional Requirement 2.1.2

The decomposition of functional requirement 2.1 .2, acquire strain measurements, [Table 10] shows the development of the circuit components required for our tester. The functional requirements of the circuit components were broken down into six functional requirements. The first, FR 2.1.2.1, describes the requirement for a power source. The second, FR 2.1.2.2, describes how strain measurements need to be collected from the cylindrical applicator. The third, FR 2.1.2.3, describes how these signals need to

be amplified to be read. The fourth, FR 2.1.2.4, describes how the output analogue signals need to be converted to digital signals for processing by the computer. The fifth, FR 2.1.2.5, describes the need to read the initial data and export it to software which can process it further. Finally, the sixth functional requirement, FR 2.1.2.6, describes the need to synthesize the output data and export it to analysis software, where it can be calibrated.

The circuit components that we used for our forward bending torque tester were mainly created and applied in the same manner as the components used in our twist torque tester. In the following section where the two designs are the same will be noted, but the design parameters will only be explain where they vary from previously mentioned components.

Table 10: FR 2.1.2 Acquire strain measurements

2.1.2	FR	Acquire strain measurements	DP	Full Wheatstone Bride Configuration Strain Gauges and NI MAX Software and Labview Signal Express
2.1.2.1	FR	Provide power supply to circuit	DP	Two 9V batteries in a dual polarity power supply configuration
2.1.2.2	FR	Collect strain signals from cylindrical applicator	DP	Four strain gauges in a Full Wheatstone bridge configuration
2.1.2.3	FR	Amplify signals to readable level	DP	Instrumentation Amplifier
2.1.2.4	FR	Convert analogue to digital signals readable by the computer	DP	DAQ module
2.1.2.5	FR	Read and export data signals	DP	NI Measurement and Automation
2.1.2.6	FR	Synthesize data and export to analysis software	DP	Labview Signal Express

To acquire strain measurements we utilized a full Wheatstone bridge configuration, DP 2.1.2.2, to obtain the initial analogue output signals. We connected the strain gauges to the cylindrical torque applicator using the procedure outlined by the Vishay Precision group (Vishay, 2011). We connected the strain gauges onto the applicator directly across from each other on either side of the cylindrical tube in the manner shown in Figure 19. The strain gauges we purchased were $120\Omega \pm 5\%$, however, we tested each gauge and only applied those that were within 1% to mitigate bridge imbalance. The strain gauges were then connected into the full Wheatstone bridge configuration in a circuit, the full configuration of which can be seen in Figure 20. The circuit in Figure 20 has the same configuration as the circuit used for our twist release tester. Gauge 1 from Figure 19 corresponds to R1 in Figure 20, and the rest of the strain gauges can be corresponded to R2, R3, and R4 in the same manner.

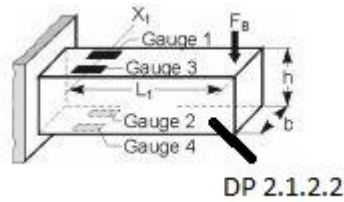


Figure 19: DP 2.1.2.2 full wheatstone bridge configuration (Hoffman, 1986)

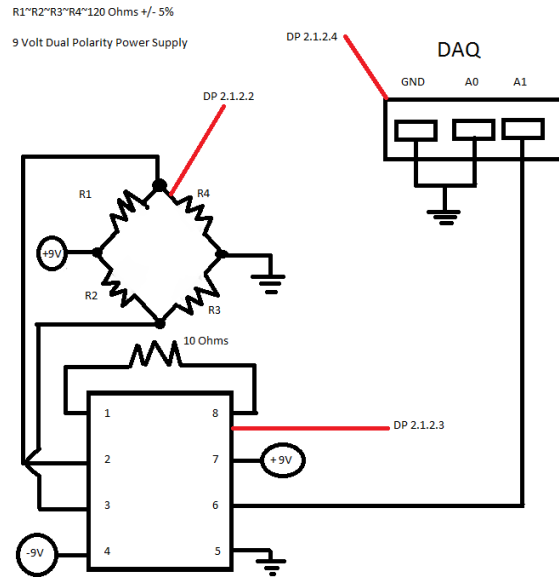


Figure 20: Complete circuit diagram including DPs 2.1.2.1 to 2.1.2.4

As previously stated Figure 21 reflects the circuit diagram for our dynamometer setup. The circuit was powered by a 9V battery dual polarity power supply, DP 2.1.2.1. The connection of the power supply is the same as described for DP 1.1.2.1. Additionally, the signals were made readable to the computer using the same DAQ, were amplified using the same model of amplifier, and the gain of the amplifier was also still set to 1000 by a 10 Ω resistor between pin 1 and 8 of the instrumentation amplifier.

After the analogue signal was converted into a digital signal by the DAQ, these readings were also read and exported to SignalExpress using NI Measurement and Automation (MAX) software, DP 2.1.2.5. Labview SignalExpress was used to synthesize the data, tracking the input voltage changes over time and converting voltage measurements to strain measurements, and to export this data into Excel where it could be analyzed, DP 2.1.2.6. For our forward bending torque tester, we used the same Signal Express program that we had created for our twist release torque tester, except that we changed the value of the voltage drop across the bridge, which we found to be slightly different upon testing. The parameters for the SignalExpress window were thus the same as those seen in Figure 16, except that the initial voltage parameter was 0.7 instead of 0.67.

3. Physical Integration

After specifying the functional requirements and design parameters, we then integrated them into components. The design was constrained to a smaller area, however the two types of binding tester contained within the design resulted in a larger amount of solutions.

3.1 Design Matrix

A design matrix (Figure 21) was used to determine if the functional requirements and design parameters were coupled. If the design was fully coupled it would not function properly, however some partially coupled pairings are acceptable in a design, though it is preferable to limit them when possible.

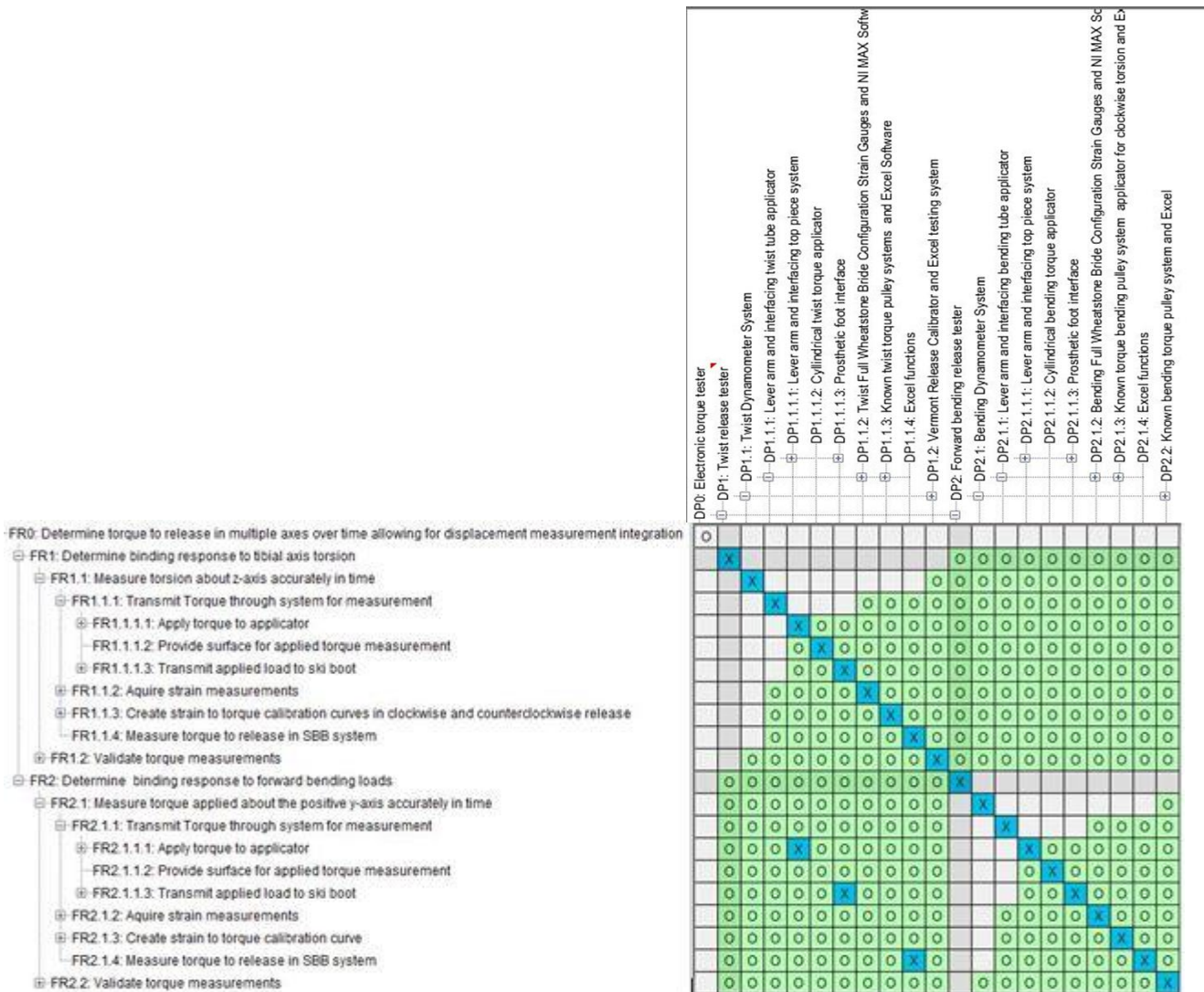


Figure 21: Design Matrix

Assessment of the design matrix reveals that there are three partial couplings between DP 1.1.1 and FR 2.1.1.1, DP 1.1.1.3 and FR 2.1.1.3, and between DP 1.1.4 and FR 2.1.4. These are due to the fact that the torque applying lever, the top piece system, bottom piece system, and Vermont Release Calibrator Prosthetic foot are used for both forward bending and twist release testing. This means that the design is limited in the fact that forward bending and twisting loads would not be able to be evaluated at the same time, however as the design was created to evaluate clockwise twist release, counter clockwise twist release, and forward bending release independently it does not impede the design.

4. Tolerancing

Prior to creating CAD models of all components, required fits and associated tolerances were determined. Correct fits ensure that all prototype components would fit together while minimizing slop in the system. *The Machinery's Handbook (27th Edition)* was used for reference and a fit calculator was used (AMES, 2013). The calculator uses fits as defined by *The Machinery's Handbook* and determines the appropriate clearances.

From *The Machinery's Handbook (27th Edition)*: "Close running fits are intended chiefly for running fits on accurate machinery with moderate surface speeds and journal pressures, where accurate location and minimum play are desired" (Jones et al., 2004). These RC4 fits were used for the pocket features on both top and bottom components. This fit does not need to be exceptionally precise, with the pin mechanism limiting play. Per this close running fit, a 38mm diameter should be opened to 38.141mm. The measured dimension of the component was 38.20mm, a design change made by the team.

The 2 – 6.35mm pin holes had to be aligned and drilled through-holes. A close running fit was chosen on these as well to ensure that simple assembly was possible. Due to the precision of alignment, any increase in clearance would enable slop. When fully loaded during testing, there should be no play. A 6.35mm pin requires a 6.37mm hole for a close running fit. This dimension required a bit of this size. The next bit up is an F drill bit, or 6.528mm. This dimension is close to our measured holes, within 0.43%.

The Machinery's Handbook (27th Edition) defines a locational clearance fit as: "Locational clearance fits are intended for parts which are normally stationary, but which can be freely assembled or disassembled" (Jones et al., 2004). The top's interface with the Epitax handle is an LC fit. The slot of the handle was measured using a micrometer, 25mm x 15mm. Using fit standards this interface should

measure 24.999mm x 14.998mm. This fit was excellent in our prototype. This fit allowed minimal play yet easy assembly.

An LC fit was also used for the prosthetic foot interface on the bottom component. Initially, the size of the socket was measured with a micrometer. The socket measured just larger than 13mm x 13mm. Using a locational clearance fit the interface size should be decreased by 1/100th of a millimeter on both sides.

Issues arose with the initial interface with the prosthetic foot. During bending testing, serious amounts of stress were induced on this joint. Initial fit clearances were not tight enough and slippage between the two parts occurred. Initial fits called for a close running fit. Clearances were changed to locational translation fits, where accuracy of location is essential but small clearance is permissible. By decreasing the fit clearance, slippage and induced deformation were mitigated.

5. Prototype Construction

Axiomatic design is used to reduce complexity and increase robustness of a design [Appendix B]; thus increasing design manufacturability. In order to simplify the design, standard parts and geometries were used wherever possible. The initial prototype was made entirely of aluminum. Aluminum is readily available, inexpensive and easy to machine. Standard bar stock size of 2" was used for both the top and bottom interfaces, tubing stock of 1.5" and 0.049" thickness and 0.25" thickness was used for the twist and bending cylindrical torque applicators, respectively, and standard ¼" diameter quick-release pins were used for disassembly.

First a model of the assembly was completed in *Solidworks*. Machined part models were imported into *ESPRIT* and tool paths were created. After defining part features and specifying tools, CNC lathe machining can be utilized for all parts. Each part was created with a Haas Minimill using standard fixturing soft-jaws and v-blocks to secure cylindrical pieces when necessary.

The top and bottom pieces of the dynamometer were created separately, in five machining operations using a $\frac{1}{4}$ " non-ferrous end mill to create the extruded features and a $\frac{7}{8}$ " end mill, with a smaller tool radius, for the slot interfaces with the selected tube applicators. First the stock was cut to approximate size using a band saw. A facing operation was then utilized to ensure a level surface to the top of the pieces. A pocketing op utilizing the island feature created the interfaces with the prosthetic foot and Epitax handle for the bottom and top pieces, respectively. A second facing operation leveled the

bottom surface of the pieces and ensured proper part length. Next, a pocketing op then created the slot for the tube applicators. Finally, 6.527mm thru holes were drilled in the bottom piece and top piece, with the diameter of the holes being located 9.830mm from the bottom rim of the part. The cylindrical applicators were then cut to size using a band saw and 6.527mm thru holes were drilled 9.830mm from each end to allow for alignment with the thru holes in the bottom and top pieces. Figure 22 below shows each finished component.



Figure 22: Completed device components

Once all parts were manufactured, the assembly was completed as shown in figure 23 below.

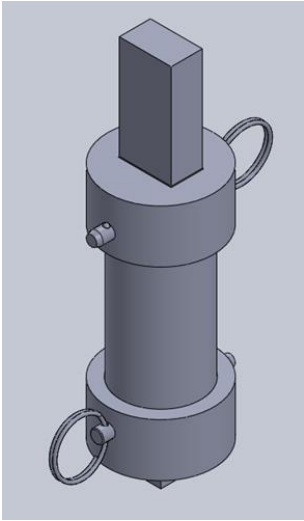


Figure 23: Completed part assembly

Measurements were made to ensure accuracy, recognize any variation and define error [Table 11]. These measurements reveal that the Haas Minimills used for part production were highly accurate, with percent differences from the CAD model being well under 1%. However, the differences in the heights of the created pieces were greater than 1%. The exact height of the different components is a critical dimension, as it did not affect the fit, form or function of the assembly.

Table 11: Machining error analysis

Machining - Error Analysis				
Part	Feature	CAD	Measured	% Difference
Top	Handle Interface (Long)	25.00x15.00	25.03x15.00	0.12
	Hole Diameters	6.50	6.50	0.00
	Depth of Pocket	19.05	19.03	0.10
	Pocket Diameter	38.50	38.50	0.00
	Overall Diameter	50.80	51.07	0.53
	Overall Length	75.40	77.02	2.15
Bottom	Handle Interface (Long)	13.00x13.00	13.00x13.04	0.31
	Hole Diameters	6.50	6.50	0.00
	Depth of Pocket	19.05	19.00	0.26
	Pocket Diameter	38.50	38.43	0.18
	Overall Diameter	50.80	51.04	0.47
	Overall Length	40.00	39.08	2.30
Bending Cylinder	Outer Diameter	38.00	38.10	0.26
	Inner Diameter	25.00	24.91	0.36
	Length	101.60	102.00	0.39
	Hole Diameters	6.50	6.61	1.69
Twist Cylinder	Outer Diameter	38.00	38.11	0.29
	Inner Diameter	35.00	35.25	0.71
	Length	101.60	102.30	0.69
	Hole Diameters	6.50	6.62	1.85

*all measurements in millimeters

6. Testing of the Final Design and Results

As discussed in the design section, testing was integrated into the decomposition of our design on multiple levels. In order to produce torque measurements a calibration scale that related the output of our circuit, strain, into torque had to be produced for clockwise, counterclockwise and twist release testing. This was encompassed by FR 1.1.3, create strain to torque calibration curves in clockwise and counterclockwise release and FR 2.1.3, create a strain to torque calibration curve in forward bending release as seen in Table 12 and Table 13. To create these calibration curves pulley systems that applied known torque values in the clockwise and counterclockwise direction, as well as in forward bending

were created, DP 1.1.3.1, DP 1.1.3.2, and DP 2.1.3.1, respectively. Information from these calibration tests were also used to determine the initial percent difference and relative range of our measurements under a constant torque, before using it to test the torque over time of a SBB system.

Table 12: FR 1.1.3 Create a strain to torque calibration curve for twist release

1.1.3	FR	Create strain to torque calibration curves in clockwise and counterclockwise release	DP	Known twist torque pulley systems and Excel Software
1.1.3.1	FR	Create strain to torque calibration curves in clockwise release	DP	Pulley system for clockwise loads and Excel
1.1.3.2	FR	Create strain to torque calibration curves in counterclockwise release	DP	Pulley system for counterclockwise loads and Excel
1.1.4	FR	Measure torque to release in SBB system	DP	Excel functions

Table 13: FR 2.1.3 Create a strain to torque calibration curve for forward bending release

2.1.3	FR	Create strain to torque calibration curve in forward bending release	DP	Known torque bending pulley system applicator for clockwise torsion and Excel Software
2.1.3.1	FR	Apply known torque	DP	Clockwise pulley system
2.1.3.2	FR	Create calibration curve	DP	Excel trendline

The testing of our design with a SBB system was also expressed in our decomposition on the third level of decomposition, as seen in Table 14. FR 1.2 encompasses the need to validate twist release torque measurements for use with a SBB system through comparative testing with an established torque tester, a Vermont Release Calibrator, DP 1.2. FR 2.2 encompasses the need to validate, or further explore, the percent difference and repeatability range of torque values obtained through the usage of our system with our produced calibration curve with the previously designed pulley system and Excel functions.

Table 14: FR 1.2 and 2.2 Validate torque measurements

0	FR	Determine torque to release in multiple axes over time allowing for displacement measurement	DP	Electronic torque tester
1	FR	Determine binding response to tibial axis torsion	DP	Twist release tester
1.1	FR	Measure torsion about z-axis accurately in time	DP	Twist Dynamometer System
1.2	FR	Validate torque measurements	DP	Vermont Release Calibrator and Excel testing system
2	FR	Determine binding response to forward bending loads	DP	Forward bending release tester
2.1	FR	Measure torque applied about the positive y-axis accurately in time	DP	Bending Dynamometer System
2.2	FR	Validate torque measurements	DP	Known bending torque pulley system and Excel

All of the data from our testing was collected through Labview SignalExpress, as described in the design section. Before running any test logging options must be specified in the Recording Options window in SignalExpress [Figure 24]. Folders for each type of testing can be created by specifying different folder names in “Log destination folder”, and can also be nested into pre-existing folders. The name for each individual test within this folder can be specified in “Log title” and a description of each individual test and testing conditions can be entered into “Log description”. Once the individual test has been defined, returning to the “Step Setup” window allows for viewing of data as the test is run. In this window the “Run” button should be selected first, this allows for the presentation of data without collection, which

is useful to verify that the circuit is properly connected. Using the “Run” button allows for simultaneous display and recording of data.

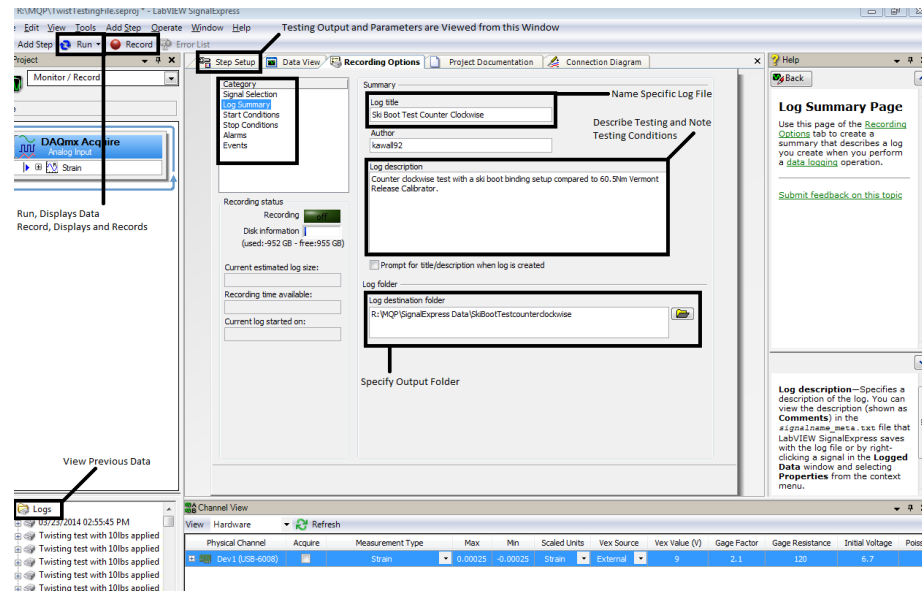


Figure 24: Running and Recording Testing Information

Each logged test produced an Excel file that contained a cover sheet with an overview of testing information, as well as a second sheet that showed the time versus the output strain. Test results for each individual test conducted, were handed in as a physical deliverable for this report to the advisor.

In all of our testing there was an offset between zero strain and zero torque. These offsets were different between clockwise, counterclockwise, and forward bending testing; however they were found to be constant for each test. The source of this offset is suspected to be either an error in the function that balances the bridge for strain measurements, or that the bridge offset we entered was not precise enough to cancel out the entire offset. Additionally, the output strain was calculated in a program that did not account for voltage amplification, this means that the output strain values were 1000 times larger than they should have been. Due to these factors the raw strain values produced through our testing were considered as “output” values instead of strain values. To create our calibration curves the output values were used, as they were directly related to the applied torque. A second order polynomial equation, produced through an Excel trendline, was used to fit calibration curve data as section 9.5 of ASTM F1062 specifies a second order polynomial, produced by the least squares method, for fitting a plotted calibration curve (ASTM, 2013). The equations for the fitted trendline were used to calculate the torque values measured by our device. For each calibration test we also determined the relationship

between strain and torque by removing the offsets from the output values and plotting it against the torque values.

To test our device's fulfillment of our constraints the equation from ASTM F1062 was used to find the agreement between our device and the known applied torque at each torque value tested for calibration testing. The original equation from the standard, however was used to "find the agreement between the test device and the standard apparatus described in Test Method F504" (ASTM, 2013). Due to this, the original equation was slightly modified to serve our means. The original equation, represented in terms of percent, from section 9.3 of ASTM F1062 is as follows (ASTM, 2013):

$$d = \frac{\bar{X}_{td} - \bar{X}_{sa}}{\bar{X}_{sa}}$$

where:

d = agreement between the test device and the standard apparatus

X_{sa} = mean measurement from the standard apparatus

X_{td} = mean measurement from the test device

To determine the agreement between the test device and the known applied torque at each tested torque value in calibration testing we defined the variable " X_{sa} " as the known applied torque. To meet the constraints determined by the group the agreement, or difference, between the known torque value and the value produced by our tester must be within $\pm 5\%$ of the known torque value, " X_{sa} " in all testing configurations .

This equation was also adapted to find the agreement between our device and the release torque measured with the Vermont Release Calibrator. To do this we defined the variable " X_{sa} " as the mean measurement from the Vermont Release Calibrator. To meet the constraints determined by the group the agreement, or difference, between the mean torque measurement from the Vermont Release Calibrator and the value produced by our tester must be within $\pm 5\%$ of the known torque value, " X_{sa} " in all testing configurations .

We also assessed the relative range of values produced by the tester, in both calibration and SBB system testing for all testing configurations, using a slight alteration to the equation used to calculate the difference between results produced by a tester to the expected results from a calibration curve. The original equation can be seen A1.3 of ASTM F1062 (ASTM, 2013). The altered form that we used to find the relative range of measured torque values is as follows (ASTM, 2013):

$$a = \frac{M_d - M_t}{M_t} \times 100$$

where:

a = Range of measured torque values relative to the magnitude of the mean measured torque value

M_d = Range of measured torque values, the difference between the maximum measured value and the minimum measured value

M_t = Mean measured torque value

This equation was also applied to assess the relative range of output, initial strain, values. These results give an indication of the size of the range of measured torque values relative to the size of the mean measured torque value. This provides information on the relative size of the variance of the measurements. However, these results served as a basic assessment and have no associated constraints.

6.1 Calibration Testing for Clockwise Twist Release Testing

Before conducting calibration testing, a range of torque values for testing was determined. To produce an accurate calibration curve, many different points should be tested. Due to time constraints however, we defined our calibration curve by testing done at six different known torques, including zero. These values were determined from using anthropometric data combined with the ASTM standards for the selection of release torque (CDC, 2010; ASTM, 2005). As this tester was designed for adult users, we felt it was most important to have an accurate calibration curve in the range of release torque values used by adult skiers. From our anthropometric data we determined that the 10th percentile female was 53.6 kg and from the ASTM release torque standards we established that this would encompass a type “I” skier, who would have a release torque value of 37 Nm in twist releases. We then established that a 90th percentile male was 114.4kg, as the highest defined weight by the ASTM for release torque selection is 95 kg, we decided that our highest torque value measured should be at least 105 Nm, which was the release torque value for skier type “P” and the highest listed for twist releases. The torque values that our calibration curve was tested with were 0, 37.81, 56.72, 94.53, and 113.4 Nm.

6.1.1 Test setup and methods for clockwise twist release testing

To apply the selected known torque values we created a pulley system that would connect to either side of the one meter long lever that interfaced with our dynamometer. The decomposition for the designed pulley system and calibration curve creation can be seen in Table 15.

Table 15: FR 1.1.3.1 Create strain to torque calibration curves in clockwise release

1.1.3	FR	Create strain to torque calibration curves in clockwise and	DP	Known twist torque pulley systems and Excel Software
1.1.3.1	FR	Create strain to torque calibration curves in clockwise release	DP	Pulley system for clockwise loads and Excel
1.1.3.1.1	FR	Apply known torque	DP	Clockwise pulley system
1.1.3.1.1.1	FR	Generate predetermined force	DP	Mirrored pulley system on either side of lever
1.1.3.1.1.1.1	FR	Apply equal forces	DP	Olympic weights of same mass
1.1.3.1.1.1.2	FR	Apply forces perpendicular to torque tester	DP	Pulley system of nominal height
1.1.3.1.1.1.2.1	FR	Locate pulley at correct height	DP	Adjustable, wood support structure
1.1.3.1.1.1.2.2	FR	Allow room for gravity-weighted load	DP	Framed box structure
1.1.3.1.1.2	FR	Apply force at known lever arm length	DP	1 meter lever arm
1.1.3.1.2	FR	Calibrate strain to torque calibration curve	DP	Excel trendline

Our pulley system for our clockwise calibration testing involved two simple wooden box frames constructed with four 3"x3" pine columns, eight 2"x4" pine support boards, eight wood braces, and 24 3" wood screws. The top 2"x4" support board of each frame had a stainless steel metal pulley, for use with 3/8" diameter rope, with a 165 lb work load rating. The center of each pulley was aligned with a point on the lever arm 0.076 m away from its respective end. The height of the pulleys, and the support boards, was adjusted so that the 3/8" diameter polypropylene and mixed synthetic rope attached perpendicularly to the lever arm. Olympic weight(s) were attached to the polypropylene ropes and used to apply known torques to the lever. A SolidWorks model of our testing setup, with important reference geometries, can be viewed in Figure 25.

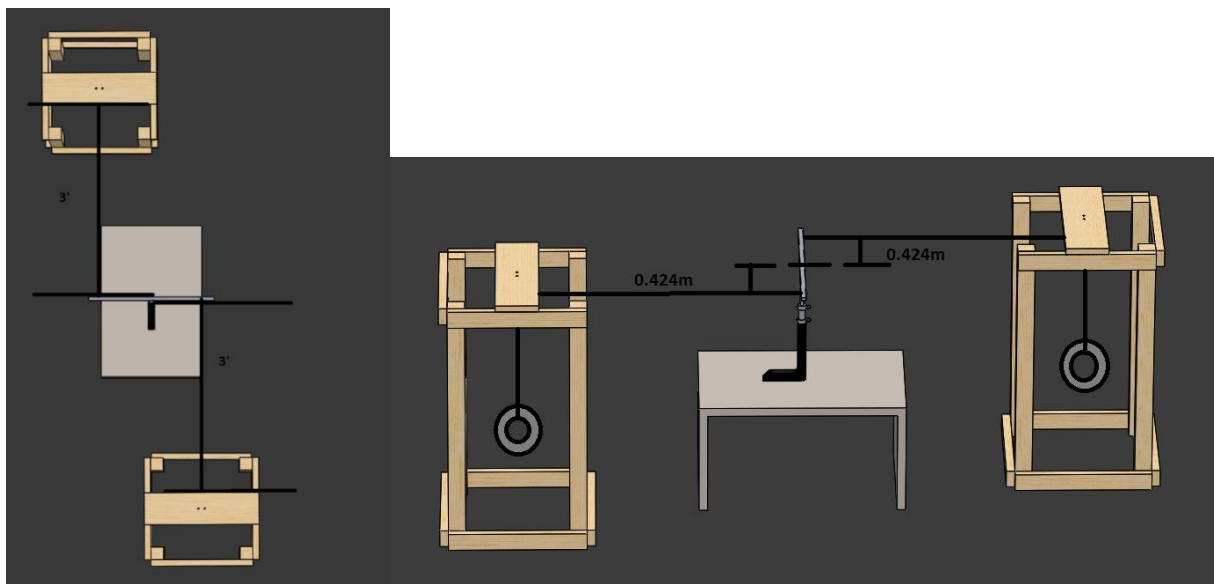


Figure 25: Clockwise calibration pulley applicator system

The amount of weight needed for each side of the pulley system was calculated using the relationships between pounds and kilograms, mass and force, and the equation:

$$M_o = Fxd$$

where M_o was the moment at the center of the lever around which torque was applied, d was the distance of the applied force from the center of the lever, 0.424m, and 90° was the angle between the lever arm and the force caused by the tension of the rope

Using this equation we found that 5, 10, 15, 25, and 30 lb weights would be required to obtain the desired amount of applied torque to the system. Table 16 shows the relationship between the mass applied per side of the pulley system to the applied torque.

Table 16: The relationship between the mass applied to each side of the pulley system and the applied torque

Mass per Side (lb)	Mass (kg)	Force (N)	Torsion (Nm)
5	2.27	22.30	18.91
10	4.55	44.59	37.81
15	6.82	66.89	56.72
25	11.36	111.48	94.53
30	13.64	133.77	113.44

6.1.2 Calibration curve, results, and analysis for clockwise twist release testing

Calibration testing was performed five times at each of the specified torque values, as well as at 0 Nm. Each of these individual tests were run for at least 10 seconds, which at a 1k sampling rate, meant that there were at least 10,000 data points for each individual test. Within each test run there were low standard deviations, which were dwarfed by the deviations seen between test runs, for this reason these deviations were not included for our calculations for percent difference and relative range of the system. Between each test the system was disassembled and then reassembled to ensure the robustness of the measurements.

The mean of the outputs of each of the five tests for each torque value was recorded. The maximum, minimum, range, and mean values of these five mean output values were then calculated. The relative range of the output, in terms of the mean measured output, was then determined by determining the percent value of the range in terms of the mean output. The range represents the possible variation of output values to the mean output value, which was used to create the calibration curve. The results of this analysis can be viewed in Table 17.

Table 17: Relative Rang of Output Values from Clockwise Testing

Applied Torque (Nm)	Mean Output (unitless)	Output Range	± Relative Range (%)
0	0.0341	0.0008	2.35
18.9	0.2793	0.0087	3.12
37.81	0.4312	0.0336	7.79
56.72	0.4947	0.0215	4.35
94.53	0.6773	0.0031	0.46
113.44	0.7030	0.0040	0.57

The range of output values relative to the mean measured output value was generally quite low. The relative range of the values was, at most, ±7.79%, of the mean. The mean output values taken at each of the specified torque values, along with their standard deviations can be viewed in Figure 26.

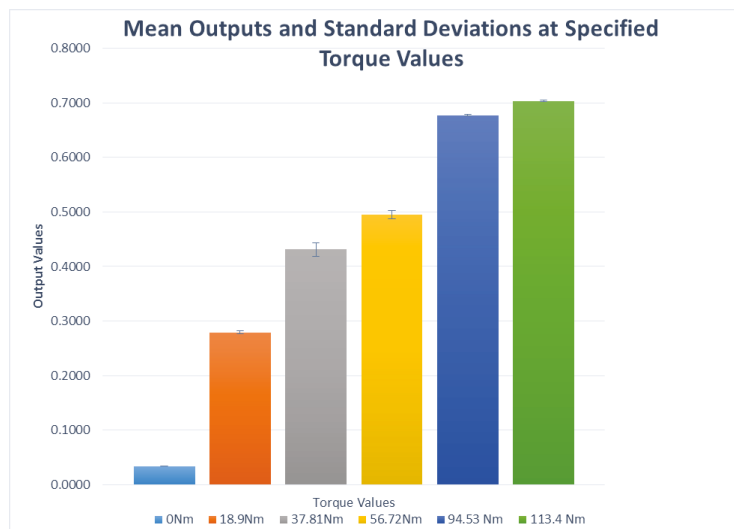


Figure 26: Mean Outputs and Standard Deviations at Specified Torque Values

Using the mean output value from the means of the five separate tests, a curve was created that plotted output values vs. the applied torque, Figure 27. Using the created curve an Excel trendline was created that formed a function to define the relationship between the output values and the applied torque. The generated function was described to fit the data with an R^2 value of 0.9912. Figure 27 also displays the standard deviations of each of the means.

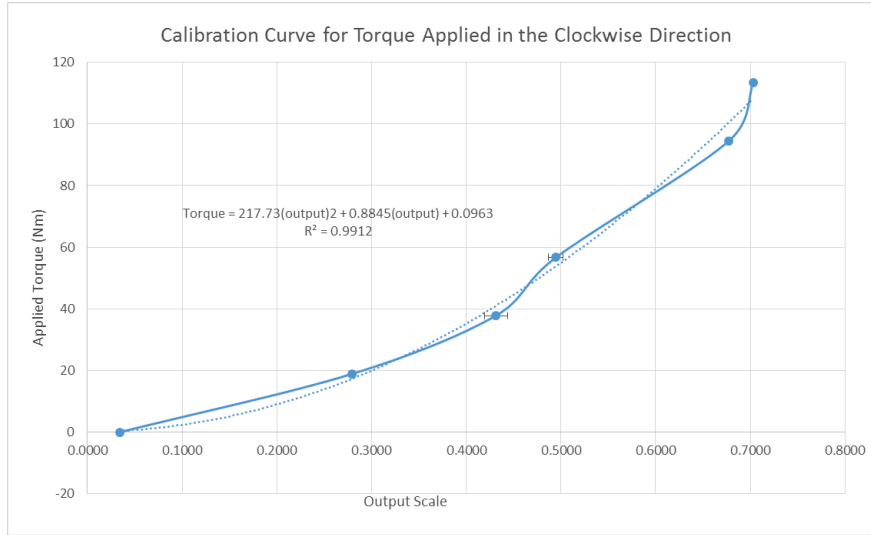


Figure 27: Calibration Curve for Torque Applied in the Clockwise Direction

The trendline generated equation that related output values to torque values is as follows:

$$Torque = 217.73(output)^2 + 0.8845(output) + 0.0963$$

Using this equation torque values were generated for each of the five tests performed at each known torque value. The mean, maximum, and minimum torque values were then determined at each known torque value. The relative range of these values was then determined by calculating the percent value of the range in terms of the mean measured torque. The range represents the possible variation of measured torque values to the mean measured torque value. The percent difference of the measurements was then determined by calculating the percent value of the mean of the measured torque to the known applied torque. These results can be viewed in Table 18.

Table 18: Percent Difference and Relative Rang of Torque Testing in the Clockwise Direction

Applied Torque (Nm)	Mean Measured Torque (Nm)	Maximum Measured Torque (Nm)	Minimum Measured Torque (Nm)	± Relative Range (%)	± Difference (%)
0	0.38	0.39	0.37	*3.33*	*280.38*
18.9	17.33	17.74	16.67	6.14	8.31
37.81	40.97	45.60	39.15	15.73	8.36
56.72	53.82	55.90	51.26	8.62	5.11
94.53	100.58	101.13	100.20	0.92	6.40
113.44	108.31	108.85	107.62	1.13	4.52

As a note the percent relative range and difference for 0Nm torques was obtained by attributing the known torque the value of 0.1Nm. Due to this low torque value the range of the percent difference and relative range will be high. The range of the measured torque values, relative to the mean measured values, were extremely different depending on the measured torque value. This indicates that the results produced by the tester are highly variable between approximately 38 and 47 Nm of applied torque. The percent difference between the known torque and applied torque were all under 10%, however only the percent difference at 113 Nm was under 5%, meeting our performance constraints. However, the lower relative ranges seen in the testing of the output values indicates that a better defined calibration curve could produce better results. An enhanced calibration curve could be produced through testing at more known torque values. Using an alternative program such as MATLAB to produce the curve might also result in a better fit.

Due to the inherent offsets between the outputs produced by our system and strain, we adjusted our output values to account for these offsets and graphed the true strain outputs verse the applied torque values, Figure 28.

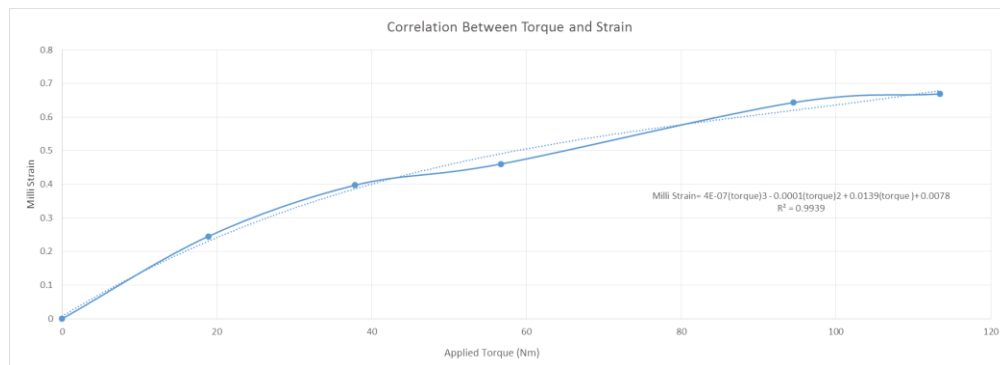


Figure 28: Correlation between Applied Torque and Strain

A trendline for this data was produced, which related the applied torque to the true strain, expressed in milli-units. This trendline was found to fit the plotted data with an R^2 value of 0.9939. The equation that related torque to strain is as follows.

$$\text{Milli Strain} = 4 \times 10^{-7}(\text{torque})^3 - 0.0001(\text{torque})^2 + 0.0139(\text{torque}) + 0.0078$$

This equation would be useful for determining the strain experienced by the dynamometer during testing.

6.2 Calibration Testing for Counterclockwise Twist Release Testing

The known release torques that were applied in counterclockwise testing were the same as those used for clockwise testing. The same values were used because release torque values for clockwise and counterclockwise release are theoretically the same for the same skier type.

6.2.1 Test setup and methods for counterclockwise twist release testing

The testing frames, pulleys, weights, and reference geometries used for clockwise testing were also used for counterclockwise testing. The only difference between the two types of testing were that the orientation of the testing frames and the direction in which the ropes attached to the lever arm were reversed, so that torsion of the dynamometer occurred in the counterclockwise direction, as seen in Figure 29.

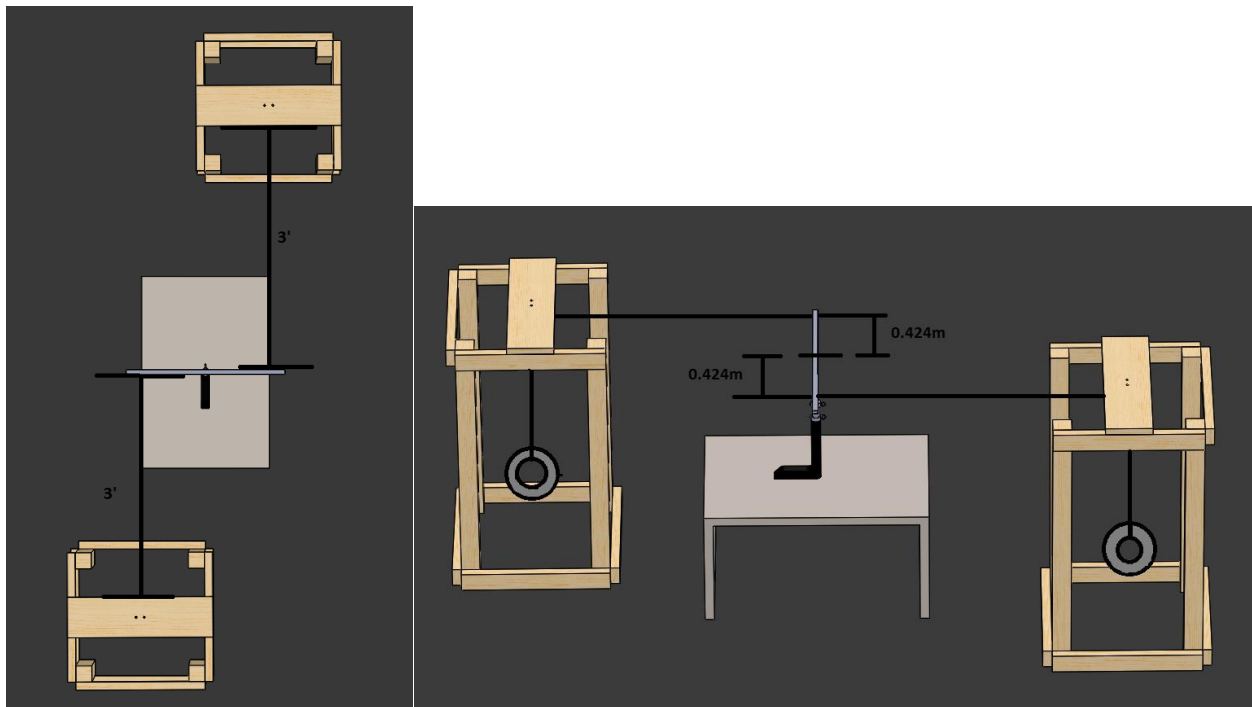


Figure 29: Counterclockwise torque applicator pulley system

6.2.2 Calibration curve, results, and analysis for counterclockwise twist release testing

For initial counterclockwise testing, there were again five test runs at each of the specified torque values, as well as at 0 Nm. Each of these individual tests were run for at least 10 seconds, which at a 1k sampling rate, meant that there were at least 10,000 data points for each individual test. Within each test run there were low standard deviations, which were dwarfed by the deviations seen between test runs. These deviations were also not included for our calculations for percent difference and relative

range of the system. Between each test the system was disassembled and then reassembled to ensure the robustness of the measurements.

The mean of the outputs of each of the five tests for each torque value was recorded. The maximum, minimum, range, and mean values of these five mean output values were then calculated. The percent relative range of the output was then determined by determining the percent value of the range in terms of the mean output. The range represents the possible variation of output values to the mean output value, which was used to create the calibration curve. The results of this analysis can be viewed in Table 19.

Table 19: Relative range of output values from counterclockwise testing

Applied Torque (Nm)	Mean Output (unitless)	Output Range	± Relative Range (%)
0	0.1548	0.0047	3.02
18.9	0.0592	0.0003	0.49
37.81	0.0145	0.0003	2.24
56.72	0.0022	0.0006	29.50
94.53	-0.0387	0.0064	16.53
113.44	-0.0546	0.0012	2.11

Interestingly, the percent relative range of the output values has a much higher range for the counterclockwise values, than the clockwise values. This could be due to the fact that the counterclockwise outputs reduce to small values before becoming negative; so even though the range of outputs from counterclockwise testing are smaller than those from clockwise testing, they account for a larger difference in proportion to the size of the output values. This is corroborated by the fact that the relative range of the 113 Nm measurement was much lower than at 57 and 95 Nm. The mean output values taken at each of the specified torque values, along with their standard deviations can be viewed in Figure 30.

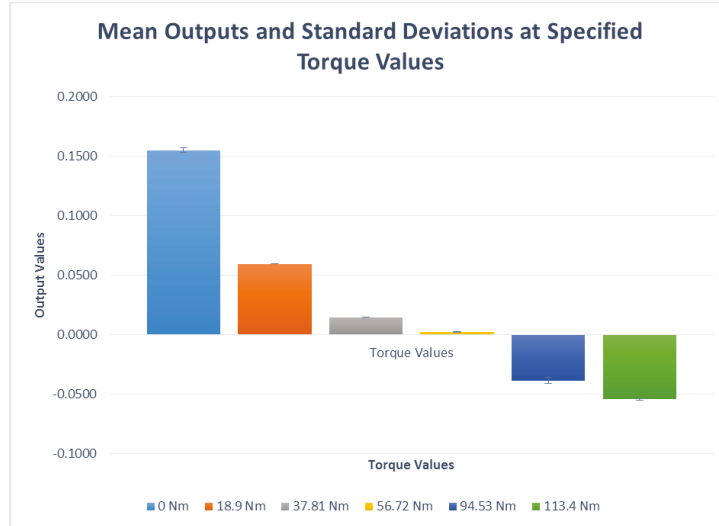


Figure 30: Mean outputs and standard deviations at specified torque values applied in the counterclockwise direction

Using the mean output value from the means of the five separate tests, a curve was created that plotted output values vs. the applied torque, Figure 31. Using the created curve an Excel trendline was created that formed a function to define the relationship between the output values and the applied torque. The generated function was described to fit the data with an R^2 value of 0.99. This calibration curve fits the majority of the data well, however, has a poor fit for low torque values. However, as we had determined previously, we are most interested in the torque values that span from 37.81 Nm to 113.44 Nm, so discrepancies in this portion of the curve are more allowable. Figure 31 also displays the standard deviations of each of the means.

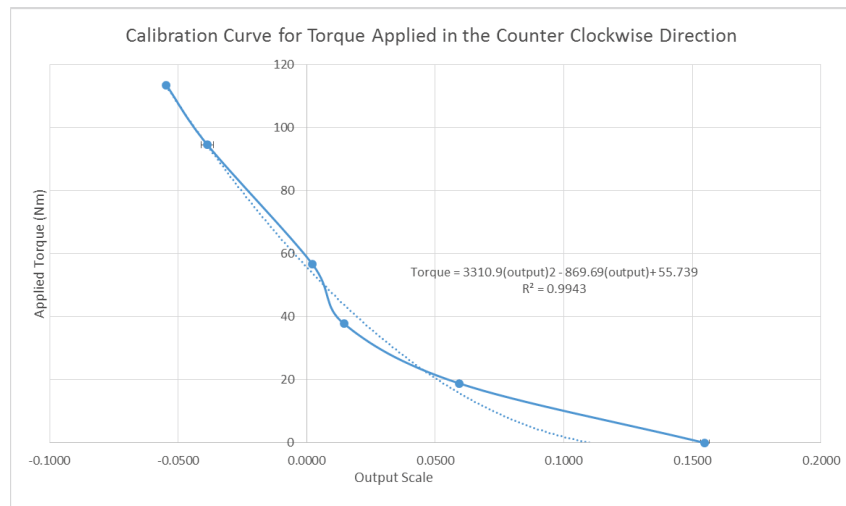


Figure 31: Calibration Curve for Torque Applied in the Counter Clockwise Direction

The trendline generated equation that related output values to torque values is as follows:

$$Torque = 3310.9(output)^2 - 869.69(output) + 55.739$$

Using this equation torque values were generated for each of the five tests performed at each known torque value. The mean, maximum, and minimum torque values were then determined at each known torque value. The percent relative range of these values was then determined by calculating the percent value of the range in terms of the mean measured torque. The range represents the possible variation of measured torque values to the mean measured torque value. The percent difference of the measurements was then determined by calculating the percent value of the mean of the measured torque to the known applied torque. These results can be viewed in Table 20.

Table 20: Percent Difference and Relative Rang of Torque Measurements in the Counter Clockwise Direction

Applied Torque (Nm)	Mean Torque (Nm)	Maximum Torque (Nm)	Minimum Torque (Nm)	± Relative Range (%)	± Difference (%)
0	0.46	0.83	0.10	*159.18*	*356.06*
18.9	15.84	15.91	15.77	0.87	16.17
37.81	43.85	43.97	43.72	0.57	15.98
56.72	53.87	54.15	53.60	1.01	5.02
94.53	94.32	96.15	89.03	7.56	0.23
113.44	113.06	113.85	112.43	1.25	0.34

Again, the percent relative range and difference for 0Nm torques was obtained by attributing the known torque the value of 0.1Nm. Due to this low torque value the range of percent difference and relative range will be high. The results of this testing reveal that the relative range of measured torque values, compared to the mean values, was generally lower and more constant than the measured values in the clockwise direction, with the majority of the values being under 2%. The percent difference between the measured torque and applied torque was also lower than with clockwise measurements, with three of the tested torque values being within 5% of the known applied torque. However, there were large percent differences at the lower tested torque values, this can be explained by the poor fitting of the trendline to the plotted data at lower torque values. This can be seen in figure 31 where output values 0.1548 through 0.0145 represent the torque values from 0 to 37.81 Nm. Due to this fact, an enhanced calibration curve could result in measurements with much lower percent differences, especially in the lower torque regions.

Due to the inherent offsets between the outputs produced by our system and strain, we adjusted our output values to account for these offsets and graphed the true strain outputs verse the applied torque values, Figure 32.

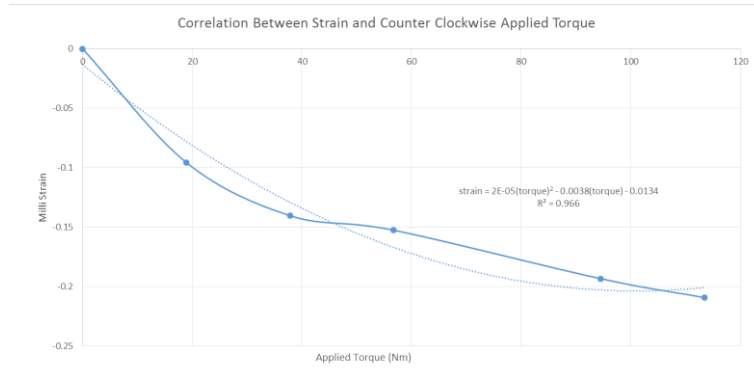


Figure 32: Correlation between strain and torque applied in the counterclockwise direction

A trendline for this data was produced, which related the applied torque to the true strain, expressed in milli-units. This trendline was found to fit the plotted data with an R^2 value of 0.966. The equation that related torque to strain is as follows.

$$\text{Milli Strain} = 2 \times 10^{-5}(\text{torque})^2 - 0.0038(\text{torque}) - 0.0134$$

This equation would be useful for determining the strain experienced by the dynamometer during testing.

6.3 Calibration Testing for Forward Bending Release Testing

Before conducting calibration testing, a range of torque values for testing was determined. To produce an accurate calibration curve, many different points should be tested. Due to time constraints however, we defined our calibration curve by testing done at six different known torques, including zero. These values were determined from using anthropometric data combined with the ASTM standards for the selection of release torque (CDC, 2010; ASTM, 2005). As this tester was designed for adult users, we felt it was most important to have an accurate calibration curve in the range of release torque values used by adult skiers. From our anthropometric data we determined that the 10th percentile female was 53.6 kg and from the ASTM release torque standards we established that this would encompass a type “I” skier, who would have a release torque value of 141 Nm in forward lean release. We then established that a 90th percentile male was 114.4kg, as the highest defined weight by the ASTM for release torque selection is 95 kg, we decided that our highest torque value measured should be at least 452 Nm, which was the release torque value for skier type “P” and the highest listed in forward lean release. However,

due to later concerns about the possibility of the extruded interface of the bottom piece deforming under the higher loads, we determined to set our highest torque value measured to 297 Nm. This value is slightly above that specified for skier type “M”, which encompasses skiers 95kg and greater, and is the last skier type with an associated weight range. The torque values that our calibration curve was tested with were thus 0, 118.88, 178.32, 237.75, and 297.19 Nm.

6.3.1 Test setup and methods for forward bending release testing

To apply the selected known torque values we created a pulley system that would connect to the top end of our one meter long lever at an angle fifteen degrees below the horizontal. The decomposition for the designed pulley system and calibration curve creation can be seen in Table 21.

Table 21: Create strain to torque calibration curve in forward bending release

2.1.3	FR	Create strain to torque calibration curve in forward bending release	DP	Known torque bending pulley system applicator for clockwise torsion and Excel Software
2.1.3.1	FR	Apply known torque	DP	Clockwise pulley system
2.1.3.1.1	FR	Generate predetermined force	DP	Pulley system that pulls lever arm forward
2.1.3.1.1.1	FR	Apply force to lever arm	DP	Olympic weights
2.1.3.1.1.2	FR	Apply forces at a fifteen degree angle to the lever arm	DP	Pulley system of a nominal height a nominal distance away from the lever arm
2.1.3.1.1.2.1	FR	Locate pulley at correct height	DP	Adjustable, wood support structure
2.1.3.1.1.2.2	FR	Allow room for gravity-weighted load	DP	Framed box structure
2.1.3.1.2	FR	Apply force at known lever arm length	DP	1 meter lever arm
2.1.3.2	FR	Create calibration curve	DP	Excel trendline

Our pulley system for our clockwise calibration testing involved a simple wooden box frame constructed with four 3"x3" pine columns, eight 2"x4" pine support boards, eight wood braces, and 24 3" wood screws. The top 2"x4" support board of each frame had a stainless steel metal pulley, for use with 3/8" diameter rope, with a 165 lb work load rating. The rope used for the pulley system was 3/8" diameter polypropylene and mixed synthetic rope. Olympic weight(s) were again attached to the rope to apply the known torque values. Due to the spacial constraints of our workspace and the Olympic weights that were available to us, we chose to apply our bending loads via a pulley located fifteen degrees below the horizontal plane of the point of the lever to which we attached the rope, a point 1.38m, 4' 6", from the surface of the table we were testing on. To accomplish this, our pulley was located 1.22m, 4', away from the attachment point in the horizontal direction and 0.33m, 1.07', away from the attachment point in the vertical direction. A SolidWorks model of our testing setup, with important reference geometries, can be viewed in Figure 33.

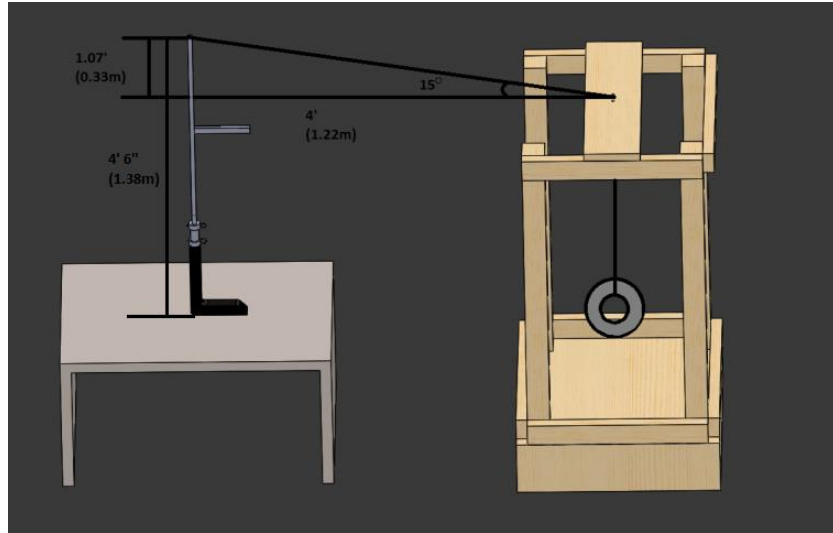


Figure 33: Forward bending torque applicator pulley system

The amount of weight needed for each side of the pulley system was calculated using the relationships between pounds and kilograms, mass and force, and the equations:

$$Mo = F(d\cos(\theta))$$

where Mo was the moment at the center of the lever around which torque was applied, d was the distance of the applied force, 1.38m, and θ was the angle between the lever arm and the force caused by the tension of the rope, 15°

Using this equation we found that 20, 30, 40, and 50 lb weights would be required to obtain the desired amount of applied torque to the system. Table 22 shows the relationship between the mass applied to the pulley system to the applied torque.

Table 22: The relationship between the applied mass and the applied torque

Mass (lbs)	Mass (kg)	Force (N)	Applied Torque (Nm)
20	9.09	89.18	118.88
30	13.64	133.77	178.32
40	18.18	178.36	237.75
50	22.73	222.95	297.19

6.3.2 Calibration curve, results, and analysis for forward bending release testing

Calibration testing was performed five times at each of the specified torque values, as well as at 0 Nm. Each of these individual tests were run for at least 10 seconds, which at a 1k sampling rate, meant that there were at least 10,000 data points for each individual test. Within each test run there were low standard deviations, which were dwarfed by the deviations seen between test runs, for this reason these deviations were not included for our calculations for percent difference and relative range of the system. Between each test the system was disassembled and then reassembled to ensure the robustness of the measurements.

The mean of the outputs of each of the five tests for each torque value was recorded. The maximum, minimum, range, and mean values of these five mean output values were then calculated. The percent relative range of the output was then determined by determining the percent value of the range in terms of the mean output. The range represents the possible variation of output values to the mean output value, which was used to create the calibration curve. The results of this analysis can be viewed in Table 23.

Table 23: Relative range of output values from forward bending testing

Applied Torque (Nm)	Mean Output (unitless)	Output Range	± Relative Range (%)
0	0.4877862	0.0009	0.18
118.88	0.654881	0.0015	0.23
178.32	0.695762	0.0012	0.18
237.75	0.7052584	0.0007	0.10
297.19	0.7129448	0.0010	0.14

The range of output values, relative to the mean measured outputs, was consistently much lower than in both clockwise and counterclockwise testing, with all values being well under 1%. The mean output values taken at each of the specified torque values, along with their standard deviations can be viewed in Figure 34.

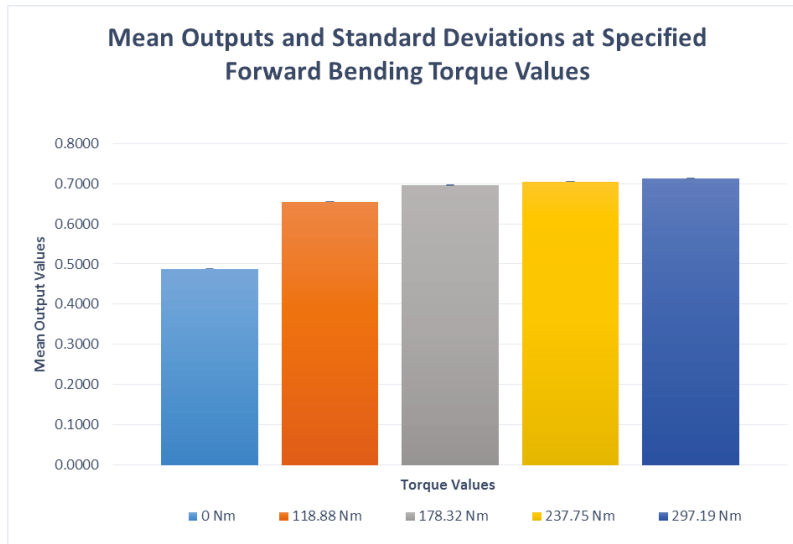


Figure 34: Mean outputs and standard deviations at specified forward bending torque values

Using the mean output value from the means of the five separate tests, a curve was created that plotted output values vs. the applied torque, Figure 35. Using the created curve an Excel trendline was created that formed a function to define the relationship between the output values and the applied torque. The generated function was described to fit the data with an R^2 value of 0.94. This calibration curve fits the output values poorly compared to the other produced calibration curves. Figure 35 also displays the standard deviations of each of the means.

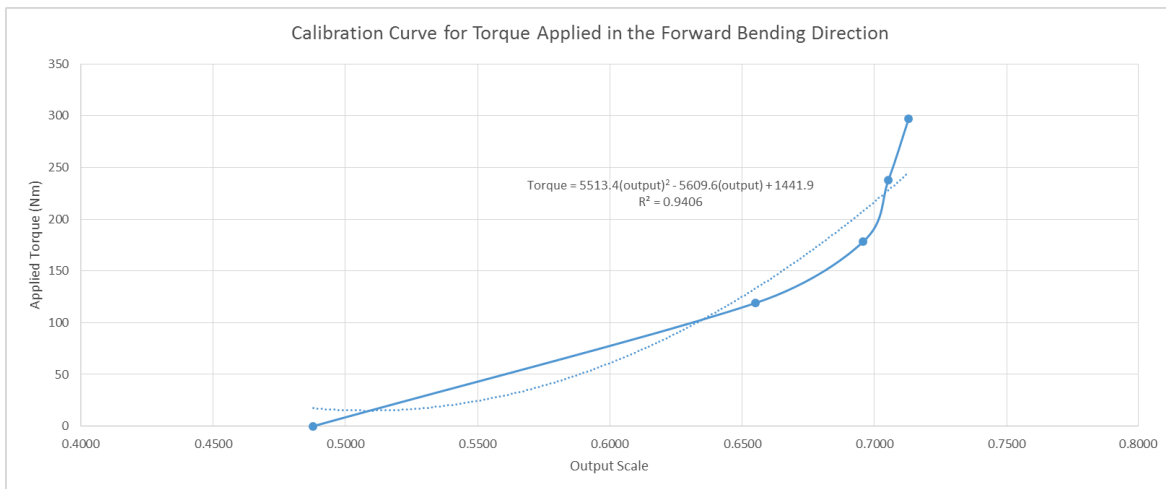


Figure 35: Calibration curve for torque applied in the forward bending direction

The trendline generated equation that related output values to torque values is as follows:

$$Torque = 5513.4(output)^2 - 5609.6(output) + 1441.9$$

Using this equation torque values were generated for each of the five tests performed at each known torque value. The mean, maximum, and minimum torque values were then determined at each known torque value. The relative range of these values was then determined by calculating the percent value of the range in terms of the mean measured torque. The range represents the possible variation of measured torque values to the mean measured torque value. The percent difference of the measurements was then determined by calculating the percent value of the mean of the measured torque to the known applied torque. These results can be viewed in Table 24.

Table 24: Percent Difference and Relative Range of Torque in the Forward Bending Direction

Applied Torque (Nm)	Mean Torque (Nm)	Maximum Torque (Nm)	Minimum Torque (Nm)	± Relative Range (%)	± Difference (%)
0	17.45	17.56	17.35	*1.18*	*17347*
118.88	132.81	134.04	131.61	1.83	11.71
178.32	207.91	209.21	206.69	1.21	16.59
237.75	227.99	228.68	227.11	0.69	4.11
297.19	244.97	245.96	243.65	0.94	17.57

As in previous sections, the percent difference and relative range for 0Nm torques was obtained by attributing the known torque the value of 0.1Nm. Due to this low torque value the percent difference and relative range will be high. The results of this testing reveal that torque measurements within the range of 0-297Nm would all have a range torque values that would be within $\pm 2\%$ of the measured torque. This suggests that the tester would produce torque measurements with small amounts of variance. The suspected reason that these results had a smaller range of torque values than those attained for clockwise and counterclockwise testing, is that someone with professional experience with applying strain gauges applied the strain gauges to the applicator tube we used for forward bending testing. However, there was a consistently large difference between the measured and applied torque values. This is due to the poor fit of the produced trendline to the plotted data, which can be seen in figure 35. The only measured value which is within 10% of the applied torque, is the measured value at 238 Nm, which corresponds to an output value of 0.705. However, due to the repeatable nature of the produced values and that the calibration curve was shown to poorly fit the produced data, an enhanced calibration curve could result in lower percent differences at each of the measured values. However, a second order polynomial may not be the best method of fitting this curve.

Due to the offsets between the outputs produced by our system and strain, we adjusted our output values to account for these offsets and graphed the true strain outputs verse the applied torque values, Figure 36.

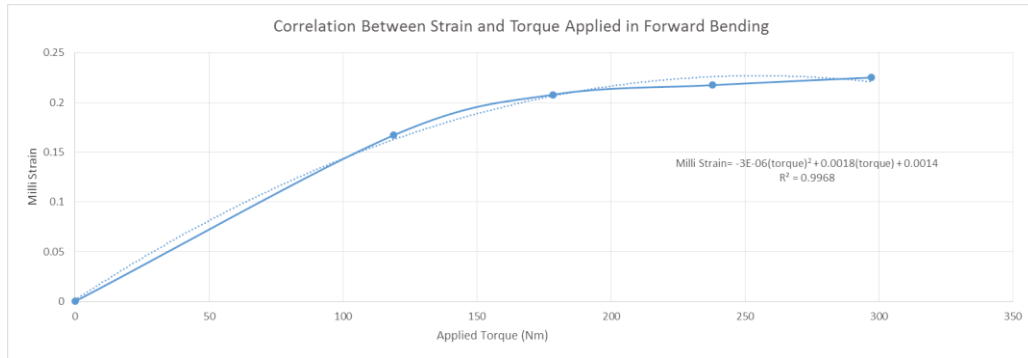


Figure 36: Correlation between strain and torque applied in forward bending

A trendline for this data was produced, which related the applied torque to the true strain, expressed in milli-units. This trendline was found to fit the plotted data with an R^2 value of 0.9968. The equation that related torque to strain is as follows.

$$\text{Milli Strain} = -3 \times 10^{-6}(\text{torque})^2 + 0.0018(\text{torque}) + 0.0014$$

This equation would be useful for determining the strain experienced by the dynamometer during testing.

6.4 SBB System Testing for Clockwise and Counterclockwise Release Testing

After calibration curves were produced and initial testing for percent difference and relative range was conducted on clockwise, counterclockwise, and forward bending applied loads, the device was tested in a ski boot binding system. This testing was done to determine the percent difference and relative range of our system under non-constant loading situations, specifically when used to release a ski boot from its binding. The testing also served to provide information on the torque experienced by the binding over time. The control “known” release torque values were taken from the release torque values taken from Vermont Release Calibrator testing. However, there is some error associated with using the Calibrator for our known release torque values as it is only guaranteed to be within $\pm 5\%$ of the actual release torque, so for our experiment it would have a percent difference range of ± 3.02 Nm of the mean measured release torque value, approximately 60.45 Nm (ASTM, 2008).

The setup for our SBB system testing was the same for both clockwise and counterclockwise testing, the only difference was the direction of the force applied to the lever arm. The SBB system was secured to

our testing station using a Tilt Vise from Vermont Ski Safety (Vermont Ski Safety, 2010). Two c-clamps were used to connect the Tilt Vise to our testing surface was of the correct dimensions for direct vise attachment. The Vermont Release Calibrator Prosthetic foot was used as the interface between the SBB system and both testing devices. An explanation of how the Vermont Release Calibrator can be used can be viewed in the State of the Art section of the paper. Figure 37 shows the testing setup for the Vermont Release Calibrator tester, left, and for our electronic dynamometer tester, right. The blue markers seen in the picture to the right are markers that we used to identify each strain gauge lead, to facilitate correct connection of the leads to the full-Wheatstone bridge circuit.



Figure 37: Ski Boot Binding Testing Setup for the Vermont Release Calibrator (left) and the designed device (right)

For both clockwise and counterclockwise testing five tests were run with both the Vermont Release Calibrator and our testing device. Testing with both devices was conducted until the boot released from the binding. In regards to the designed tester, testing of release occurred over a period of approximately 4.2 to 8 seconds, which at a 1k sampling rate, meant that 4,200 to 8,000 data points were collected during each test. Data acquisition through SignalExpress was also performed in the same manner for these tests as it was for prior testing.

6.4.1 Clockwise testing results and analysis

Over a series of five test runs the Vermont Release Calibrator measured the mean release torque of the SBB system to be 60.45 Nm, with four of the five release values being 60.5 Nm. These values can be seen in Table 25. Subsequent testing of the same SBB system with our device produced a characterization of all torque experienced by the tester during release over time. Due to this, our produced data included a ramping section where torque was initially being applied and section between when the binding was released and when we stopped the test. To account for these ramping and cut-off sections the acquired data was only analyzed from the 2 to 4 second timeframe for their mean, maximum, and minimum values for all tests. This was due to the fact that all of the tests evaluated were

at a stable state from 2 to four sections as seen by one example of the generated torque vs time graphs in Figure 38. All of the generated torque vs time graphs can be viewed in Appendix F. However, as our tests showed that the binding absorbed the load until an instantaneous release at a certain time-point, we took the last non-zero, or near non-zero, torque value to be the release torque value, which generally occurred after the 4 second mark. These values, as well as the range of torque values from 2 to 4 seconds can also be seen in Table 25. These values in combinations with the curves generated from each test, Figure 38, serve to define the behavior of release.

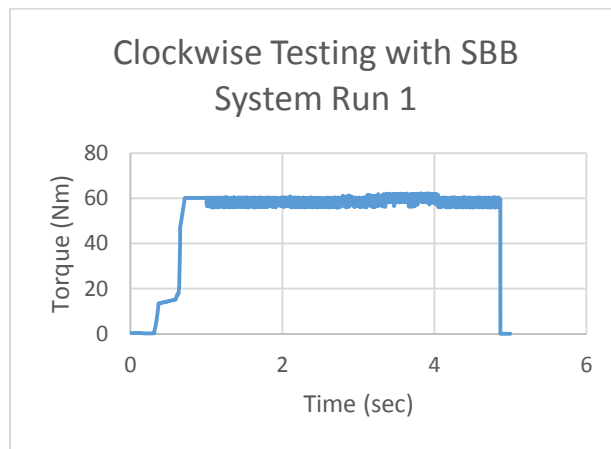


Figure 38: Torque to release over time for clockwise run 1 with our device

Table 25: Characterization of torque to release measurements from a Vermont Release Calibrator and the designed device

Run Number	Vermont Release Calibrator Measurement (Nm)	Maximum Torque (Nm)	Minimum Torque (Nm)	Mean Torque (Nm)	Torque at Release (Nm)	Torque Range (Nm)
1	60.5	62.214	55.88	58.956	57.94	6.331
2	60.5	61.536	59.010	60.281	60.80	2.526
3	60.5	61.539	59.009	60.269	61.13	2.530
4	60.25	61.538	59.011	60.259	61.53	2.527
5	60.5	61.538	59.012	60.264	59.93	2.527

These results suggest that the binding responds to the applied load by gradually displacing the boot within the binding and then releasing instantaneously once the boot has reached a certain threshold of displacement. This hypothesis would have to be corroborated with displacement testing in order to

determine its validity. These results also indicate that the maximum torque experienced by the system is not necessarily the torque that the boot is released from the binding at. This is significant as torque to release testers such as the Vermont Release Calibrator assess the greatest magnitude of torque experienced by the binding.

After analyzing the generated torque vs time curves, we determined the percent difference and relative range of our tester. The relative range of the Vermont Release Calibrator was established by calculating the percent value of the range of release torque values in terms of the mean measured torque, over the five measurement series. The range represents the possible variation of the measured torque value to the mean measured torque value. The Vermont Release Calibrator was assumed to have a maximum percent difference of $\pm 5\%$ from the actual release torque (ASTM, 2008). The relative range of the results generated by the developed tester was established by calculating the percent value of the range of the maximum measured torque values, in terms of the mean of the maximum measured torque values, over the five measurement series. The maximum measured torque values, column 3 of the preceding table, were used as the Vermont Release Calibrator technically measures to the highest registered torque value and not the torque at the moment of release. The percent difference of the measurements from our tester, from the values shown by the Vermont Release Calibrator, was then determined by calculating the percent value of the mean of the maximum measured torque to the mean of the release torque values obtained from the Vermont Release Calibrator. These results can be viewed in Table 26.

Table 26: Percent difference and relative range of the Vermont Release Calibrator and the designed device

Mean Maximum Measured Torque (Nm)	Minimum, Maximum Measured Torque (Nm)	Maximum, Maximum Measured Torque (Nm)	\pm Relative Range (%)	\pm Difference (%)
61.67	61.54	62.21	1.01	2.02
Mean Vermont Release Calibrator Measurement (Nm)	Minimum Vermont Release Calibrator Measurement (Nm)	Maximum Vermont Release Calibrator Measurement (Nm)	\pm Relative Range (%)	\pm Difference (%)
60.45	60.25	60.5	0.41	*5*

These results indicate that the measurements taken with our device within a $\pm 1.01\%$, ± 0.63 Nm, range to the mean maximum measured torque and were within $\pm 2.02\%$, ± 1.22 Nm, of the mean release torque measured by the Vermont Release Calibrator. These results are surprising as the relative range of continuously applied clockwise torques, during calibration, at 56Nm and 94Nm were $\pm 8.62\%$, ± 4.8 Nm,

and $\pm 0.92\%$, ± 0.86 Nm, respectively, while the percent difference at these torque values were $\pm 5.11\%$, ± 2.86 Nm, and $\pm 6.4\%$, ± 6.02 Nm, respectively. Possible reasons why our results with the SBB system had a smaller relative range and percent difference were that these tests were all conducted on the same day, at the same time, unlike the calibration tests. Also, we did not remove the tester between each test as we did with calibration testing. The tested torque value 60.4 Nm also lies between the two torques values mentioned on the calibration curve, so the percent difference of the results is completely dependent on the fit of the counterclockwise calibration curve at this value.

6.4.2 Counter clockwise testing results and analysis

Over a series of five test runs the Vermont Release Calibrator measured the mean release torque of the SBB system to be 60.4 Nm. The values for these runs can be seen in Table 27. Subsequent testing of the same SBB system with our device produced a characterization of all torque experienced by the tester during release over time. Due to this, our produced data included a ramping section where torque was initially being applied and section between when the binding was released and when we stopped the test, which was the same as the behavior of the applied torque in the clockwise direction. To account for these ramping and cut-off sections the acquired data was only analyzed from the 2 to 4 second timeframe for their mean, maximum, and minimum values for all tests. This was due to the fact that all of the tests evaluated were at a stable state from 2 to four sections as seen by one example of the generated torque vs time graphs in Figure 39. All of the generated torque vs time graphs can be viewed in Appendix G. However, as our tests showed that the binding absorbed the load until an instantaneous release at a certain time-point, we took the last non-zero, or near non-zero, torque value to be the release torque value, which generally occurred after the 4 second mark. This procedure was the same as that used for the characterization of the torque vs time data from clockwise testing. These values, as well as the range of torque values from 2 to 4 seconds can also be seen in Table 27. These values in combinations with the curves generated from each test, Figure 39, serve to define the behavior of release.

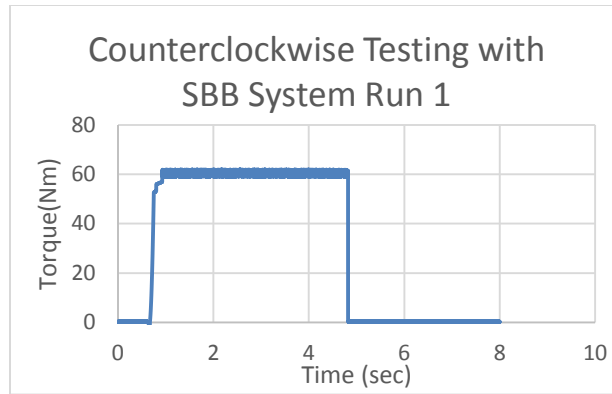


Figure 39: Torque to release over time for counterclockwise run 1 with our device

Table 27: Characterization of torque to release measurements from a Vermont Release Calibrator and the designed device

Run Number	Vermont Release Calibrator Measurement (Nm)	Maximum Torque (Nm)	Minimum Torque (Nm)	Mean Torque (Nm)	Torque at Release (Nm)	Torque Range (Nm)
1	60.25	61.996	58.960	60.474	61.43	3.036
2	60.5	61.995	58.959	60.501	60.98	3.035
3	60.5	61.996	58.963	60.472	60.28	3.033
4	60.5	61.997	58.960	60.466	61.65	3.037
5	60.25	61.993	58.959	60.468	61.62	3.034

These results corroborate the response patterns we identified in clockwise release; that the binding responds to the applied load by gradually displacing the boot within the binding and then releasing instantaneously once the boot has reached a certain threshold of displacement. This hypothesis would have to be corroborated with displacement testing in order to determine its validity. The maximum torque experienced by the system was also not the same value as the torque that the boot is released from the binding at.

After analyzing the generated torque vs time curves, we determined the percent difference of the values measured from our tester from the values measured with the Vermont Release Calibrator and relative range of the values measured from our tester. The percent difference and relative range of the Vermont Calibrator measurements and of our designed device were assessed in the same manner as they were for clockwise testing. The relative range of the Vermont Release Calibrator was established by calculating the percent value of the range of release torque values in terms of the mean measured torque, over the five measurement series. The range represents the possible variation of the measured

torque value to the mean measured torque value. The Vermont Release Calibrator was assumed to have a maximum percent difference of $\pm 5\%$ from the actual release torque (ASTM, 2008). The relative range of the results generated by the developed tester was established by calculating the percent value of the range of the maximum measured torque values, in terms of the mean of the maximum measured torque values, over the five measurement series. The maximum measured torque values, column 3 of the preceding table, were used as the Vermont Release Calibrator technically measures to the highest registered torque value and not the torque at the moment of release. The percent difference of the measurements from our tester, from the values shown by the Vermont Release Calibrator, was then determined by calculating the percent value of the mean of the maximum measured torque to the mean of the release torque values obtained from the Vermont Release Calibrator. These results can be viewed in Table 28.

Table 28: Percent difference and relative range of the Vermont Release Calibrator and the designed device

Mean Maximum Measured Torque (Nm)	Minimum Maximum Measured Torque (Nm)	Maximum Maximum Measured Torque (Nm)	\pm Relative Range (%)	\pm Difference (%)
61.995	61.993	61.997	0.007	2.64
Mean Vermont Release Calibrator Measurement (Nm)	Minimum Vermont Release Calibrator Measurement (Nm)	Maximum Vermont Release Calibrator Measurement (Nm)	\pm Relative Range (%)	\pm Difference (%)
60.4	60.25	60.5	0.414	*5*

These results indicate that the measurements taken with our device had a range of $\pm 0.007\%$, ± 0.004 Nm, in respect to the mean maximum measured torque and were within $\pm 2.64\%$, ± 1.6 Nm, of the mean release torque measured by the Vermont Release Calibrator, 60.4 Nm. These results are surprising as the relative range of continuously applied counterclockwise torques at 56Nm and 94Nm were $\pm 1.01\%$, ± 0.56 Nm, and $\pm 7.56\%$, ± 7.1 Nm, respectively, while the percent difference from the known applied torque at these values were $\pm 5.02\%$, ± 2.91 Nm, and $\pm 0.23\%$, ± 0.22 Nm, respectively. Possible reasons why our results with the SBB system were more accurate and reproducible were that these tests were all conducted on the same day, at the same time, unlike the calibration tests. Also, we did not remove the tester between each test as we did with calibration testing. The tested torque value 60.4 Nm also lies between the two torques values mentioned on the calibration curve, so the percent difference of

the results from the known value is completely dependent on the fit of the counterclockwise calibration curve at this value.

6.5 Additional Calibration Curve Validation Testing for Forward Bending Testing

Additional validation of the calibration curve for forward bending testing was done instead of testing with the SBB system. This was due to the fact that the calibration curve for bending was shown have high percent differences, between $\pm 4.11\%$ and $\pm 17.57\%$, over the range of tested values. Additionally, the Vermont Release Calibrator would not stay in the test boot during attempts at forward bending release, as the tongue of the tested boot would displace and come out. It was later determined that for this mode of release testing, a strap is placed under the heel of the boot. This strap allows for the upward load to be transmitted. Validation of the calibration curve for forward bending was carried out using the same test methods used for creating the calibration curve and testing the measured torque values against the known applied torque values in forward bending. However, for these tests we evaluated the percent difference and relative range of the measured torque values generated by the device outputs and calibration equation at a known torque value of 148.6 Nm. Using the equation,

$$M_o = F(d\cos(\theta))$$

*where M_o was the moment at the center of the lever around which torque was applied,
 d was the distance of the applied force, 1.38m,
and θ was the angle between the lever arm and the force caused by the tension of the rope, 15°*

from section 6.3.1 we determined that a load of 25 lbs would be needed to generate a torque of this magnitude.

6.5.1 Testing results and analysis

Calibration testing was performed five times at 148.6Nm, with each of these individual tests being run for at least 10 seconds, which at a 1k sampling rate, meant that there were at least 10,000 data points for each individual test. Within each test run there were low standard deviations, which were dwarfed by the deviations seen between test runs, for this reason these deviations were not included for our calculations for percent difference and relative range of the system. Between each test the system was disassembled and then reassembled to ensure the robustness of the measurements. This procedure was the same used as the procedure used for initial calibration curve testing.

The same trendline generated equation, derived in section 6.3.2, that related output values to torque, for calibration testing was used for the validation testing:

$$Torque = 5513.4(output)^2 - 5609.6(output) + 1441.9$$

Using this equation torque values were generated for each of the five tests performed at each known torque value. The mean, maximum, and minimum torque values were then determined at each known torque value. The relative range of these values was then determined by calculating the percent value of the range in terms of the mean measured torque. The range represents the possible variation of measured torque values to the mean measured torque value. The percent difference of the measurements was then determined by calculating the percent value of the mean of the measured torque to the known applied torque. These results can be viewed in Table 29.

Table 29: Percent difference and relative range of the forward bending calibration curve at 148.6 Nm of applied torque

Run Number	Mean Measured Torque (Nm)	Maximum Measured Torque (Nm)	Minimum Measured Torque (Nm)	± Relative Range (%)	± Difference (%)
1	168.66	169.95	167.96	2.66	12.57
2	168.01	168.95	166.97		
3	167.23	167.96	166.48		
4	166.55	167.47	165.98		
5	165.96	166.48	165.49		

These results further demonstrate the unreliability of the torque values generated by our device with torque applied in forward bending. The difference of the measurements from the applied 148.6 Nm was within ±12.57%, ±18.68 Nm, which is a reflection of the poorly defined calibration curve. The relative range of the measured values, ±2.66%, ±4.49 Nm, was also greater than from the initial calibration testing, where the worst percent relative range was 1.83%, ±2.17 Nm. This leads to concerns about the consistency of our device and suggests that further testing is needed.

7. Design Iteration

Torque to release may be insufficient to identify injurious situations from non-injurious situations, as is the case with the “bow effect” [Appendix A] (Brown and Ettlinger, 1985; Young, 1989). An electronic torque tester interfaced with a displacement sensor provides several advantages. A torque-displacement binding test system has the ability to test for both torque-to-release and work-to-release. Measuring work-to-release will identify a bindings shock absorptive capabilities and thus its susceptibility for inadvertent releases caused by such mechanisms as the “bow effect”.

A displacement sensor for this system must meet previously established constraints of the project; sensor uncertainty must be within ± 0.2 mm and remain within the project budget. Uncertainty was defined using the standards described in ASTM E2655, which defines uncertainty as “an indication of the magnitude of error associated with a value that takes into account both systematic errors and random errors associated with the measurement or test process” (ASTM E2655, 2008). The equation for uncertainty from ASTM E2655 is as follows:

$$\text{Uncertainty} = \sigma / \sqrt{n}$$






Where σ = the standard deviation, and
 n = the number of measurements

$$\sigma = \pm \sqrt{\frac{\sum (x - \bar{x})^2}{n}}$$

n = the number of measurements
 x = the sample
 \bar{x} = the sample mean

Several sensor options were considered during preliminary research [Table 30]. The parameters compared between the sensor options were measurement method, uncertainty, and cost.

Table 30: Displacement sensor comparison

	Optical Mouse	NDI Polaris	Leap Motion	Rotary Potentiometers	Rotary Encoder
Picture					
How does it measure?	Pixel displacement	Two passive markers are attached to a reference and moving object. Translation is recorded.	Using a 300 fps camera, this device will accurately track all ten fingers. It creates a 6 cubic foot an is accurate up to 0.01mm.	Output is ratiometric voltage with regards to length of cable. LabView capable with two solder points.	Use incremental rotary encoder. Highly accurate. Capacitance; easy data recording.
Uncertainty	See Previous MQP	0.4 mm	0.01 mm	0.15 - 0.25 mm	0.0004 mm
Simplicity? (1-10 scale)	7	5; Expensive surgical precision. Access in WPI AIM Lab.	3; will likely need to be programmed to recognize anything other than fingers.	8; simple set-up and integration. Accurate and repeatable.	5; displacement system design gets more complex.
Cost?	\$20	> \$1,000	\$80	\$169	< \$100
Website		http://www.ndigital.com/medical/products/polaris-family/#specifications	https://www.leapmotion.com/	http://www.celesco.com/_datasheets/sm1.pdf	http://www.baumer.com/us-en/products/rotary-encoders

Initial design requirements were defined using Nam Suh’s axiomatic design theory [Appendix B], and fundamental requirements and design parameters of the system were defined in *Acclaro* software. The utmost fundamental requirement of this displacement sensor system is the ability to measure angular displacement of the boot in binding during several loading conditions [Table 31]

Table 31: Initial decomposition for torque-displacement binding tester

0	FR	Determine a bindings ability to release only in response to injurious loads	DP	Torque-displacement binding tester
1	FR	Determine binding response to tibial axis torsion	DP	Twist release tester
1.1	FR	Measure torsion about z-axis accurately in time	DP	Dynamometer System
1.2	FR	Measure angular x-y axis displacement of boot in binding	DP	Displacement Sensor system
2	FR	Determine binding response to forward bending loads	DP	Forward bending release tester
2.1	FR	Measure torque applied about the positive y-axis accurately in time	DP	Dynamometer System
2.2	FR	Measure angular displacement of the boot in the x-z plane accurately in time	DP	Displacement Sensor system
3	FR	Determine binding response to backwards bending loads	DP	Backwards bending release tester
3.1	FR	Measure torque applied about the negative y-axis accurately in time	DP	Dynamometer System
3.2	FR	Measure angular displacement of the boot in the x-z plane accurately in time	DP	Displacement Sensor system
4	FR	Analyze signals for Work to Release	DP	Excel equation and graphing functions

7.1 Optical Mouse

Recent work at Worcester Polytechnic Institute was completed titled ‘Torque-Displacement Binding Tester’ by (Merrill, 2013). In this project feasibility testing was performed using an optical mouse as a displacement sensor. ‘The optical mouse as a two-dimensional displacement sensor’ also validates a mouse for x-y displacement measurement (Ng, 2003). Testing included linearity, repeatability, and uncertainty. At roughly \$20, a mouse was an affordable sensor. Electronic integration was easily performed using readily available National Instruments software. Considering the aforementioned, the initial displacement system design utilized an optical mouse as the sensor.

7.1.1 Design Decomposition

First, a design decomposition was created to determine how the mouse would be used to obtain accurate data over time [Table 32].

Table 32: Decomposition for a displacement measurement system utilizing an optical mouse

1.2	FR	Measure angular displacement of boot in binding	DP	Displacement Sensor system
1.2.1	FR	Connect mouse and boot	DP	Detachable lever-arm fixation device
1.2.1.1	FR	Secure arm to mouse	DP	Spring Loaded Pin
1.2.1.2	FR	Secure arm to boot	DP	Mounting system
1.2.1.2.1	FR	Secure arm to mounting bracket	DP	Collar
1.2.1.2.2	FR	Secure Mounting bracket to boot	DP	Bracket and Threaded Rod
1.2.2	FR	Provide signal measurement readable by computer	DP	Signal conditioning amplifier and DAQ module
1.2.3	FR	Read and export displacement data to analysis software	DP	Labview
1.2.4	FR	Analyze displacement signals appropriately	DP	Excel equation and graphing functions
1.2.4.1	FR	Determine maximum displacement	DP	Excel
1.2.4.2	FR	Determine displacement at different percent torques	DP	Excel graphing and equation functions

In order to measure displacement of the boot accurately, simultaneous and stiff articulation of the mouse is necessary. To satisfy this requirement a ‘detachable and stiff fixation arm’ would grapple the mouse on the side of the boot. This arm would articulate the mouse with any boot displacement. Due to the several loading conditions during test, a detachable and adjustable solution is required. In order to connect the arm and mouse, a spring loaded pin would be used to ensure precise z-axis distance. An optical mouse is inoperable without a proper surface to image from. The arm/mouse must also be secured to the ski boot. To accomplish this, a pair of brackets would locate a rod along the length of the side of the boot. The arm would then secure to this rod using a shaft collar. This would complete the physical design. For twist release only x-y position is considered, and only x-z position is considered for bending.

Measuring displacement also requires the ability to read and export displacement data electronically. To satisfy this requirement we utilized the virtual instrument capabilities of *National Instruments Labview* software. As the mouse travels across the computer screen during binding release, the x-y location of the mouse and time data is exported to Excel for analysis. With this decomposition, a fully exhausted and mutually exclusive design is accomplished.

7.1.2 Shortcomings of Optical Mouse

Despite the findings of other scholarly works, testing was performed to fully validate linearity, repeatability and uncertainty within the scope of our design. Despite exhaustive experimentation (Appendix H), the level of uncertainty of an electronic mouse was not within our constraint of 0.2 mm. Despite a rated resolution of 2000 dpi, an optical mouse is not a viable sensor in this application. Several sources of error were analyzed and documented.

Firstly, an optical mouse's accuracy is strictly dependent on a precise z-axis distance. With any separation from the imaging surface, the mouse becomes inoperable. In binding testing procedures the boot may twist and roll along the x-axis creating z-axis separation. This is difficult to mitigate in a binding test. A third source of error with a mouse is top speed. Binding testing is to be performed with applied torque for a maximum of 5 seconds (ASTM, 2009). This quick release may be difficult to capture with an electronic mouse, a 1000 dpi gaming mouse has a top speed around 0.5 m/s (Windows, 2002). This is not adequate for this application.

Additional error can be incurred due to smoothing or anti-aliasing functions built in to the mouse hardware. Designed to smooth the translation of the cursor on the screen, these minor adjustments can affect trajectory across the screen as well as cause significant lag. These properties will dramatically decrease the accuracy of a computer mouse. Lastly, screen size will limit the amount of recordable displacement distance. If the cursor runs into the edge of the screen during testing, data is halted at that point. This limitation requires additional preliminary setup, and may go unnoticed.

7.2 NDI Polaris

A highly accurate spatial measurement system, the Northern Digital Polaris, was developed to further image-guided surgery in operating rooms. Using advanced tracking algorithms this system provides exceptional accuracy, a 95% confidence interval of 0.4 mm (Wiles et al., 2004). Producing a large virtual measurement volume [Figure 40], both passive and active markers can be tracked within the working space. Active markers produce infrared light that are activated by an electrical signal, while passive markers use retro-reflective coatings to reflect infrared light back to the sensor. The price of such a system is in upwards of \$1500, making this an unmarketable solution. Despite this price tag, further testing was performed in order to understand the technology and the potential for this application. This portable solution was provided by the Worcester Polytechnic Institute 'Automation and Interventional Medicine Laboratory', providing the means to analyze image tracking hardware for this application.

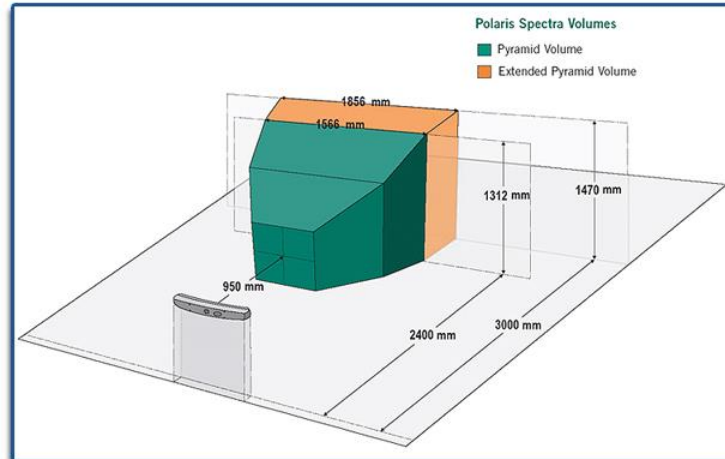


Figure 40: Volume of Polaris measurement range (NDI, 2014)

2.2.1 Design Decomposition

The following decomposition demonstrates how the NDI Polaris would be used to obtain accurate displacement data [Table 33].

Table 33: Decomposition for a displacement measuring system utilizing the NDI Polaris

1.2	FR	Measure angular displacement of boot in binding	DP	Displacement Sensor system
1.2.1	FR	Track boot displacement	DP	NDI Polaris
1.2.1.1	FR	Track reference position	DP	Passive markers and position sensor
1.2.1.2	FR	Track displacement of boot	DP	Passive markers and position sensor
1.2.2	FR	Provide displacement signal measurement readable by computer	DP	Wireless optical mouse
1.2.3	FR	Read and export displacement data to analysis software	DP	Optical Measurement System and API software
1.2.4	FR	Analyze displacement signals appropriately	DP	Excel equation and graphing functions
1.2.4.1	FR	Determine maximum displacement	DP	Excel
1.2.4.2	FR	Determine displacement at different percent torques	DP	Excel graphing and equation functions

The NDI Polaris can reproduce a transformation of movement using 3D Euclidean positioning data (Wiles et al., 2004). In order to obtain necessary data, the boot's position is tracked with respect to a reference position. This reference was located directly along the x-axis with a passive marker. As the boot moves during testing, this motion is also tracked with a second passive marker. Comparing the initial to the final position yields a complete transformation of displacement. For twist release only x-y position is considered, and only x-z position is considered for bending.

The Polaris system also has the capability to electronically read and export data to Excel. This feature produces 3D Euler angle point per frame. This complete data set can be ignored, only focusing on the necessary axis transformations.

7.2.2 Shortcomings of NDI Polaris

Validation testing was performed with the Polaris device in an attempt to validate its use as a displacement sensor. A simple displacement test was conducted in attempt to obtain data regarding the linearity, repeatability and accuracy of the system (Appendix I). Despite several tests, results were unfavorable. With a nominal uncertainty of 0.4mm, data estimated an additional error magnitude of 0.3mm (NDI, 2014; Wiles et al., 2004). Based on the required accuracy of ASTM standard testing procedures, this tool does not meet constraints. These series of experiments did however provide excellent insight into imaging technology for tracking purposes.

Several other shortcomings were recognized through experimentation. Firstly, the working space required by the Polaris is quite large. Nearly a 10'x10' testing area is required. This requirement is not ideal in local ski shops where space is a premium. Another difficulty with this device is with its integration with a torque-to-release tester. Polaris data can be exported to *Excel* as a running series of frames and associated 6D position. No time stamp data is included however, increasing difficulty of aligning the two peaks of torque and displacement data. The cost of the equipment must also be considered. With a price tag of greater than \$1,000, this does not meet project constraints set previously. Overall the NDI Polaris is not a viable displacement sensor for this application.

7.3 Additional Displacement Sensors

Following difficulty with the Mouse and the NDI Polaris, several other displacement sensor options were explored. Inadequacies of these two systems were recognized and improved upon. A major necessity was the level uncertainty. Constraints requiring uncertainty of 0.2mm require a highly accurate, and therefore more expensive, sensor. The required space for such a sensor was also a concern. Ideally a working space would be a table top. With an electronic torque-displacement sensor, access to a computer is vital. Budgetary constraints were also considered.

7.3.1 Rotary and String Potentiometers

Rotary potentiometers express angular rotation in terms of voltage output. These highly accurate devices are sensitive to within 0.1mm, sufficient for this application. They can be used to measure both linear and angular displacement and can be easily integrated with a torque-to-release tester. Rotary potentiometers can also be spring loaded, called a string potentiometer. By attaching two of these spring loaded string pots can be attached to the boot, measuring both x and y axis displacement [Figure 41]. The potentiometer on the toe of the boot measures x position, and the side mounted pot measures position on the y axis. The following equation can then be used to calculate displacement:

$$Displacement = \sqrt{(\Delta x)^2 + (\Delta y)^2}$$

Where Δx = change in position in the x – direction

Δy = change in position in the y – direction

With a stroke length of over 200mm, this is adequate capability for expected boot-binding displacement. The price of these sensors can be upwards of \$300 for a pair. This is a direct result of its high precision and repeatability capabilities. Despite this somewhat high cost, expected results are much better with these sensors. This is a potentially viable option for a torque-displacement tester.

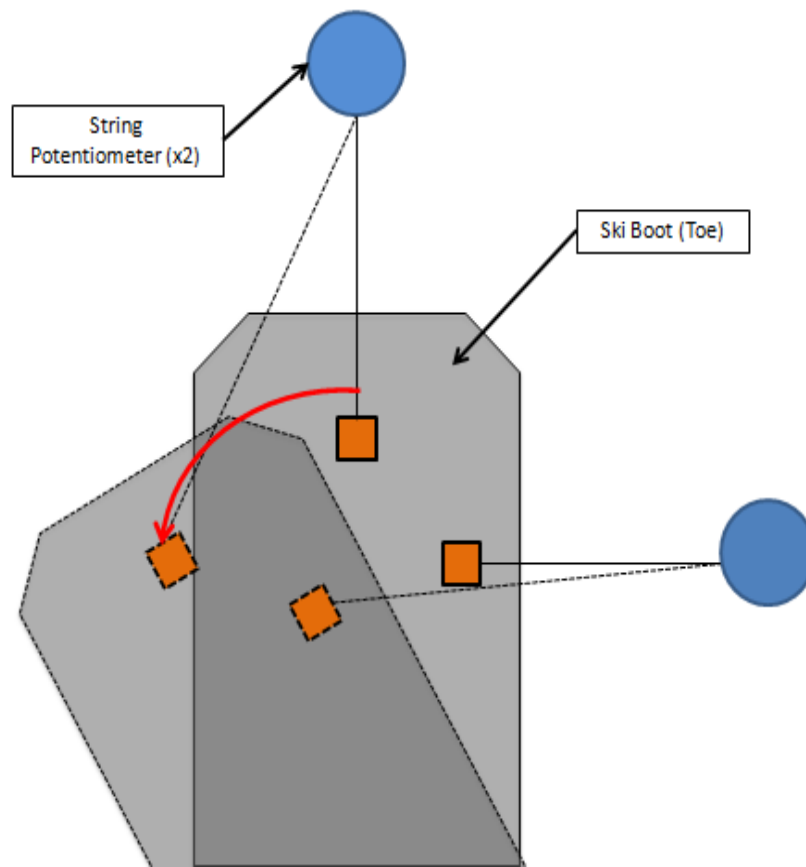


Figure 41: Displacement measurement with string potentiometers

7.3.2 Rotary Encoders

Another sensor to be considered is rotary encoders. These devices measure displacement by converting angular position to analog or digital code. There are two main types of rotary encoders: incremental and absolute. Absolute rotary encoders maintain position information when power is removed. Incremental rotary encoders record changes in position, but do not initiate with a fixed relation to physical position. The capability to “zero” the sensor with its initial position, make

incremental encoders the better choice for this application. With a precision up to 2/1000 of a millimeter and a cost of \$100 per encoder, rotary encoders are promising. Designing a displacement system with these sensors is more difficult however. Typically, rotary encoders are shaft driven, a motion not easily captured over two axes. Setup is similar to string potentiometers, using a tether to turn the shaft of the encoder. Highly precise and affordable, rotary encoders are a viable option for this application. Additional design time would yield an effective displacement tool (BEI Sensors, 2014).

7.3.3 Leap Motion

Another possibly effective tool for measuring displacement is the Leap Motion. This new product is used to translate hand and finger motion and translate the motion electronically, analogous to a mouse. This system requires no touching or contact and manipulation is responsive to all ten fingers at once. Three infrared LEDs and two IR cameras create a 6 cubic foot workspace [Figure 42]. Analyzing 300 frames per second, information is sent through USB to the computer (LeapMotion, 2014).

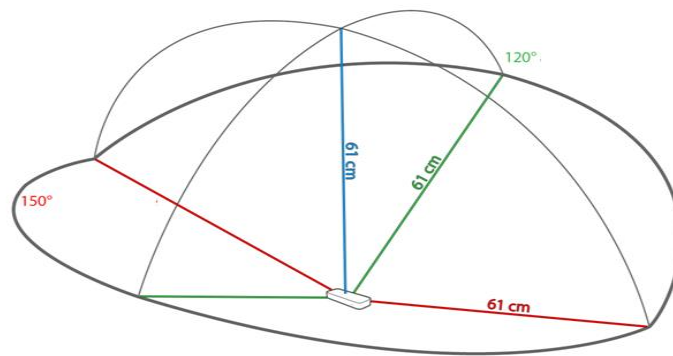


Figure 42: Working range of a LeapMotion (LeapMotion, 2014)

The Leap Motion is listed with a precision of 1/100th of a millimeter (LeapMotion, 2014). With a cost of only \$80, the specifications are extremely impressive. However, this is a new technology. As a venture backed project, applications for the device are broad. Currently the system is only capable of reading hand motion. That being said, Leap Motion provides developer resources regarding the device API. This access provides application development. In order to measure ski boot displacement, the system must be able to track a marker on the boot. With someone who is knowledgeable of Computer Science there is a great opportunity for precise image tracking. This small device is an excellent candidate for a torque-displacement system.

8. Discussion

8.1 Satisfaction of the Objective

The objective of this Major Qualifying Project was to design an alpine ski binding testing device that measures the torque, displacement, and work to release ski boots from bindings in response to multiple quasi-static loading configurations in the y and z axis. Such a test device would be able to identify ski binding devices' susceptibility for inadvertent release [Appendix A].

This objective was partially satisfied with the successful design and manufacture of an electronic torque dynamometer. Several tests were performed in clockwise, counter-clockwise, and forward bending loading configurations, y and z axes, respectively. A torque-to-release calibration curve was calculated for each direction of testing by plotting the output of our tester against known applied torque values and creating a second order polynomial trendline using the least squares method in Excel. The equations that defined these trendlines were used to determine an unknown applied torque.

Due to ineffectual displacement sensors, work-to-release was not measured. Several additional options were explored and described regarding the feasibility for successful system integration; the Polaris Optical Tracker, rotary encoders, string potentiometers, and Leap Motion optical controller.

8.1 Results and Satisfaction of Constraints

The satisfaction of project constraints are shown in Table 34 below.

Table 34: Satisfaction of project constraints

	<u>Constraint</u>	<u>Final Design</u>	<u>Success</u>
<u>Constraints for Calibration Testing Based on ASTM Standards:</u>	Torque testing must be no greater than $\pm 5\%$ of the known applied torque during calibration testing, using the equation from ASTM F1062, in the Z-axis.	$\pm 16.2\%$	No
	Torque testing must be no greater than $\pm 5\%$ of the known applied torque during calibration testing, using the equation from ASTM F1062, in the Y-axis.	$\pm 17.6\%$	No
<u>Constraints for Testing with a Ski Boot Binding System Based on ASTM Standards:</u>	Torque testing must be no greater than $\pm 5\%$ of the release torque determined through testing with a Vermont Release Calibrator, using the equation from ASTM F1062, in the Z-axis.	$\pm 2.64\%$	Yes
	Torque testing must be no greater than $\pm 5\%$ of the release torque determined through testing with a Vermont Release Calibrator, using the equation from ASTM F1062, in the Y-axis.	N/A	No
<u>Additional Constraints:</u>	The device must be compatible with existing ski boot binding setups.	Yes	Yes
	Displacement testing must be accurate within 0.2 mm (ASTM, 2009; ISO, 2009).	0.45mm	No
	Customer cost must be under \$350.	\$350	Yes
	Design prototype must be under \$500.	\$500	Yes

The range of measurements indicated that our measured torque values had a higher degree of variability in both modes of twist testing than in bending testing. Initial torque testing revealed that the greatest difference, in percent, between known and applied torques in the clockwise direction was $\pm 8.4\%$ of 38 Nm, or ± 3.2 Nm. The greatest difference in the counterclockwise direction was $\pm 16.2\%$ of 18.9 Nm, or 3.06 Nm. While the greatest difference in the forward bending direction was $\pm 17.6\%$ of 297 Nm, or 52.2 Nm. The percent difference between the known torque and the measured torque is displayed as a percentage of the magnitude. This percentage was determined as a result of the calculated calibration curve. This calibration curve was calculated using six data points in the twist directions and five data points in bending testing. Overall results could be improved by creating a better defined calibration curve through testing at more reference points. This will dramatically increase the likelihood of satisfying the first two constraints.

The percent difference between the applied torque and the known torque during ski boot-binding testing met specified constraints about the z-axis. Clockwise testing revealed a 2.02% difference in magnitude between the Vermont Release Calibrator value and the calculated data, while counter clockwise measurement resulted in a 2.64% difference. The constraints that we developed based on ASTM standards require that these measurements must be no greater than $\pm 5\%$ of the release torque measured with the Vermont Release Calibrator, therefore this constraint is met. However, these results were far superior than those obtained in calibration testing, which suggests that further testing should be conducted to verify these results.

Continued validation of the calibration curve for forward bending testing was done instead of testing with the SBB system. This was due to the fact that the calibration curve for bending was shown to be highly inaccurate, between $\pm 4.11\%$ and $\pm 17.57\%$, over the range of tested values and the fact that the Vermont Release Calibrator would not stay in the test boot during attempts at forward bending release, as the tongue of the tested boot created major sources of error. These results further demonstrate the unreliability of the torque values generated by our device with torque applied in forward bending. The difference of the measurements from the applied 148.6 Nm was within $\pm 12.57\%$, ± 18.68 Nm, which is a reflection of the poorly defined calibration curve. The relative range of the measured values, $\pm 2.66\%$, ± 4.49 Nm, was also greater than from the initial calibration testing, where the worst percent relative range was 1.83%, ± 2.17 Nm. This leads to concerns about the consistency of our device and suggests that further testing is needed.

This system was designed under compatibility requirements for existing adult ski boot binding technology. All makes and models of adult ski-boot-binding systems can be tested using the prototype dynamometer as it interfaces with the universal Vermont Release Calibrator prosthetic foot.

Displacement sensor results were inadequate, as the measured uncertainty for both the NDI Polaris and optical mice were greater than $\pm 0.2\text{mm}$. The mouse was determined to have an uncertainty of $\pm 0.68\text{mm}$. The NDI Polaris system is listed with a nominal precision of 0.4mm , and an error of $\pm 1.6\text{mm}$ was calculated when using the system to track the position of a ski boot.

Throughout the design and implementation process the prototype and projected consumer costs were documented and an effort was made to keep both costs within their respective constraints. We met the \$500 prototype constraint easily, as most of the necessary components and software required were provided by the school. We also avoided manufacturing costs by machining the required pieces ourselves. Our final prototype costs were \$61.49 excluding tax and shipping fees. Tax and shipping fees were mitigated by ordering all circuit components from DigiKey and all stock material from McMaster-Carr. The projected consumer cost was much higher than our initial prototype cost as the consumer would have to pay for the National Instruments DAQ, which is \$189, and for machining. Under the assumption that our device would take two hours to machine, we projected manufacturing costs to be \$50. However, the software needed for using our device, Labview SignalExpress, as well the necessary NI-MAX drivers can be downloaded for free from the National Instruments Website (National Instruments, 2014). The final consumer cost for our device was \$338.56, not including the Vermont Release Calibrator Prosthetic Foot, which costs \$200 (Vermont Ski Safety, 2010). The cost of the prosthetic foot was ignored when assessing the satisfaction of our constraint due to the prevalence of the Vermont Release Tester among ski shops and teams. Tables that document the cost of each component and the amount spent, excluding tax and shipping fees, can be seen in Appendix J.

8.3 Impact of Solution

The existing torque to release testers have no way to interface with future displacement to release measurements. Although we were unable to create a work to release testing device, we were able to create an electronic testing device that measures the applied torque to the ski-boot-binding system over time, which would be able to interface with later displacement measuring devices. The target market is ski shops and ski racers who wish to mitigate inadvertent binding release. Providing the ability to further differentiate between effective and ineffective bindings, through work to release testing, is

pivotal in preventing associated injuries. Successful, design, development and testing of such a device would create a new technology that would advance the safety of skiing.

Using stock parts, simple CAD models and machining processes, the developed electronic torque tester could easily be duplicated. Due to the design's low cost, weight, and size it provides a viable option for both large and small ski shops, as well as the individual ski racer.

8.4 Future Recommendations

Despite our design's ability to measure torque applied to a ski-boot-binding system multiple improvements could be made to the design. The top and bottom pieces could be machined out of a material with a higher elastic modulus as the bottom piece of the design can currently only withstand a maximum load of 297 Nm without plastic deformation. By machining both pieces out of the same higher elastic modulus stock, only one type of 2 inch diameter stock would have to be purchased.

In future designs work to release could be incorporated through developing a displacement measuring system. This system would have to have an analogue or digital output that could be measured with the portable NI DAQ to produce displacement measurements over time. This would allow for direct correlation between the torque and displacement measurements. The uncertainty of the displacement sensors would have to be within ± 0.2 mm, without being exorbitantly expensive. To this end the string potentiometers and LeapMotion controller are potentially viable future options.

9. Conclusions

The initial main objective of this MQP was to design an alpine ski binding tester that could measure the simultaneous torque and displacement experienced by a ski boot-binding system under quasi-static loading conditions. This would allow for the identification of the work required to release a ski boot from its binding. The greater the evaluated binding's measured work to release, the greater its ability to prevent inadvertent release at large, instantaneously applied loads. However, due to the tested displacement sensors having an unacceptably high uncertainty of ± 0.68 mm or greater, and additional restrictions that made them unsuitable options for use with a ski boot-binding system, a work-to-release device was not created. However, an electronic torque to release dynamometer that could be integrated with several identified possible future displacement methods, was designed, manufactured, and tested.

Design Accomplishments:

- The design was able to measure applied torque over time under constant loading situations and when used to measure the torque to release a ski boot from a binding
- The design could be integrated with future displacement measuring devices
- The design could be reproduced for approximately \$339 by ski shops or ski teams

Assessment of the effectiveness of the design method:

- Allowed for the design of a modular device where functional requirements of the system were addressed through separate design parameters
- The design of the device allowed for easy identification of malfunction within the separate components. If a function of the device was not operational, the specific design parameter that accomplished that functional requirement could be easily identified and repaired.

Remaining Issues:

- The device was unable to measure torque within $\pm 5\%$ of the known applied torque in clockwise, counterclockwise, or forward bending during initial calibration testing.
- The measured torque values produced by the device under forward bending loads had a larger percent difference from the known applied torques than in clockwise and counterclockwise loading configurations. These differences constituted up to 17.57% of the applied torque, or 52.2 Nm.
- The torque measurements could be improved through improving the fit of the produced calibration curve. The calibration curves relating output strain measurements and applied torque could be improved through evaluating the strain outputs at more known applied torques.
- The bottom piece of the device would deform under loads over 297 Nm in forward bending, which could be addressed by re-machining the top and bottom pieces out of a higher modulus material.
- Strain gauges are highly temperature dependent; the torque values measured by the device could vary under large variations in temperature.

- The robustness of the design should be continued to be tested. The calibration curves used to compare output strain to known applied torque values should be replicated to test the systems reproducibility over time.
- Displacement measurement options such as the LeapMotion and string potentiometers should be continued to be assessed for future incorporation with the design.

Appendix A: Causes and Effects of Inadvertent Release

Inadvertent release is often caused by inappropriate retention; the inability of the binding to retain the boots to the ski during normal skiing maneuvers (Ettliger et al., 2009). This can be caused by a number of mechanisms including hardware problems and bad skiing practice coupled with under defined heel release mechanisms. Hardware problems include sluggish or faulty forward pressure mechanisms in the toe or heel piece. A flaw in either of these mechanisms will cause a gap to form between the boot and binding. This allows the boot to escape from either the toe or heel piece, depending on the situation, without opening of the heel piece (Ettliger, 2010). Ettliger also describes a method of release that usually happens to less experienced skiers moving at a slower speed, and in heavier snow, called the “superman effect”. In the superman effect the skier applies a torque through forced clockwise and counterclockwise motions of the lower leg, setting off the twist release mechanism in the toe piece.

Another method of inadvertent release, “the bow effect” [Figure 9] is caused by both skier error and the under design of the heel piece. The typical mechanism for the bow effect is when a forward leaning skier presses the shovel of his ski into a depression, loading the tip of the ski, causing the heelpiece to release (Brown and Ettliger, 1985; Ettliger, 2010, Young, 1989). This type of release is recognizable by the rearward trajectory of the released ski, caused by the forces acting on the shovel of the ski. In the bow effect the heelpiece releases at a much lower bending moment because it can only sense vertical forces. In 1985 Brown and Ettliger completed testing to evaluate retention characteristics part of which included reproducing the bow effect using an alteration of Test 2.5 in ASTM Method F 504-77. Using this test method they found that they could reduce the bending moment at which heel release occurred from 240 Nm to 120 Nm, without adjusting the binding settings. In a correlating study about elevated binding settings in alpine racers, Young found that bow releases had occurred despite the heel settings often being four or five, in one instance ten, above ASTM recommendations for expert fast skiers. This is especially dangerous because the heel piece will release seemingly regardless of the release setting.



Figure 43: "Bow Effect" Inadvertent Release (Brown and Ettliger, 1985)

Skiers who experience the bow effect, or other retention related inadvertent releases, often blame the pre-release on the release torque settings of the binding, which leads to a phenomenon called the “ratchet effect” (Ettlinger, 2010). This is when expert skiers, who already have the highest release torque setting standards per ASTM F 939-05a, continue to raise the release torque levels on their bindings in order to avoid inadvertent releases. In the case of the bow effect, faulty forward pressure mechanisms, or other types of retention related issues, raising the release torque is not going to stop inadvertent release. However, raising the release torque beyond the standards increases the chance of binding release failure under high loading situations, and subsequent lower leg damage. A severe demonstration of this was when Matthias Lanzinger’s left ski failed to release after a crash in a World Cup Super-G run in 2008 [Figure 10], the crash was so severe that it led to his leg being amputated (New York Times, 2008; Merrill, 2013).



Figure 44: Failure of Ski to Release

Although the release settings defined by ASTM F 939-05a have helped reduce lower leg injuries and overall injuries by 80-90% over the last thirty years, there are still some problems with binding release accuracy in regards to the heel piece (Beynnon et al., 1997; Paletta et al., 1994). This largely because the bending moment sensed by the leg does not always agree with the moment sensed by the binding [Figure 11] (Brown et al., 1985). The moment sensed by binding (M_B) is the vector product of the force on the ski and the distance between this

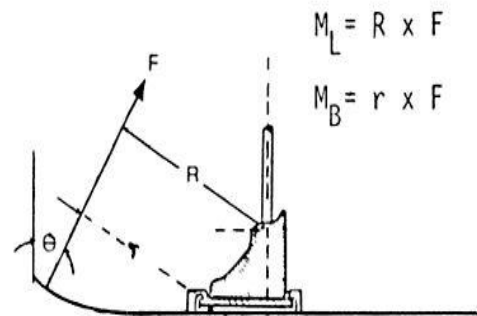


Figure 45: Bending Moment Sensed by the Binding vs. the Tibia (Brown and Ettlinger, 1985)

force and the bending fulcrum, r . However, the moment experienced by the leg (M_L) is the product of the force and distance of that force from the center of the distributed load on the tibia, R . As the r displacement remains constant, a skier’s ability to change the R displacement through forward lean, coupled with a small deceleration force on the shovel of the ski can cause the binding to release at a much higher moment than desired. However, a large deceleration force at the shovel of the ski in these same conditions can cause inadvertent release. Though ASTM F504-05 testing methods, 2.3 and 2.5, have been developed to test for these issues, they have not been able to demonstrate most retention issues (ASTM, 2005).

Appendix B: Axiomatic Design Concepts

Nam Suh's Axiomatic Design method was utilized to decrease design time and increase efficacy. To do this the designer first determines the design objectives by defining them in terms of specific requirements known as functional requirements (FRs)

(Suh, 1990). To satisfy these functional requirements solutions, design parameters (DPs), of the physical domain, must be generated. FRs and DPs are naturally organized into a hierarchical structure from which they can be decomposed; the first level FRs are the most fundamental of a design. To develop the FR and DP hierarchies the designer has to travel back and forth between the functional and physical domains of the FRs

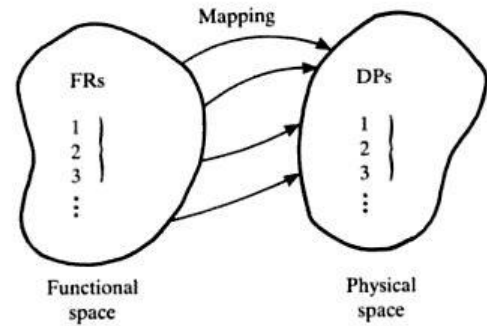


Figure 46: Relationship Between FRs and DPs (Suh, 1990)

and DPs [Figure 12]. After completing first level FRs first level DPs have to be established in order to identify the next level of FRs. The alternating pattern helps to streamline decomposition by allowing the designer to look at fewer FRs, or objectives, at a time. This reduces the complexity of the design process and results in a more robust design. This is also the principle behind the definition of good FRs, which are collectively exhaustive, mutually exclusive, and minimum in number.

Axiomatic design is decomposed both horizontally and vertically. Horizontally it is divided into five domains including the functional, FRs, and physical, DPs, already discussed. The other domains are the customer needs, constraints, and process variables. The customer needs define what elements will add value to a design and are referred to as CNs. The constraints, CONs, must be adhered to and describe what needs to be avoided. Process variables, PVs, are addressed in relation to lower levels of DPs and define how the DPs are accomplished using various formulas.

Axiomatic design is used to reduce design complexity and increase robustness; it does this by establishing the two axioms of independence and information (Suh, 1990). The independence axiom explains that a good design should be uncoupled; meaning that FRs and DPs should be related on a one to one ratio. If one DP is used to address two FRs then it is impossible to address

	DP1	DP2
FR1 temperature	X	X
FR2 flow rate	X	X

Fully coupled

Figure 47: Failure of Independence Axiom

and adjust the two FRs separately. For example, in the classic two handled faucet temperature and flow rate are both controlled by the adjustment of the hot water and cold water valves; meaning that you cannot control the flow rate without also changing the temperature of the water [Figure 13].

The information axiom is considered after the independence axiom and involves minimizing the amount of information required for the design (Suh, 1990). Where axiom one is about adapting to change; axiom two is about robustness with respect to change. For example, a clamping mechanism is defined by the equation $F=kx$,

with k being a linear spring constant and x being clamp displacement. As the spring constant is the only adjustable part of the design, the

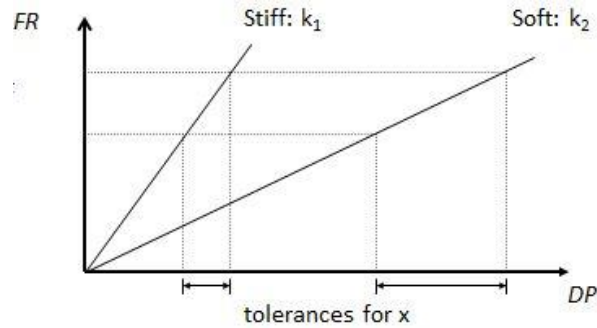


Figure 48: Information Axiom Satisfied by Altering k

question is whether or not it should be a stiff or soft spring. With a softer spring there is a greater range of acceptable x values [Figure 14], which maximizes the probability of success. The information axiom is especially useful for machining and manufacturing purposes where small tolerances are particularly problematic.

Appendix C: Supplements to Our Approach

Initial Client Statement:

The initial client statement was to reduce the risk of ski injuries by designing and building a better binding test device. This device was to measure the work to release boots from bindings and the torques about three axes at the knee in quasi-static release conditions. The device should also be capable of demonstrating response to multiple loading configurations. Some version of the device should be usable by sports shops and ski teams. The possibility of making the designs available on the web so anyone could make and use them should be considered. In order to measure work to release, displacement should be measured as well as torque. In order to test bindings that are designed to protect the knee from injury, the loads at the knee must be assessed. It is expected that the group will apply for patents and publish and present the results outside of WPI.

Objectives:

Based on this client statement the primary objective of this project is to design an alpine ski binding testing device that measures the torque and work to release ski boots from bindings in response to multiple quasi-static loading configurations in the y and z axis. The test device would be able to identify ski binding devices' susceptibility for inadvertent release [Appendix A]. We also initially planned to make the design available online for use by skiers and ski teams. An objectives tree describing the different objectives and sub-objectives of this project can be seen in Figure 9.

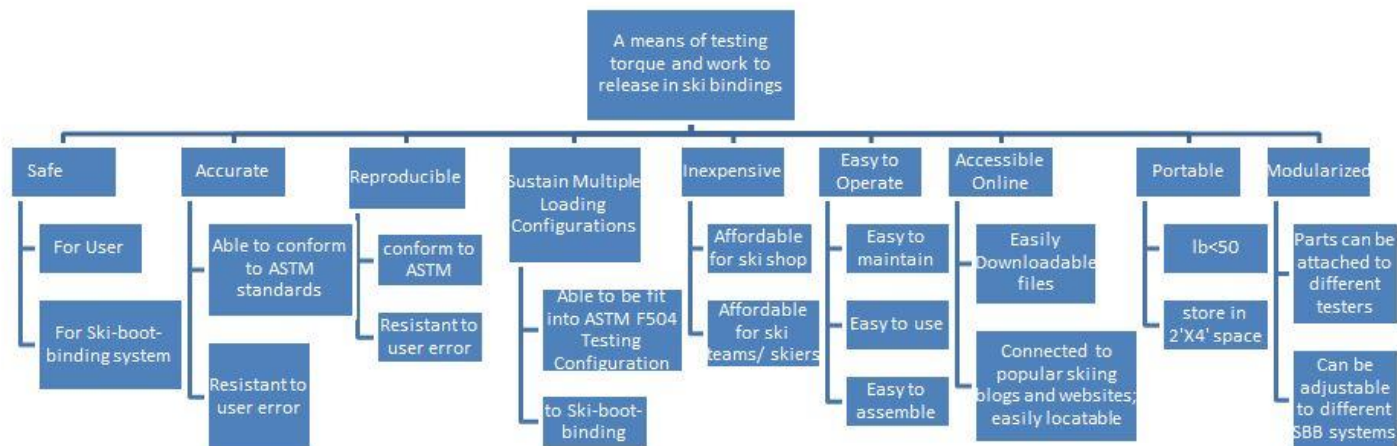


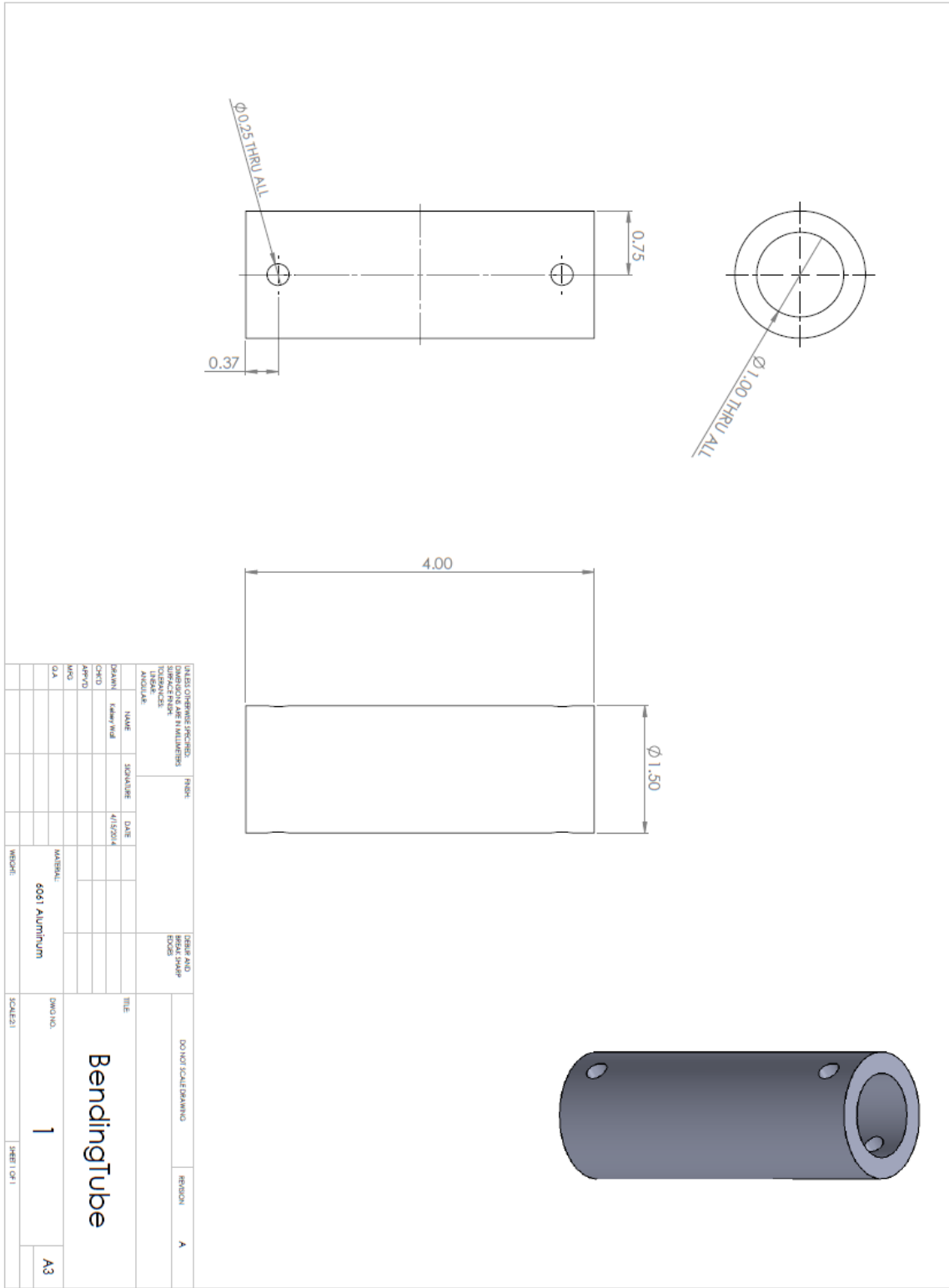
Figure 49: Objectives Tree Representation of Objectives and Sub-Objectives

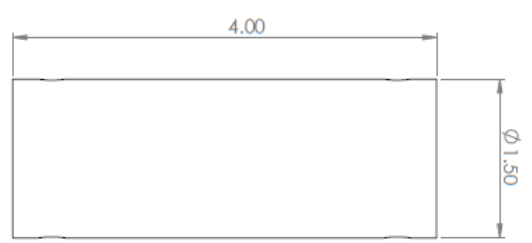
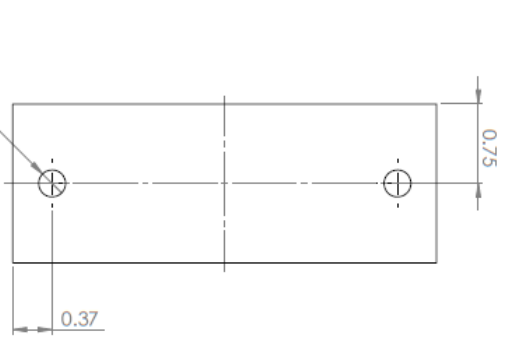
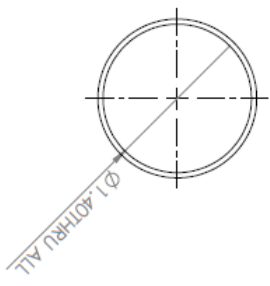
The main objectives of this project, in order of importance, are that the device needs to be safe for the user, safe for the ski boot binding system, accurate, reproducible, able to sustain multiple loading configurations, inexpensive, easy to assemble, maintain, and use, accessible online, portable, and modularized. Modularization means that our final design, as opposed to our testing prototype, will be compatible with a wide range of different binding testers, and that it will be independent from specific supplementary release equipment. This objective is ranked lowest on our list because it was determined that creating a preliminary testing device that articulated well with a Vermont Release Calibrator foot prosthetic, the most common commercial tester in the US, was the primary focus. These objectives and their order of importance were discussed and agreed upon with our advisor, as demonstrated in our pairwise comparison chart [Table 1].

Table 35: Pairwise Comparison Chart of Objectives

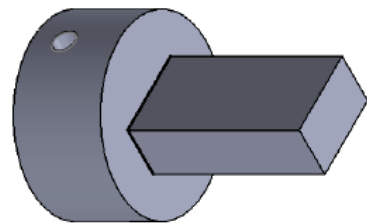
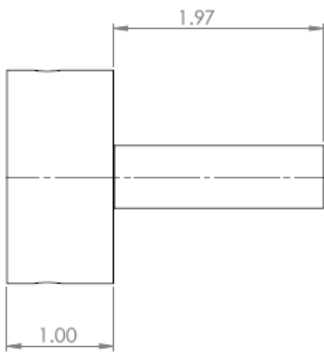
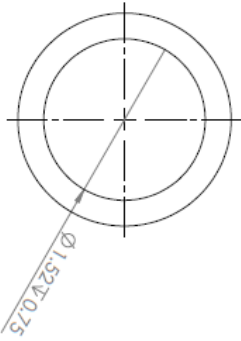
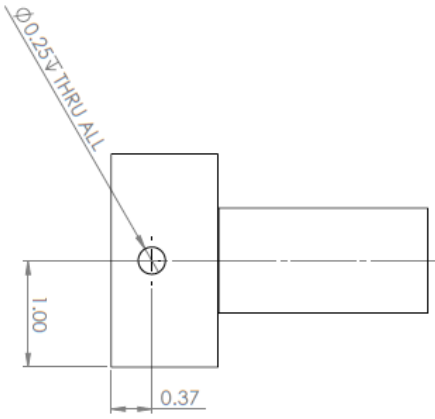
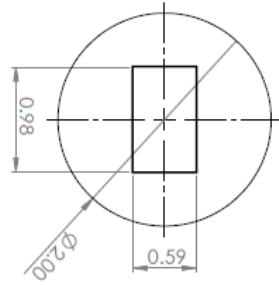
OBJ.	Safe	Accurate	Reproducible	Sustain Multiple Loading Conf.	Inexpensive	Easy to Operate	Accessible Online	Portable	Modularized	SCORE
Safe	X	1	1	1	1	1	1	1	1	8
Accurate	0	X	1	1	1	1	1	1	1	7
Reproducible	0	0	X	1	1	1	1	1	1	6
Sustain Multiple Loading Conf.	0	0	0	X	1	1	1	1	1	5
Inexpensive	0	0	0	0	X	1	1	1	1	4
Easy to Operate	0	0	0	0	0	X	1	1	1	3
Accessible Online	0	0	0	0	0	0	X	1	1	2
Portable	0	0	0	0	0	0	0	X	1	1
Modularized	0	0	0	0	0	0	0	0	X	0

Appendix D: CAD Drawings of System

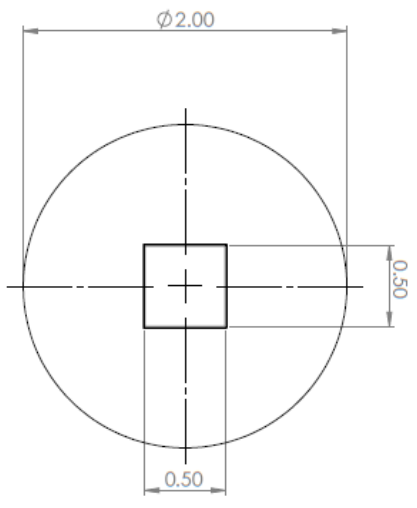
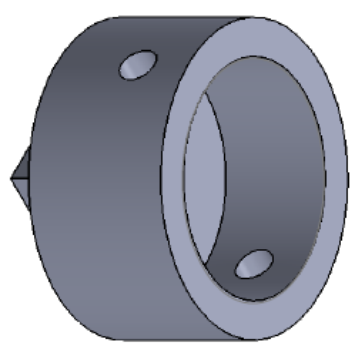
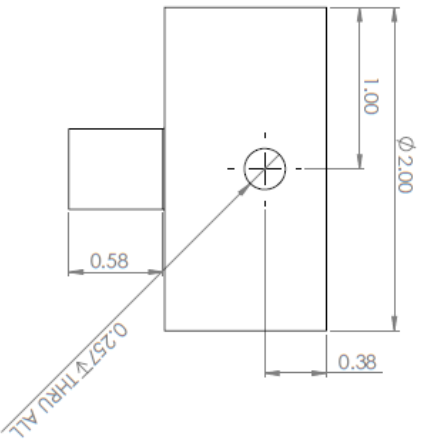
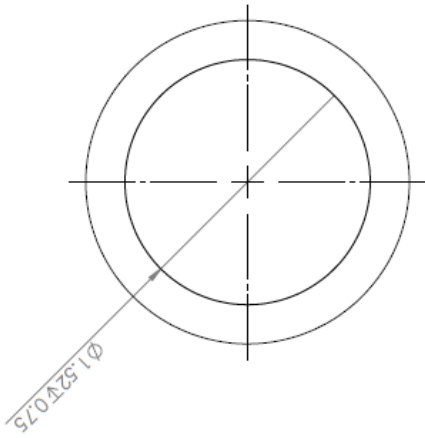




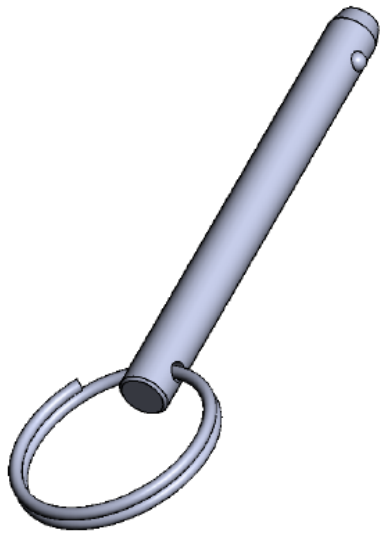
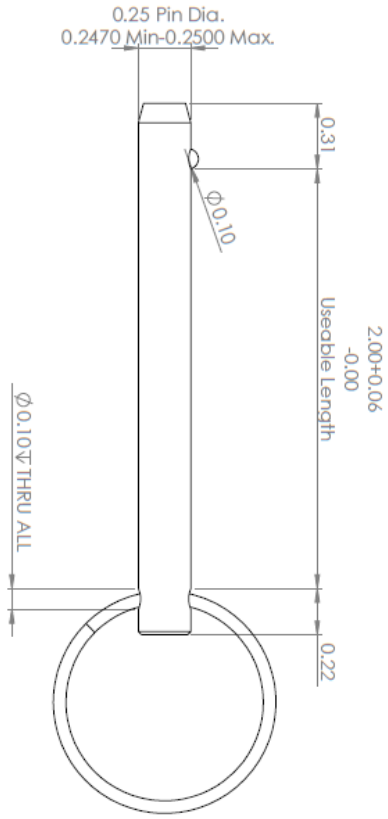
UNLESS OTHERWISE SPECIFIED, DIMENSIONS ARE IN MILLIMETERS UNLESS OTHERWISE INDICATED		FINISH		DRILL AND REAM SHARP EDGES		DO NOT SCALE DRAWING		REGION		A	
DATE	BY	DATE	BY	DATE	BY	DATE	BY	DATE	BY	DATE	BY
4/12/2014											
DRAWN: Eddy Wif		SIGNATURE		DATE		TITLE		MATERIAL		DOWNS	
CHECKED						TorsionTube		6061 ALUMINUM		2	
APPROVED								WEIGHT		SHEET 1 OF 1	
MFG										A3	
QA											



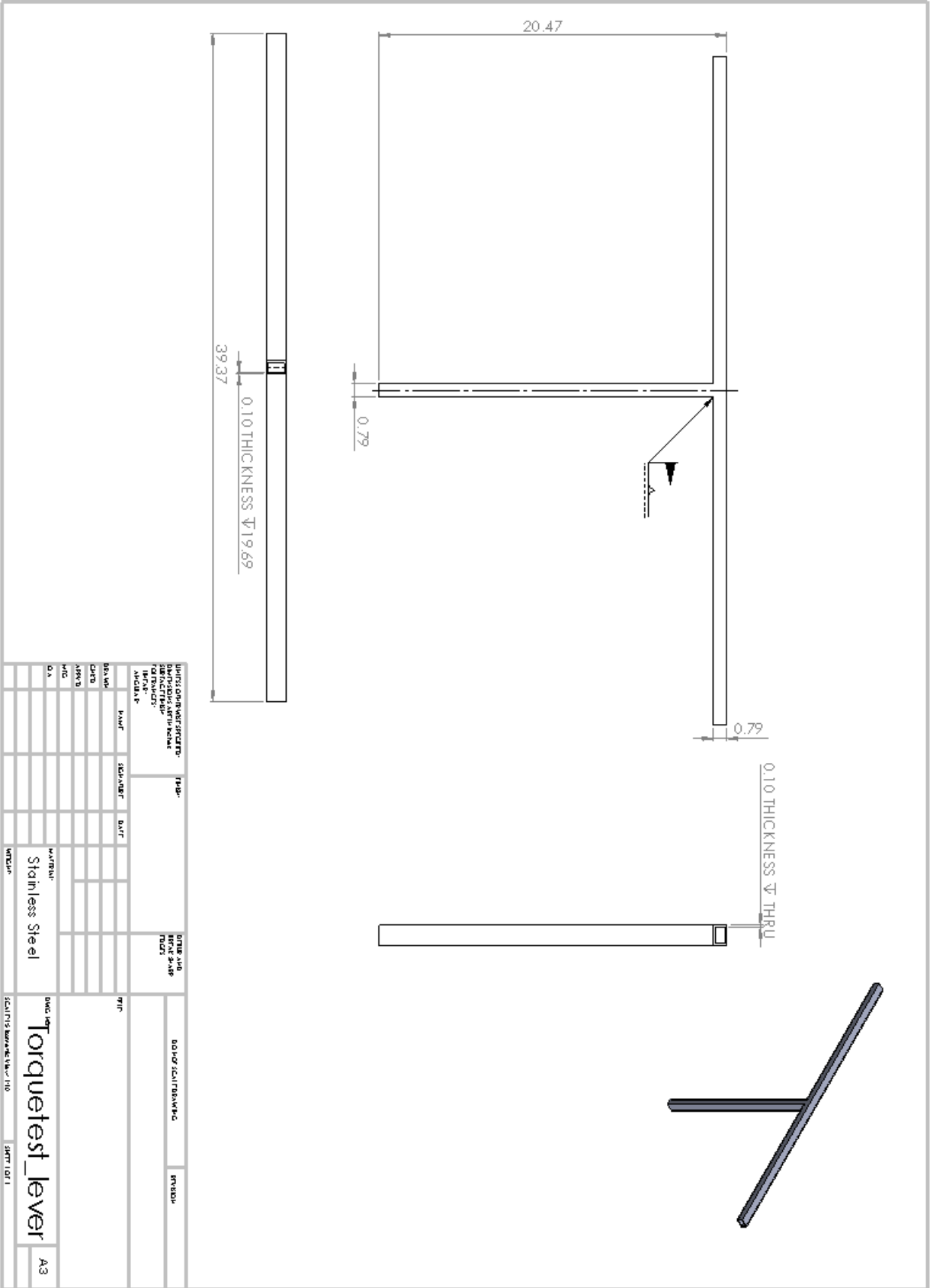
DATE: 08/28/2014				DRAWN: [blank]		CHECKED: [blank]		APPROVED: [blank]		DATE: 4/15/2014		MATERIAL: 6061 ALUMINUM		WEIGHT: [blank]		SCALE: [blank]		
DIMENSIONS ARE IN MILLIMETERS				SURFACE FINISH: [blank]		TOLERANCES: [blank]		UNLESS OTHERWISE SPECIFIED		TITLE: StrainTop		DRAWING NO: 3		SHEET NO: 1 OF 1		REVISION: A		
NO.	DESCRIPTION	DATE	BY	APPROVED	DATE	BY	APPROVED	DATE	BY	APPROVED	DATE	BY	APPROVED	DATE	BY	APPROVED	DATE	BY



INSTEAD OF THESE SPECIFIED DIMENSIONS ARE IN MILLIMETERS				RISK		DIE AND BRASS SHARP EDGES		DO NOT SCALE DRAWING		REGION			
NAME	DATE	DATE	DATE	DATE	DATE	DATE	DATE	DATE	DATE	DATE	DATE		
DESIGNER													
CHECKED													
APPROVED													
QA													
MATERIAL: 6061 ALUMINUM				WEIGHT:				SCALE: 1:1					
StrainBottom										DWG NO. 4		SHEET 1 OF 1	
										A3		A	



DESIGN APPROVALS		DATE		TITLE	
DESIGNER	NAME	DATE			
CHECKED	NAME	DATE			
APPROVED	NAME	DATE			
QA	NAME	DATE			
MATERIAL: 316 STAINLESS STEEL			DWG NO:	5	A3
WEIGHT:			SCALE:	1:1	



Appendix E: SignalExpress Instructions (NI, 2010)

DAQ Getting Started Guide

This guide describes how to confirm your NI data acquisition (DAQ) device is operating properly. Install your application and driver software, then your device, using the instructions packaged with your device.

Confirm Device Recognition

Complete the following steps:

1. Double-click the **Measurement & Automation** icon on the desktop to open MAX.
2. Expand **Devices and Interfaces** to confirm your device is detected. If you are using a remote RT target, expand **Remote Systems**, find and expand your target, and then expand **Devices and Interfaces**. If your device is not listed, press <F5> to refresh MAX. If the device is still not recognized, refer to ni.com/support/daqmx.

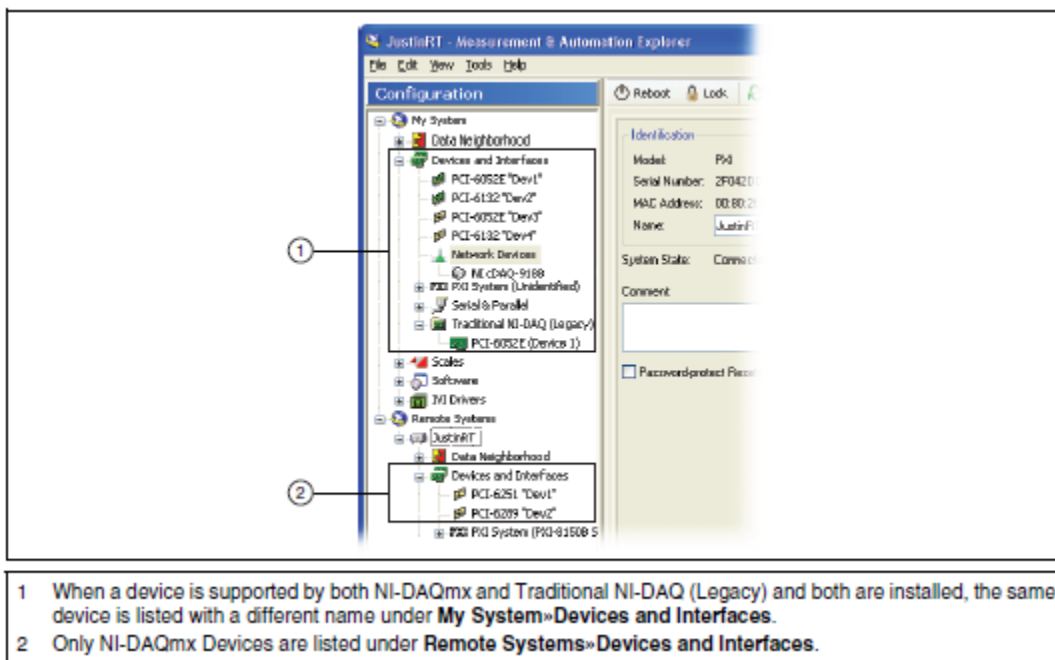


Figure 50: MAX Configuration

For a Network DAQ device, do the following:

- If the Network DAQ device is listed under **Devices and Interfaces > Network Devices**, right-click it and select **Add Device**.
- If your Network DAQ device is not listed, right-click **Network Devices**, and select **Find Network NI-DAQmx Devices**. In the Add Device Manually field, type the Network DAQ device's host name or IP address, click the + button, and click **Add Selected Devices**. Your device will be added under **Devices and Interfaces > Network Devices (Figure 50)**.

Note If your DHCP server is set up to automatically register host names, the device registers the default host name as cDAQ<model number>-<serial number>, WLS-<serial number>, or

Attach sensors and signal lines to the terminal block or accessory terminals for each installed device. Table 36 lists device terminal/pinout locations.

Table 36: Terminal/pin locations

Location	How to Access Pinout
MAX	Right-click the device name under Devices and Interfaces and select Device Pinouts .
	Right-click the device name under Devices and Interfaces and select Help»Online Device Documentation . A browser window opens to ni.com/manuals with the results of a search for relevant device documents.
DAQ Assistant	Select the task or virtual channel, and click the Connection Diagram tab. Select each virtual channel in the task.
NI-DAQmx Help	Select Start»All Programs»National Instruments»NI-DAQ»NI-DAQmx Help .
ni.com/manuals	Refer to the device documentation.

Use NI-DAQmx with Your Application Software

The DAQ Assistant is compatible with version 8.2 or later of LabVIEW, version 7.x or later of LabWindows™/CVI™ or Measurement Studio, or with version 3 or later of LabVIEW SignalExpress. LabVIEW SignalExpress LE, an easy-to-use configuration-based tool for data logging applications, is at **Start»All Programs»National Instruments»LabVIEW SignalExpress**.

To get started with data acquisition in your application software, refer to the tutorials seen in Table 37:

Table 37: Location for software tutorials

Application	Tutorial Location
LabVIEW	Go to Help»LabVIEW Help . Next, go to Getting Started with LabVIEW»Getting Started with DAQ»Taking an NI-DAQmx Measurement in LabVIEW .
LabWindows/CVI	Go to Help»Contents . Next, go to Using LabWindows/CVI»Data Acquisition»Taking an NI-DAQmx Measurement in LabWindows/CVI .
Measurement Studio	Go to NI Measurement Studio Help»Getting Started with the Measurement Studio Class Libraries»Measurement Studio Walkthroughs»Walkthrough: Creating a Measurement Studio NI-DAQmx Application .
LabVIEW SignalExpress	Go to Help»Taking an NI-DAQmx Measurement in SignalExpress .

Examples

NI-DAQmx includes example programs to help you get started developing an application. Modify example code and save it in an application, or use examples to develop a new application or add example

code to an existing application.

To locate LabVIEW, LabWindows/CVI, Measurement Studio, Visual Basic, and ANSI C examples, go to ni.com/info and enter the info code `daqmxexp`. For additional examples, refer to zone.ni.com.

To run examples without hardware installed, use an NI-DAQmx simulated device. In MAX, select **Help»Help Topics»NI-DAQmx»MAX Help for NI-DAQmx** and search for simulated devices.

Troubleshooting

If you have problems installing your software, go to ni.com/support/daqmx. For hardware troubleshooting, go to ni.com/support and enter your device name, or go to ni.com/kb.

If you need to return your National Instruments hardware for repair or device calibration, refer to ni.com/info and enter the info code `rdsenn` to start the Return Merchandise Authorization (RMA) process.

Go to ni.com/info and enter `rddq8x` for a complete listing of the NI-DAQmx documents and their locations.

Appendix F: Clockwise SBB System Torque vs. Time Graph

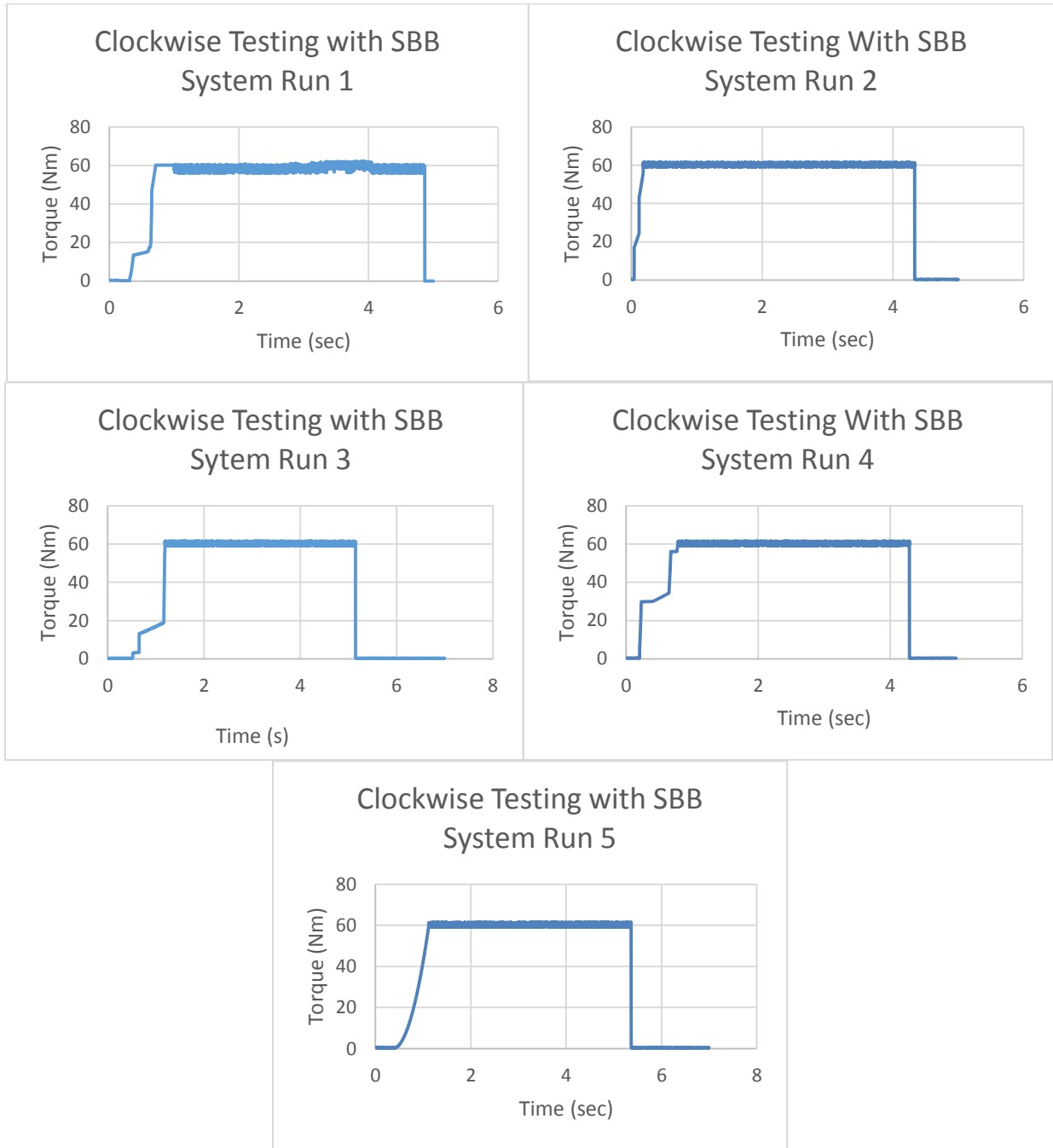


Figure 51: A compilation of all torque vs time graphs generated during clockwise SBB system testing

Appendix G: Counter Clockwise SBB System Torque vs. Time Graph

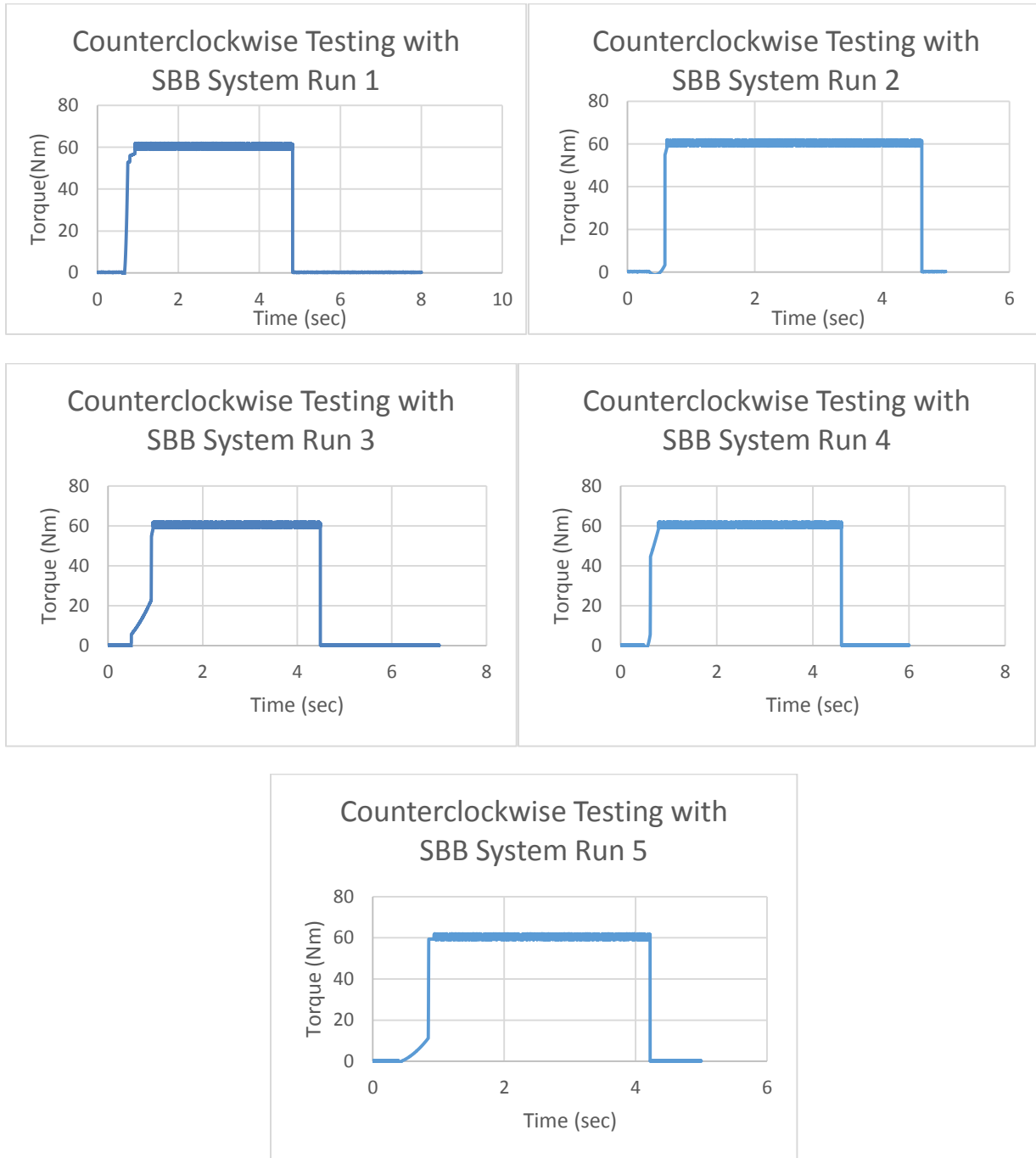


Figure 52: A compilation of all torque vs time graphs produced during counter-clockwise SBB system testing

Appendix H: Optical Mouse Data Analysis

In order to successfully validate a device as a capable displacement sensor, several criteria must be met. Established system constraints must be considered; both cost of the device and its precision capabilities. The tolerance and precision of the device must satisfy ISO 9462 return-to-center test. This test requires that the boot return to within 2mm of the binding's center, requiring a precision 1/10th of that measurement. A displacement sensor for this system must meet these previously established constraints of the project; sensor uncertainty must be within ±0.2 mm and remain within the project budget. Uncertainty was defined using the standards described in ASTM E2655, which defines uncertainty as “an indication of the magnitude of error associated with a value that takes into account both systematic errors and random errors associated with the measurement or test process” (ASTM E2655, 2008). The equation for uncertainty from ASTM E2655 is as follows:

$$\sigma/\sqrt{n}.$$

Where σ = the standard deviation, and
 n = the number of measurements

$$\sigma = \sqrt{\frac{\sum(x-\bar{x})^2}{n}}$$

n = the number of measurements
 x =the sample
= the sample mean

A displacement sensor must also be capable of integration with the torque-to-release sensor. This electronic integration should be as simple as possible, increasing chances of sustained accurate measurements.

An optical mouse converts an electromagnetic signal, or light, to an electrical signal. This is accomplished by reflecting LED light off a surface onto a CMOS (complementary metal-oxide semiconductor) sensor. This sensor compares these reflected images thousands of times per second with a Digital Signal Processor. Position is then determined relative to translation motion between frames (Ng, 2003).

An electronic mouse provides several benefits as a potential displacement sensor. Optical mice offer accurate sensing at nearly 2% of the cost of other conventional displacement sensors (Merrill, 2013).

Due to high production volumes, a “high-precision” mouse can be obtained for less than \$20. Additionally, a 2003 study by T.W. Ng of the National University of Singapore determined that an optical mouse can be used as effective displacement sensor for small distances on an opaque surface. Displacement of 1mm in both horizontal and vertical directions was performed; a mean square error of 0.018mm² and a mean R² value of 0.9914 was determined (Ng, 2003). These specifications were satisfactory motives to perform further testing in regards to the boot-binding application.

H.1 Testing Setup and Procedure

H.1.1 Labview Program for Tracking Mouse Position

Electronic integration is a necessity for displacement measurements. A mouse’s movements across the screen can easily be tracked using National Instrument’s *Labview*. A Virtual Instrument can be created in order to track the x and y position of the cursor in relation to time. Using an ‘Initialize Mouse’ command to Generate Data, the x and y coordinates can be bundled together with a time stamp.

Mouse position is tracked relative to an origin in the top left corner of the screen (0,0). As the mouse moves, the cursor on the screen displaces a certain number of dots, or pixels. This change in position can be calibrated by measuring a known distance, a function relating actual displacement to pixel displacement can be calculated. Validation of the precision, repeatability and linearity of the output data is paramount for an accurate function.

By setting additional parameters, 100 data points are measured over a 5 second collection period. The start of data collection is prompted by keystroke. This removes user interaction with the mouse, increasing simplicity and mitigating potential sources of error. Using *Labview* ‘Write’ functions, all data is labeled and exported to Excel. Figure 53 below shows the Virtual Instrument for collecting mouse position.

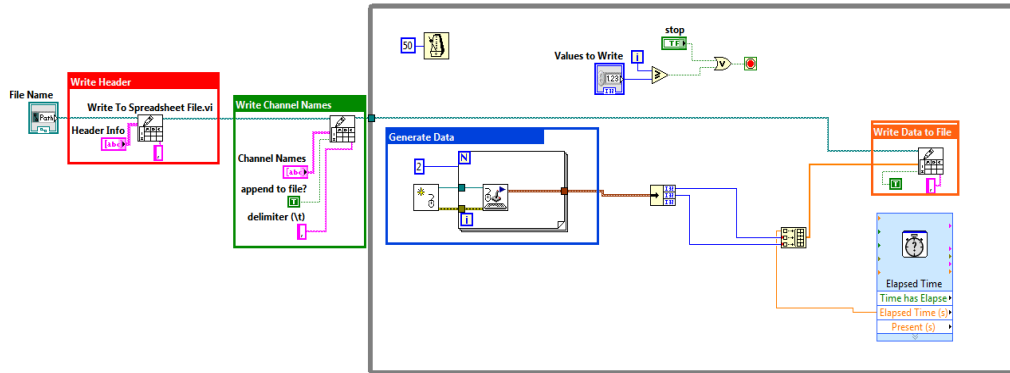


Figure 53: Labview program for documenting mouse position

H.1.2 Physical Testing Setup

The position data that was recorded using Labview was obtained while the team moved an optical mouse by a known increment. To do so required a test setup with two hard stops to ensure repeatable displacement. These stops were positioned to ensure that the mouse would travel 30mm for initial tests with a standard mouse. However, this increment was changed to 10mm, while using the 2000 DPI gaming mouse, as larger displacements would cause the cursor of the mouse to reach the edge of the computer screen. This was done so that the position, in units, of the mouse recorded through the Labview Program could be compared to the known distance traveled by the mouse. Measuring the length of the mouse and the distance between the hard stops will yield the amount of travel by the mouse. As seen in Figure 54 below, this test setup was performed to verify y-axis displacement.

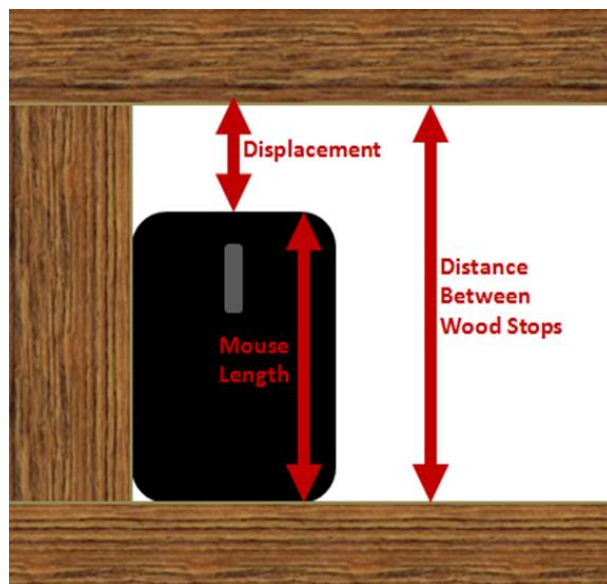


Figure 54: Physical test setup for mouse position data acquisition

A mouse is a sensitive sensor. With every small movement of the mouse, the cursor is displaced on the screen by a certain amount of pixels, depending on the sensitivity settings of the mouse. The sensitivity of a mouse is a user defined setting; defining the ratio of pixels displaced per centimeter displaced. This setting can be adjusted from the 'Control Panel' window (Figure 55). This setting has a large effect on precise displacement measurements, as a higher setting corresponds to a higher ratio of pixels to centimeters displaced. Several experiments were conducted in order to establish the most effective displacement sensor settings with this application.

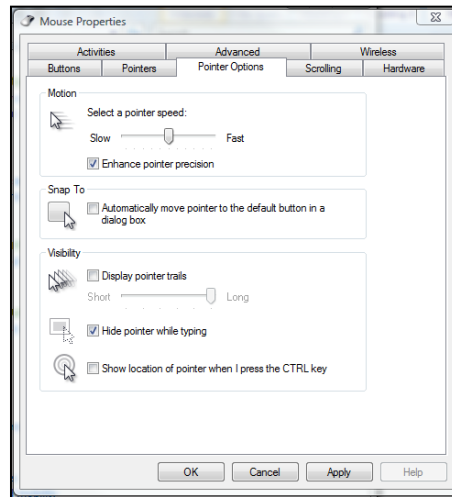


Figure 55: Changing the pointer speed, or sensitivity, of an optical mouse

H.1.3 Data and Analysis

Linear displacement can be found using the function:

$$s[t] = (\Delta x^2 + \Delta y^2)^{1/2}$$

Where Δx is the change in x position and Δy is the change in y position. Using *Labview*, the position of the mouse was tracked along the rigid path. In order to simplify the validation, only motion along the y axis was tracked. It was found easiest to apply the displacement function within the raw Excel data; however built-in functions within the VI could be applied.

Using the initial starting point as an offset, $\Delta x = x_{\text{Final}} - x_{\text{Initial}}$ and $\Delta y = y_{\text{Final}} - y_{\text{Initial}}$.

Displacement was then calculated accordingly, as seen in Table 38.

Table 38: Mouse position and linear displacement calculations

	A	B	C	D	E	F
1	Test Name					
2	Displacement Test	Kelsey and Brendan				
3	Time	X Location	Y Location	Change X	Change Y	Linear Displacement
4	0	334	942	0	0	239.6768658
5	0.045	334	942	0	0	
6	0.095	335	942	1	0	
7	0.145	338	942	4	0	
8	0.195	343	942	9	0	
9	0.245	347	942	13	0	
10	0.295	353	942	19	0	
11	0.345	359	942	25	0	
12	0.395	367	941	33	1	
13	0.445	373	941	39	1	
14	0.495	379	941	45	1	
15	0.545	384	940	50	2	
16	0.595	391	940	57	2	
17	0.645	398	939	64	3	
18	0.695	404	939	70	3	
19	0.745	409	938	75	4	
20	0.802	416	938	82	4	
21	0.845	420	937	86	5	
22	0.895	424	937	90	5	
23	0.945	426	937	92	5	
24	0.995	429	937	95	5	
25	1.045	431	936	97	6	
26	1.099	435	936	101	6	
27	1.145	438	936	104	6	
28	1.195	443	935	109	7	
29	1.245	447	935	113	7	
30	1.295	451	935	117	7	
31	1.345	456	934	122	8	
32	1.395	460	934	126	8	
33	1.445	464	933	130	9	
34	1.495	467	933	133	9	
35	1.545	471	933	137	9	
36	1.595	474	933	140	9	
37	1.645	477	932	143	10	

Preliminary trials analyzed the mouse at speed, or sensitivity, settings 1, 5, and 10. Hard stops were placed so that the mouse would only displace 30 millimeters. 100 data points were recorded per run and linear displacement was recorded. The mean amount displaced, in unspecified units, was taken to correlate to 30mm of displacement. Seven identical tests revealed the range, standard deviation and uncertainty of mouse displacement measured through the Labview program. Tables 39, 40, and 41 correspond to the measurements obtained with a standard optical mouse at pointer speeds 1, 5, and 10, respectively.

Table 39: Displacement measurements obtained by a standard mouse at pointer speed 1

Test #	Linear Displacement (units)	Linear Displacement (mm)	Average Linear Displacement (mm)		Displacement (mm)
1	405.36	42.42	30.00	Average	30.00
2	330.12	34.55		S.D.	6.55
3	265.70	27.80		Uncertainty	2.67
4	253.34	26.51			
5	241.30	25.25			
6	224.29	23.47			

Table 40: Displacement measurements obtained by a standard mouse at pointer speed 5

Test #	Linear Displacement (units)	Linear Displacement (mm)	Average Linear Displacement (mm)		Displacement (mm)
1	597.55	27.29	30.00	Average	30.00
2	718.10	32.79		S.D.	1.85
3	692.06	31.60		Uncertainty	0.76
4	664.08	30.33			
5	621.43	28.38			
6	648.44	29.61			

Table 41: Displacement measurements obtained by a standard mouse at pointer speed 10

Test #	Linear Displacement (units)	Linear Displacement (mm)	Average Linear Displacement (mm)		Displacement (mm)
1	852.00	32.50	30.00	Average	30.00
2	838.01	31.96		S.D.	1.67
3	747.01	28.49		Uncertainty	0.68
4	782.03	29.83			
5	738.02	28.15			
6	762.00	29.07			

Overall, the minimum uncertainty was found with the mouse at the highest and most sensitive speed; setting 10. With a standard deviation of 1.67, this was our best result. The range of calculated displacement was 28.15mm to 32.50mm. With an uncertainty of 0.68, the mouse does not preliminary meet our constraints.

A mouse setting of 10 also creates additional sources of error. The high speed of the cursor limits the amount of measureable displacement due to screen size. With the high speed setting, more pixels are displaced per millimeter moved and the cursor will hit the edge of the screen with less movement.

With that in mind, an ideal setting of 7 was used for final testing. This would provide a maximum sensitivity and mitigate the likelihood of the cursor hitting the side of the screen. A precise, high dot-per-inch wireless mouse was also purchased. With 2000 dpi, this mouse is designed for performance. Table 42 and figure 56 correspond to the measurements obtained with the 2000 dpi mouse at a pointer speed setting of 7.

Table 42: Displacement measurement from a 2000 DPI mouse at pointer speed 7

Test #	Displacement (units)	Displacement (mm)	Average Linear Displacement (mm)		Total Displacement (mm)
1	680.00	9.32	10.00	Average	10.00
2	795.00	10.90		S.D.	0.75
3	720.00	9.87		Uncertainty	0.28
4	728.00	9.98			
5	745.00	10.22			
6	724.00	9.93			
7	713.00	9.78			

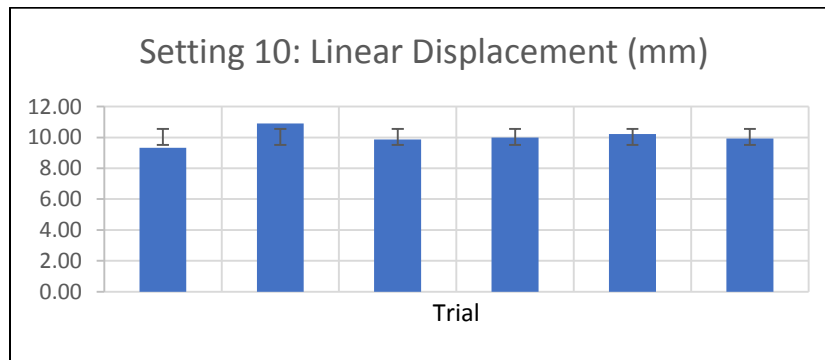


Figure 56: Mean and standard deviation of mouse displacement measurements from a 2000 DPI mouse at pointer speed 7

This trial was our most successful, but still not within constraints. With a standard deviation of 0.75, uncertainty for these trials is 0.28. These results would be considered promising for a mouse as a displacement sensor, but there were many additional negative characteristics of the electronic mouse in this application. Additionally, using a 2000 DPI mouse at pointer speed 7, restricts the user to displacements within 10mm, which is unsuitable for this application. This means the low uncertainty measured at this setting was meaningless, as it could not be used with a ski boot binding test setup.

H.1.4 Findings

Despite the findings of other scholarly works, testing was performed to fully validate linearity, repeatability and uncertainty within the scope of our design. Despite exhaustive experimentation (Appendix H), the level of uncertainty of an electronic mouse was not within our constraint of 0.2 mm. Despite a rated resolution of 2000 dpi, an optical mouse is not a viable sensor in this application. Several sources of error were analyzed and documented.

Firstly, an optical mouse's accuracy is strictly dependent on a precise z-axis distance. With any separation from the imaging surface, the mouse becomes inoperable. In binding testing procedures the boot may twist and roll along the x-axis creating z-axis separation. This is difficult to mitigate in a binding test. A third source of error with a mouse is top speed. Binding testing is to be performed with applied torque for a maximum of 5 seconds (ASTM, 2009). This quick release may be difficult to capture with an electronic mouse, a 1000 dpi gaming mouse has a top speed around 0.5 m/s (Windows, 2002). This is not adequate for this application.

Additional error can be incurred due to smoothing or anti-aliasing functions built in to the mouse hardware. Designed to smooth the translation of the cursor on the screen, these minor adjustments can affect trajectory across the screen as well as cause significant lag. These properties will dramatically decrease the accuracy of a computer mouse. Lastly, screen size will limit the amount of recordable displacement distance. If the cursor runs into the edge of the screen during testing, data is halted at that point. This limitation requires additional preliminary setup, and may go unnoticed.

Appendix I: Polaris Measurement Analysis

I.1 Test Setup

Our displacement measurements were made by applying removable fiducials, also known as passive markers, onto the tested ski boot in order for the Polaris Spectra to optically track the three-dimensional motion of the boot, while other passive markers were used to provide a reference frame for the displacement (Figure 57). This setup was placed approximately 5 feet from the NDI Polaris sensor. The passive markers on the toe of the boot can be seen extending above, while the reference markers are on the tabletop in front.



Figure 57: Ski boot with attached passive marker and passive marker reference marker on testing bench

The position of the boot in relation to the reference marker was determined by the Polaris' optical measurement system and Application Program Interface (API), which allowed for tracking of specific passive markers and output data to Excel. During Polaris testing, the position of the tracking markers was measured and recorded via calipers, and then compared to the positions documented by the Polaris to validate the precision of the measurements. The passive marker affixed to the ski boot, was aligned with the mid-sole line of the boot, which was moved to a rigidly defined point. Error analysis of the

reported data was conducted in order to determine the sensors viability in a torque-displacement testing system.

I.2 Data and Analysis

The passive markers are tracked in 3D space relative to the reference passive marker, in centimeters, as x, y and z coordinates within the measurement volume. The output relative position is provided on a frame basis, but does not include a timestamp to identify the time at which these positions were documented. The output data is sent to a CSV file format in Excel, and includes the error associated with each position documented in the frame (Table 43).

Table 43: Polaris position tracking of a ski boot

	A	B	C	D	E	F	G
1	Port 3: NDI	Frame	Tx	Ty	Tz	Error	Average Error
142	3	48142	-279.038	40.161	-140.077	0.22079	
143	3	48145	-279.098	40.333	-139.914	0.213958	
144	3	48148	-278.969	40.437	-140.129	0.22076	
145	3	48151	-279.262	40.008	-139.747	0.211685	
146	3	48154	-278.881	40.391	-140.22	0.217425	
147	3	48157	-279.286	39.705	-139.69	0.228908	
148	3	48160	-278.781	40.214	-140.57	0.20673	
149	3	48163	-278.609	40.047	-140.99	0.219699	
150	3	48166	-279.397	39.701	-139.381	0.217718	
151	3	48169	-278.915	40.232	-140.385	0.216944	
152	3	48172	-278.782	39.728	-140.846	0.220583	
153	3	48175	-279.047	36.288	-141.384	0.213533	
154	3	48178	-278.407	29.287	-145.307	0.217343	
155	3	48181	-278.466	30.036	-144.409	0.20643	
156	3	48184	-278.442	34.572	-143.542	0.215714	
157	3	48187	-278.965	30.889	-143.759	0.213773	
158	3	48190	-278.79	29.729	-144.073	0.223135	
159	3	48193	-279.152	31.2	-143.124	0.224793	
160	3	48196	-278.746	29.989	-144.537	0.204887	
161	3	48199	-278.95	29.493	-143.94	0.225843	
162	3	48202	-278.781	29.381	-144.775	0.210499	
163	3	48205	-278.558	27.388	-145.896	0.220706	
164	3	48208	-278.592	27.447	-145.508	0.220028	
165	3	48211	-278.078	27.468	-146.995	0.207261	
166	3	48214	-278.985	26.581	-145.11	0.21763	
167	3	48217	-278.29	27.152	-146.423	0.20363	
168	3	48220	-278.495	27.46	-146.065	0.216387	
169	3	48223	-278.236	27.226	-146.359	0.214375	
170	3	48226	-277.885	26.996	-147.223	0.207862	

A series of four identical tests were performed to assess error in the system. Error analysis was performed by averaging the 500 error values provided by the Polaris (Table 44).

Table 44: Average Polaris Error (cm)

Average System Error (cm)				
<u>Test #1</u>	<u>Test #2</u>	<u>Test#3</u>	<u>Test#4</u>	<u>System Error</u>
0.14	0.19	0.20	0.12	0.16

A total average error was calculated to be 0.16cm, or 1.6mm. This level error, and lack of certainty, is far greater than is tolerable for this application.

Unfortunately, these results were expected with the NDI Polaris. A nominal error of the system is claimed to be as low as 0.3mm, but results show that the value was much larger. Similar to other similar technology, these sensors are more imprecise at distances and do not respond well to quick, sudden motions. This system is not designed to measure small displacements, and therefore this technology is ineffectual.

Appendix J: Prototype and Consumer Costs

Prototype Costs	
Stock Materials (Total):	\$54.71
6061 Aluminum Rod, 2" Diameter, 1' Length	\$23.99
6061 Aluminum Tube, 1-1/2" OD, 1" ID, .250" Wall Thickness, 1' Length	\$18.07
6061 Aluminum Tube, 1-1/2" OD, 1.402" ID, .049" Wall Thickness, 1' Length	\$12.65
304 Stainless Steel Rectangular Tube Stock	Provided (Epitoux Lever)
Circuit Components (Total):	\$6.78
Resistors	Provided
Wiring	Provided
2 INA217AIP Amplifiers	\$6.78
National Instruments USB-6008 DAQ:	Provided
Vermont Release Calibrator Prosthetic Foot:	Provided
Labview SignalExpress Software and NI-MAX Drivers:	Provided
Total Prototype Costs	\$61.49

Consumer Costs	
CNC Manufacturing (2 Hours):	\$50
McMaster-Carr Stock Materials (Total):	\$91.78
6061 Aluminum Rod, 2" Diameter, 1/2' Length	\$16.36
6061 Aluminum Tube, 1-1/2" OD, 1" ID, .250" Wall Thickness, 1' Length	\$10.84
6061 Aluminum Tube, 1-1/2" OD, 1" ID, 0.049" Wall Thickness, 1/2' Length	\$7.59
304 Stainless Steel Rectangular Tube Stock	\$56.99
DigiKey Circuit Components (Total):	\$7.78
Resistors:	\$0.20
Wiring:	\$0.80
2 INA217AIP Amplifiers:	\$6.78
National Instruments USB-6008 DAQ:	\$189
Vermont Release Calibrator Prosthetic Foot:	\$200
Labview SignalExpress Software and NI-MAX Drivers:	Free
Total Consumer Cost (with Prosthetic Foot)	\$538.56
Total Discluding Including Prosthetic Foot	\$338.56

References

- AMES. (2013). ANSI Standard Limits and Fits Calculator. Advanced Mechanical Engineering Solutions. Retrieved December 12, 2013, From: <http://www.amesweb.info/FitTolerance/FitTolerancelmperial.aspx>
- ASM. (2013). Aluminum 6061-T6; 6061-T651. Aerospace Specification Metals Inc. Retrieved December 18, 2013, From: <http://asm.matweb.com>
- ASTM. (2005). Standard Practice for Selection of Release Torque Values for Alpine Ski Bindings. *ASTM Standards*. Pennsylvania, United States of America: American Society for Testing and Materials.
- ASTM. (2008). Standard Specification for Ski Binding Test Devices. *ASTM Standards*. Pennsylvania, United States of America: American Society for Testing and Materials.
- ASTM E2655. (2008). Standard Guide for Reporting Uncertainty of Test Results and Use of the Term Measurement Uncertainty in ASTM Test Methods. *ASTM Standards*. Pennsylvania, United States of America: American Society for Testing and Materials.
- ASTM. (2009). Standards for Functional Inspections and Adjustments of Alpine Ski/Binding/Boot Systems. *ASTM Standards*. Pennsylvania, United States of America: American Society for Testing and Materials.
- ASTM. (2013). Standard Method for Verification of Ski Binding Test Devices. *ASTM Standards*. Pennsylvania, United States of America: American Society for Testing and Materials.
- BEI Sensors. (2014). Optical Rotary Encoders-Incremental versus Absolute and Shafted versus Hollow Shaft Encoder Products. From: <http://www.beisensors.com/technical-support-bei-rotary-encoder-vs-optical-encoder.html>
- Beynon, B. D., Ettlinger, C. F., Johnson, R. J., Natri, A., & Shealy, J. E. (1997). Alpine ski bindings and injuries. *Sports medicine*, 28(1), 35-48.
- Brown, C. A. (2006). *Axiomatic Design and the Evolution of Conventional Alpine Ski Bindings*. Retrieved June 1, 2013, from Axiomatic Design: <http://www.axiomaticdesign.org/docs/AxiomaticDesignandSkiBindings.pdf>
- Brown, C. A., & Ettlinger, C. F. (1985). A method for improvement of retention characteristics in alpine ski bindings. In *Skiing Trauma and Safety: Fifth International Symposium (ASTM STP 860)*. Philadelphia, PA: ASTM International (pp. 224-237).
- CDC. (2010). Anthropometric Reference Data for Children and Adults: United States 2007-2010. Center for Disease Control and Prevention. From: http://www.cdc.gov/nchs/data/series/sr_11/sr11_252.pdf
- Dodge, D., Ettlinger, C. F., Johnson, R. J., Sargent, M., and Shealy, J. E. (2010) Retention requirements for alpine ski bindings *Journal of ASTM International*, Vol. 7, No. 6.

Epitoux, Jacques. (1989). U.S. Patent No. 4,860,595. Washington, DC: U.S. Patent and Trademark Office

Ettlenger, Carl F. (1974). U.S. Patent No. 3,805,603. Washington, DC: U.S. Patent and Trademark Office

Ettlenger, C. F., Johnson, R. J., & Shealy, J. E. (2005). Using signal detection theory as a model to evaluate release/retention criteria in alpine skiing. *Journal of ASTM International(JAI)*, 2(7).

Ettlenger, C. F., Shealy, J. E., & Johnson, R. J. (2009). Myths Concerning Alpine Skiing Injuries *Sports Health: A Multidisciplinary Approach*, 1(6), 486-492.

Ettlenger, C. (2010). *FAQ #5 for Skiers/ Riders*. Retrieved May 28th, 2013, from Vermont Ski Safety: <http://www.vermontskisafety.com/>

Hawks, T. (2012, October 1). *NSAA Fact Sheet*. Retrieved May 30th, 2013, from National Ski Areas Association Website: www.nsaa.org

Hoffmann, K. (1986). Applying the Wheatstone Bridge Circuit. *HBM S1569-1.1 en, HBM, Darmstadt, Germany*, <http://www.hbm.com/fileadmin/mediapool/hbmdoc/technical/s1569.pdf>.

ISO. (2009). Alpine ski bindings- Requirements and test methods. *International Standards and British Standards*. London, England: British Standards Institution.

Jones, F. D., Oberg, E., & Horton, H. L. (2004). *Machinery's handbook*. Industrial Press, Incorporated.

Lagran, M. (2012). *Head Injuries on the Slopes*. Retrieved: May 31st, from: Ski Injury <http://www.ski.injury.com>

LeapMotion. (2014). Explore the World in a Whole New Way. Retrieved: February 12th, 2014

From: <https://www.leapmotion.com/product>

Lipe, Gordan C. & Hinds, Charles W. (1966). U.S. Patent No. 3,289,472. Washington, DC: U.S. Patent and Trademark Office.

Merrill, Bradley. (2013). *Torque-Displacement Binding Tester (Undergraduate Interactive Qualifying Project, E-project-031213-113928)*. Retrieved from Worcester Polytechnic Institute Electronic Projects Collection: <http://www.wpi.edu/Pubs/E-project/Available/E-project-031213-113928/>

NDI. (2014). Polaris Optical Tracking System. NDI Medical. Retrieved From: <http://www.ndigital.com/medical/products/polaris-family/>

New York Times. (2008, March 4). Alpine Skiing Men's World Cup. Retrieved July, 3 2013, from The New York Times: <http://www.nytimes.com/2008/03/04/sports/04ihtalpine4.10693330.html>

Ng, T. W. (2003). The optical mouse as a two-dimensional displacement sensor. *Sensors and Actuators A: Physical*, 107(1), 21-25.

- NI. (2010). DAQ Getting Started Guide. National Instruments. From: <http://www.ni.com/pdf/manuals/373737d.pdf>
- National Instruments. (2014). NI SignalExpress. From: <http://www.ni.com/labview/signalexpress/>
- Özkaya, N., Nordin, M., Goldsheyder, D., & Leger, D. (2012). *Fundamentals of biomechanics: equilibrium, motion, and deformation*. Springer.
- Paletta, G. A., & Warren, R. F. (1994). Knee injuries and alpine skiing. *Sports Medicine*, 17(6), 411-423.
- Shealy, J. E., Ettliger, C. F., & Johnson, R. J. (1999). Signal Detection Theory: A Model for Evaluating Release/Retention Criteria in Alpine Ski-Binding-Boot Systems. *ASTM SPECIAL TECHNICAL PUBLICATION, 1345*, 120-131.
- Ski Gear TV (2012, December 8). Ski Prophet Presents Core Shot: Ski Binding Test [Video file]. Retrieved from <http://www.youtube.com/watch?v=ORvpLjlx8Uk>
- SIA. (March, 2013). *2013 SIA Snow Sports Fact Sheet*. Retrieved September 12th, from: Snow Sports Industries America website: www.snowsports.org
- Suh, N. P. (1990). *The principles of design*. New York: Oxford University Press.
- Taylor, B. N. (2009). *Guidelines for Evaluating and Expressing the Uncertainty of NIST Measurement Results (rev. DIANE Publishing)*.
- Texas Instruments. (2005). Low-Noise, Low-Distortion Instrumentation Amplifier Replacement for SSM2017. Retrieved from: <http://www.ti.com/lit/ds/symlink/ina217.pdf>
- Vishay Precision Group. (2011, December 19). *Surface Preparation for Strain Gage Bonding*. Retrieved December 2013, from VishayPG.com.
- Vermont Ski Safety (2010). *Vermont release calibrator operation and maintenance manual*. Retrieved July 9, 2013, from <http://www.vermontskisafety.com/files/CALIBRATER-MANUAL.pdf>
- Wiles, A. D., Thompson, D. G., & Frantz, D. D. (2004, May). Accuracy assessment and interpretation for optical tracking systems. In *Medical Imaging 2004* (pp. 421-432). International Society for Optics and Photonics.
- Windows. (2002). Pointer ballistics for Windows XP. Windows Hardware Developer Center Archive. Microsoft
- Wintersteiger (2011). *Speedtronic Pro*. Retrieved June 30, 2013, from <http://www.wintersteiger.com/us/Sports/Machines/New-Machines/Binding-adjustment/84-Speedtronic-Pro/>
- Young, L. R. (1989). Elevated racer binding settings and inadvertent releases. In *Skiing trauma and safety. Seventh International Symposium, ASTM STP* (Vol. 1022, pp. 222-7).